PHASE BEHAVIOR AND RHEOLOGY OF SOLUTIONS OF ASSOCIATIVE POLYMER AND SURFACTANT

ZHAO GUANGQIANG

NATIONAL UNIVERSITY OF SINGAPORE

2007

PHASE BEHAVIOR AND RHEOLOGY OF SOLUTIONS OF ASSOCIATIVE POLYMER AND SURFACTANT

ZHAO GUANGQIANG

(B.ENG., SHANGHAI JIAOTONG UNIVERSITY)

A THESIS SUBMITTED

FOR THE DEGREE OF DOCTOR OF PHILOSOPHY

DEPARTMENT OF CHEMICAL AND BIOMOLECULAR ENGINEERING

NATIONAL UNIVERSITY OF SINGAPORE

2007

ACKNOWLEDGEMENT

This dissertation represents the successful culmination of many years of hard and deliberate work on a chemical engineering research project that would not have been possible without the efforts of many other people on my behalf.

In particular, I am indebted to Professor Chen Shing Bor for his constant guidance and inspiration throughout my graduate study. I could always count on him to help me see things from another point of view, and to foster both my professional and personal development.

I would also like to thank my oral qualifying examination committee members, Professor Chung Tai-Shung, Neal and Professor Uddin, Mohammad S. for their genuine comments on my research and valuable advice on how to be a good scientist.

This work has received a great deal of support and assistance from the lab officers Ms. Siew Woon Chee, Ms. Sylvia Wan and Ms. Chew Su Mei. I would like to acknowledge Ms. Samantha Fam and Dr. Yuan Ze Liang for their help on the operation of the laser scattering system in the initial stage of this project.

Many thanks also go to my labmates: Mr. Zhou Tong, Ms. Cho Cho Khin, Mr. Gao Yonggang, Ms. Zhou Huai, Ms. Shen Yiran and Ms. Chieng Yu Yuan, for their support and helpful discussions. Without them, the atmosphere in the lab would not have been so unforgettable. Thanks are also due to my friends at NUS, Mr. Zhu Zhen, Mr. Shao Lichun, Ms. Sheng Xiaoxia, and Mr. Chen Huan for their encouragement and enjoyable talks and jokes during the numerous afternoon tea sessions.

Finally, I express my heartful gratitude to my parents, whose support made me strong in facing with difficulties, and to my wife, who supported me through all of the lean times, both physical and emotional.

TABLE OF CONTENTS

SUMMARY

To elucidate the interactions between associative polymers and surfactants, we studied the phase behavior and rheological properties of their aqueous mixtures. In particular, clouding phenomena, phase separation behavior, steady and dynamic shear viscosity, and nonlinear rheology were examined for mixtures of hydrophobically modified hydroxyethyl cellulose (HMHEC) and nonionic surfactants.

Two nonionic surfactants, Triton X-114 and Triton X-100, in the presence of either hydroxyethyl cellulose (HEC) or the hydrophobically modified counterpart (HMHEC) were used to experimentally study the clouding phenomena and phase behaviors. Compared with HEC, HMHEC was found to have a stronger effect on lowering the cloud point temperature (CPT) of nonionic surfactant at low concentrations. The difference in clouding behavior can be attributed to different kinds of molecular interactions. Depletion flocculation is the underlying mechanism in the case of HEC, while chain-bridging effect is responsible for the large decrease in CPT for HMHEC. Composition analyses of the formed macroscopic phases were carried out to provide support for associative phase separation in the case of HMHEC, in contrast to segregative phase separation for HEC. An interesting three-phase separation phenomenon was reported for the first time in some HMHEC/Triton X-100 mixtures at high enough surfactant concentrations.

The interesting three-phase separation for Triton X-114 or Triton X-100 solutions with addition of hydrophobically modified hydroxyethyl cellulose was then investigated in detail experimentally. When the surfactant concentration was high enough, the solution slightly above the cloud point could separate into three macroscopic phases: a cloudy phase in between a clear phase and a bluish, translucent phase. The rate of phase separation was very slow in a matter of several days with the formation of the clear and cloudy phases followed by the emergence of the bluish phase. The volume fraction of the cloudy phase increases linearly with the global polymer concentration, while the volume fraction of the bluish phase increases linearly with the global surfactant concentration. Composition analyses found that

most of the polymer stayed in the cloudy phase, as opposed to most of surfactant in the bluish phase. The interesting phase behavior can be explained by an initial associative phase separation followed by a segregative phase separation in the cloudy phase.

The viscosity behavior of HMHEC solutions were investigated experimentally, focusing on nonionic surfactant and temperature effects. Weak shear thickening at intermediate shear rates took place for HMHEC at moderate concentrations, and became more significant at lower temperatures. While this amphiphilic polymer in surfactant free solution did not turn turbid by heating up to 95 °C, its mixture with nonionic surfactant showed a lower cloud point temperature than did a pure surfactant solution. For some mixture cases, phase separation took place at temperatures as low as 2 °C. The drop of cloud point temperature was attributed to an additional attractive interaction between mixed micelles via chain bridging. With increasing temperature, the viscosity of a HMHEC-surfactant mixture in aqueous solution first decreased, but then rose considerably until around the cloud point. The observed viscosity increase could be explained by the interchain association due to micellar aggregation.

Shear thickening and strain hardening behavior of HMHEC solutions were experimentally examined. We focused on the effects of polymer concentration, temperature and addition of nonionic surfactant. It was found that HMHEC showed stronger shear thickening at intermediate shear rates in a certain concentration range. In this range, the zero-shear viscosity scaled with polymer concentration as $\eta_0 \sim c^{5.7}$, showing a stronger concentration dependence than for more concentrated solutions. The critical shear stress for complete disruption of the transient network followed $\tau_c \sim c^{1.62}$ in the concentrated regime. Dynamic oscillatory tests of the transient network on addition of surfactants showed that the enhanced zero-shear viscosity was due to an increase in the network junction strength, rather than their number, which in fact decreases. The reduction in the junction number could partly explain the weak variation of strain hardening extent for low surfactant concentrations, because of longer and looser bridging chain segments, and hence lesser nonlinear chain

stretching.

The microviscosity of HMHEC aqueous solution was experimentally measured by conductometry. The microviscosity was significantly lower by more than 4 orders of magnitude than its bulk viscosity. The hydrophobic modification was found to have no effect on the solutions' microviscosity, based on the fact that the same electric conductivity reduction of a simple salt NaCl was found for both HMHEC and HEC solutions. This interesting result was explained by the fact that the conductivity reduction is merely resulted from the hydrodynamic interactions between the probe ions and the polymer segments.

LIST OF FIGURES

LIST OF TABLES

NOMENCLATURE

Abbreviations	Description
CAC	critical aggregation concentration
CMC	critical micelle concentration
CPT	cloud point temperature
CxEy	oligoethylene glycol ether
DS	degree of substitution
EHEC	Ethyl hydroxyethyl cellulose
EO	Ethylene oxide
GC-MS	Gas chromatography- mass spectroscopy
GPC	Gel permeation chromatograph
HASE	hydrophobically modified alkali-swellable emulsion
HEC	2- hydroxyethyl cellulose
HEUR	hydrophobically modified ethoxylated urethane
HMEHEC	hydrophobically modified ethyl hydroxyethyl cellulose
HMHEC	hydrophobically modified hydroxyethyl cellulose
HMHPG	hydrophobically modified hydroxypropyl guar
HMP	hydrophobically modified polymer
MS	molar substitution
PEO	poly(ethylene oxide)
PNIPAM	poly(N-isopropylacrylamide)
PVA	poly(vinyl alcohol)
PVP	poly(vinylpyrrolidone)

SANS	small-angle neutron scattering
SDS	sodium dodecyl sulfate
TOC	Total organic carbon

Symbols

c_i	Number concentration of species i
c_p	the polymer concentration, wt%
e	Fundamental charge, C
E	activation energy for hydrophobe, kJ/mol
G^*	Complex modulus, Pa
G'	Storage modulus, Pa
G"	Loss modulus, Pa
G_0	plateau modulus, Pa
G_c	crossover modulus, Pa
i	Complex number, or species
k	Boltzmann constant
M_w	weight averaged molar mass, g/mole
M_n	number averaged molar mass, g/mole
$n_{electrolyte}$	number concentration of electrolyte
R	Radius of a plate, cm
t	Time, s
t_c	Crossover time, s
T	Absolute temperature, K

z_i	Valency number
α	prefactor
α_0	Cone angle, radian
$\gamma(t)$	Sinusoidal strain function
γ_0	Amplitude of strain
$\dot{\gamma}$	shear /strain rate, s^{-1}
γ^*	Complex strain
$\dot{\gamma}_c$	Critical shear rate for the maximum viscosity
η_0	Zero shear viscosity or solvent viscosity, Pa·s
η_c	Microviscosity, Pa·s
κ	Electric conductivity, $S \cdot m^{-1}$
[κ]	Intrinsic attenuation factor
$\sigma(t)$	Sinusoidal stress function, Pa
σ_0	Amplitude of stress, Pa
σ^*	Complex stress, Pa
τ	relaxation time, s
μ	Mobility of a particle, $cm^2/s \cdot volt$
v	Network number density or scaling exponent
φ	Phase angle/lag, radian
ω_c	Crossover frequency, Hz
ω	Angular frequency, Hz

CHAPTER 1 Introduction to Associative Polymers and Surfactants

1.1 Motivation for Study of Associative Polymers

Water-soluble polymers are superior to solvent borne counterparts for safety and environmental concern, and have attracted growing attention in industry. They are widely used to modify the rheological properties of various water based formulations, such as latex paints, drilling mud, and cosmetics. In many cases, the polymer is modified by adding alkyl side chains either randomly along the backbone or to its two ends as hydrophobes, to become amphiphilic, in order to achieve higher viscosifying efficiency. Such a modification can lead to interactions of more kinds with other species in a solution, and thereby complex phase behaviors and more versatile flow properties, depending on the solution composition.

1.2 Definition of an Associative Polymer

Associative polymers are hydrophobically modified water soluble polymers, composed of both water soluble and water insoluble components; the water insoluble components interact in solution, leading to interchain or intrachain association, or both, accompanied by macroscopic consequences such as viscosifying effect, phase separation phenomena, etc. The water insoluble components are usually C_{12} ~ C_{20} linear aliphatic chains, called hydrophobes. This main feature justifies their name as associative polymers. In principle, any water soluble polymer can be modified to produce an associative polymer. In literature three popular species investigated are hydrophobically modified alkali-swellable (HASE) polymers, hydrophobically modified hydroxyethyl cellulose (HMHEC), and hydrophobically modified ethoxylated urethane (HEUR) polymers.[1]

At sufficiently high polymer concentration, a dramatically high viscosity can be attained because of the formation of a gel-like structure arising from the dominant intermolecular association.[2] The hydrophobic association may be enhanced or

weakened by an imposed flow, depending on the flow strength and polymer concentration.[3]

1.3 Interactions with Surfactants

In the presence of surfactants, the properties of HMP (hydrophobically modified polymers) solutions may often be changed dramatically, because of the interactions between the two amphiphilic species, which are mainly hydrophobic association and electrostatic interactions if at least one species is charged. One of the most important interactions is hydrophobic binding between the HMP hydrophobes and the surfactant tails to form so-called "mixed micelles" [4]. The hydrophobic interaction is due to the Van de Waals attraction between the hydrophobes. A schematic representation of the mixed micelles is shown in Figure 1.1. As a consequence, the attractive interaction between the surfactant hydrophobic tails and the hydrophobes of the polymers can lead to unusual phase/clouding behaviors[5-8] and interesting rheological properties.[8-10] A recent review on the properties of mixed solutions of surfactants and HMPs with a special emphasis on molecular interpretations was given by Piculell et al.[11]

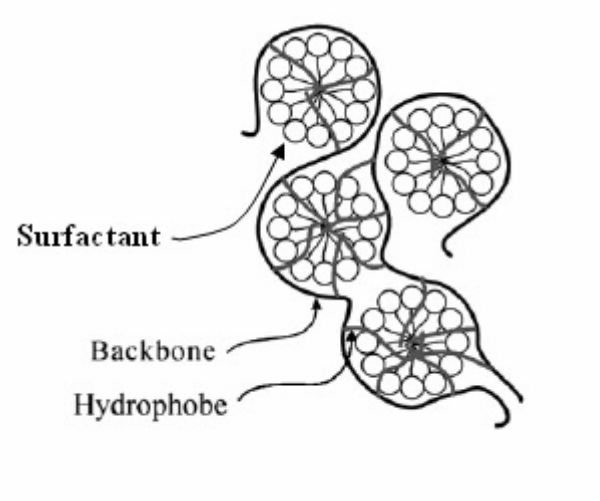

Figure 1.1: A schematic representation of the the mixed micelles formed by the surfactant molecules and the hydrophobes from the associative polymer.

1.3.1 Clouding Phenomenon and Phase Separation

A nonionic surfactant solution above its critical micelle concentration (CMC) turns turbid after heated to a certain temperature, known as the cloud point

temperature (CPT). This phenomenon is attributed to the progressive dehydration of ethylene oxide (EO) units in the hydrophilic heads of nonionic surfactants, and the resulting micellar aggregation with increasing temperature. At CPT, both the size and the number of micellar aggregates have to be sufficient for visible turbidity. Clouding phenomenon can also happen to certain nonionic water-soluble polymers. Some examples are poly(ethylene oxide) (PEO), poly(N-isopropylacrylamide) (PNIPAM), ethyl(hydroxyethyl)cellulose (EHEC) and hydrophobically modified EHEC (HMEHEC).[5]

The CPTs of nonionic surfactants or polymers are quite sensitive to additives, such as electrolytes, alcohols, non-clouding surfactants or polymers. Therefore, investigating how the CPT changes in the presence of these additives can shed light on the interactions between these molecules.[12] Although available studies have provided insight into various interactions, less attention has been paid to the separated macroscopic phases, due to experimental difficulty and workload in obtaining the compositions of each phase.[13]

An HMP/surfactant mixture may undergo an associative phase separation into a phase enriched in both the polymer and surfactant and a very dilute water phase. Although the surfactant concentration in the latter phase is thought to be equal to or below its CMC, little experimental evidence has been reported in the literature. Unlike electrostatics for oppositely charged polymer and ionic surfactant, the attractive interaction responsible for the associative phase separation of a mixture of neutral HMP and nonionic surfactant is primarily of hydrophobic nature. In contrast, a mixture of an unmodified neutral polymer and a nonionic surfactant usually segregates in two phases, each of which is rich in one of the solutes. Phase separation takes place at a temperature slightly above the cloud point temperature (CPT), which can depend strongly on the mixture composition.[14] Segregative phase separation, as opposed to its associative counterpart, was first proposed by Piculell and Lindman[15] and evidenced by experimental studies on charged HMP/surfactant mixtures[16-18] and also on neutral HMP/surfactant mixtures[19-20] in the last two decades.

Except for the excluded volume effect, the interactions between nonionic

surfactant and neutral water soluble polymer, the parent material of their hydrophobically modified derivatives, are usually very weak or even nonexistent. Examples of such polymers are poly(vinyl alcohol) (PVA), poly(ethylene oxide) (PEO), poly(vinylpyrrolidone) (PVP), and cellulose analogus.[21,22] However, these polymers at high concentrations do exert noticeable effects on lowering the cloud point of surfactants (CxEy).[23,24] The observed CPT decrease was explained by depletion flocculation because of the excluded volume interaction, leading to a segregative phase separation into a polymer-rich phase and a surfactant-rich phase.

1.3.2 Rheological Aspect

The presence of surfactant manifests its interactions with the hydrophobic association in solutions of associative polymers through not only dramatic phase changes, but also interesting variations in the rheological properties of solutions of associative polymers. At low surfactant concentration, this binding enhances the interchain association for gel-like HMP solutions, leading to an increase in viscosity.[25-28] Further addition of the surfactant can result in an increased number of mixed micelles, each of which however contains hydrophobes in a declined number. As a result, the viscosity will reach a maximum and then decrease. With excess surfactant, each hydrophobe will eventually be masked by a mixed micelle, leading to disappearance of the hydrophobe links and formation of free micelles. This behavior is reflected by a nearly constant viscosity since the HMP has been saturated with surfactant and the free micelles exert a very small effect on the viscosity. For ionic surfactant, the electrostatic repulsion between the mixed micelles can affect the polymer conformation and the corresponding gel microstructure is more expanded.[26-28]

Shear thickening phenomenon, where the steady shear viscosity increases with increasing shear rate, has been known to occur at moderate shear rates for aqueous solutions of hydrophobically modified ethoxylated urethanes (HEUR, an end-capped PEO).[29-31] The proposed mechanisms to account for the shear thickening are: (1) flow-induced loop-to-bridge transition[32-35], (2) cooperative effect of non-Gaussian

chain stretching[36], and (3) network reorganization[37]. The three mechanisms may coexist, and their relative importance depends on the polymer molecular weight, concentration, and hydrophobe size. Studying HEUR polymer (M_n = 51,000, M_w/M_n~1.7), Tam *et al.*[32] was the first to report the occurrence of a flow-induced loop-to-bridge transition, inferred from an increased plateau modulus in the experiments with superposition of a small oscillation on a steady shear flow. However, the above transition argument appears inappropriate for cases with high concentrations. Moreover, Ma and Cooper[38] experimentally found no discernible shear thickening for unimodal polydisperse HEUR polymer. They justified this observation by cooperative effect of non-Gaussian chain stretching, which can take place at certain critical shear rates only for a sample with low enough polydispersity.

Relatively weak shear thickening was observed for hydrophobically modified alkali-soluble emulsion (HASE) polymer solutions at intermediate shear stresses and low concentrations[39]. This polymer is a hydrophobically modified carboxylic acid containing copolymer, i.e., a comblike polyelectrolyte with hydrophobes randomly distributed along its backbone. The shear thickening and strain hardening behavior[39-41] is attributed to shear-induced structuring through hydrophobic association, which is inferred again from the aforementioned flow-superposition experiments. The shear thickening of HASE polymer is weaker than that observed for HEUR, primarily due to the competing effects between topological disentanglement and induced hydrophobic association at moderate shear rates.[39]

Another commercially available comblike polymer, hydrophobically modified hydroxyethyl cellulose (HMHEC), by contrast, has received little attention and is less well understood regarding the shear thickening and strain hardening behavior. Maestro *et al.*[3] observed weak shear thickening only for the HMHEC solution at 0.5 wt%, which was the lowest concentration investigated in their study. They attributed the shear thickening to flow enhanced interchain association of hydrophobes. However, no systematic studies on the shear thickening were carried out in their paper.

1.3.3 Microrheology

The transport through polymer solutions of spherical rigid microparticles of different sizes, ranging from tens of nanometers to several micrometers, has been studied extensively over the past two decades[96-97]. The microscopic material properties, such as viscosity, and modulus could be obtained through measuring the migration of the microparticle, thus this field is termed as *microrheology*. It is of paramount importance in the technological and biological processes that involve separating or removing protein and other biomolecules. Other applications include chromatography, catalysis and electrophoresis. However, the transport of small ions through an associative polymer solution is relatively less studied.

1.4 Objectives and Scope of This Work

In this work, we investigated the interactions between nonionic surfactant and HMHEC by studying the phase behavior and rheological properties of their mixtures. The influence of uncharged HMP with randomly distributed hydrophobes on the clouding phenomenon of nonionic surfactants had not yet been investigated, but was expected to be more complicated since the hydrophobic interactions were not restricted to the polymer chain ends.

Although available studies have provided insight into various interactions, less attention has been paid to the separated macroscopic phases, due to experimental difficulty and workload in obtaining the compositions of each phase. We also intended to determine the composition in each phase after the phase separation was completed. The unmodified analogue HEC was also tested for comparison. A new three-phase separation in associative polymer/nonionic surfactants mixtures was reported for the first time. We systematically studied this phenomenon, in particular with respect to the phase separation kinetics, the composition in each phase and the mechanism.

Besides the phase behavior, the rheological properties of HMHEC were examined, focusing on the effects of nonionic surfactant and temperature, in an attempt to seek the correlation between molecular interactions and flow behavior. The

nonlinear rheology, specifically, the shear thickening and strain hardening behavior of HMHEC was investigated with a commercial rheometer, focusing on the effects of polymer concentration, temperature and added nonionic surfactant. It is aimed at gaining a better understanding of the flow behavior of comblike HMP.

The microviscosity of HMHEC aqueous solutions was experimentally measured and compared with its bulk viscosity.

1.5 Organization

A thorough investigation into the phase behavior, especially the macroscopic phase separation, and the rheological properties of comb-like associative polymer in the presence of surfactants should reveal considerable insight into the hydrophobic interaction mechanism between them. The materials and experimental methods are described in Chapter 2, while the experimental results are presented in the following four chapters.

We started with a relevant literature review in Chapter 3 on the phase behavior of mixed solutions of HMPs and surfactants, before presenting the results on the phase behavior of aqueous solutions of hydrophobically modified hydroxyethyl cellulose (HMHEC) mixed with nonionic surfactant. We examined the effect of hydrophobic modification by contrasting the results obtained from HMHEC with those obtained from its parent polymer hydroxyethyl cellulose (HEC).

In the course of experiments, a new, unexpected phase separation phenomenon (termed as three-phase separation) was encountered. This finding promoted us to further investigate it in a systematic way, with the results presented in the later part of Chapter 3. These results are nontrivial in our opinion, and hopefully will advance our understanding of the phase behavior of mixed solutions of associative polymer and surfactant to a new level.

The knowledge of phase behavior of the mixed solutions is a prerequisite for the subsequent investigation of the rheological properties. An introduction to the existing literature on the viscosity behavior of mixtures of HMPs and surfactants will be given in the first section of Chapter 4, followed by the results and discussion. In Chapter 5,

we present the nonlinear rheology of HMHEC, focusing on the effects of added nonionic surfactants, temperature, and the polymer concentration. Chapter 5 was concluded by discussing the implications of the experimental findings to the industry, which maybe useful to better design daily care products, which usually contain both polymer and surfactant, and involve flows in nonlinear regime during manufacturing. Following the previous two chapters on the bulk viscosity behavior, Chapter 6 investigated the microviscosity of HMHEC solutions.

And finally, Chapter 7 concludes the dissertation with recommended extensions of the current work.

CHAPTER 2 Materials and Methods

2.1 Investigated Associative Polymer (HMHEC)

Depending on the position of the hydrophobes along the parent polymer backbone, two types of associative polymers, could be identified. The first type has a triblock molecular structure, such as the most well-known HEUR, and is often referred to as 'end-capped', or 'telechelic'. The other type has a comb-like structure with a number of hydrophobes (on the order of dozens), randomly distributed along the polymer backbone. A schematic of the comb-like structure is shown in Figure 2.1. Associative polymers are usually at the water-soluble end of the spectrum of polymeric amphiphiles, i.e., the weight fraction of the hydrophobes is usually small (a few percent). A high degree of hydrophobic modification typically leads to poor water-solubility.[11]

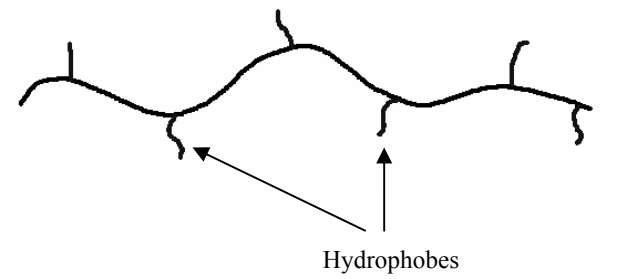

Figure 2.1: A schematic representation of the comb-like molecular structure.

The associative polymer investigated in this work is of a comb-like structure, and a water soluble derivative from cellulose, namely, 2-hydroxyethyl cellulose hydrophobically modified with hexadecyl groups (HMHEC) supplied by Aldrich and used as received. According to the manufacturer, the polymer has a mass-average molecular weight M_w=560,000 g/mol with the molar substitution (MS) and degree of substitution (DS) for hydroxyethyl groups (-OCH_2CH_2-) being 2.7-3.4 and 2.0, respectively. The degree of polymerization is estimated to be ~1880. For cellulose derivatives, DS is defined as the average number of hydroxyl groups, which have

been replaced by hydroxyethyl groups, for one anhydrous glucose residual repeating unit, so it can range from 0 up to a maximum 3. MS is the average number of hydroxyethyl groups per anhydrous glucose residual repeating unit, and thus can be any value greater than zero. The molecular structure of HMHEC is shown in Figure 2.2. The C_{16} alkyl chains act as the hydrophobes.

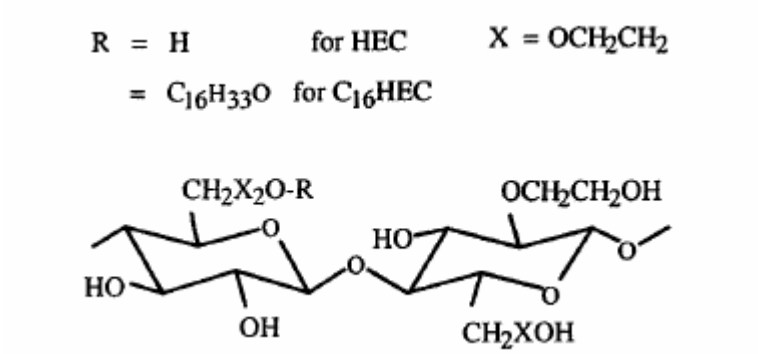

Figure 2.2: The molecular structure of hydrophobically modified hydroxyethyl cellulose, with the hydrophobic groups being -C_{16} linear alkyl chains.

Unfortunately, the information in regards to the hydrophobe substitution level for HMHEC was not provided by the manufacturer. We conducted H^1 NMR experiment to find out that each polymer molecule has on average 10 hydrophobes randomly distributed along its backbone, i.e., the degree of modification is 0.53 mol% or 1.8×10^{-5} moles of hydrophobes/g of polymer. This information is critical for interpretating the experimental results since the surfactant-to-hydrophobe ratio could not be known without knowing the number of hydrophobes beforehand. Gel permeation chromatograph (GPC) of HMHEC using water as the mobile phase gives the polydispersity index (M_w/M_n) ~4.5. The large polydispersity of the cellulose based polymer will have a possible impact on the phase behavior as studied in Chapter 3

2.2 Control Polymer (HEC)

The unmodified parent polymer of HMHEC, 2-hydroxyethyl cellulose (HEC) also from Aldrich was used without any further purification, with the weight averaged molar mass M_w=720,000 g/mol, MS and DS equal to 2.5 and 1.5. The molecular

structure of HEC is similar to that shown in Figure 2.2 except that it has no -C_{16} hydrophobes. This polymer (abbreviated as HEC72) was used as the control to study the effect of hydrophobic modification on the phase behavior, as will be discussed in Chapter 3. Another HEC, only different from HEC72 in the molar mass, has a weight averaged molecular weight M_w = 90,000 g/mol. It is used in Chapter 6 and abbreviated as HEC9.

2.3 Nonionic Surfactants

The surfactants used in this study are oligoethylene glycol ethers. The mechanism of dissolution in water is hydrogen bonding between their hydrophilic head (usually a short ethylene oxide chain) and water molecules. An increase in thermal energy (i.e., temperature rise) can weaken the bonding, causing the solution to turn turbid at a certain temperature (called CPT) because of dehydration of the ethylene oxide (EO) units.

Two nonionic surfactants from Sigma were adopted without further purification: 4-(1,1,3,3-tetramethylbutyl) phenyl-polyethylene glycol (ethylene oxide number ~7.5 and trade name as Triton X-114, abbreviated as TX114 thereafter) and 4-(1,1,3,3-tetramethylbutyl) phenyl-polyethylene glycol (ethylene oxide number ~9.5 and trade name as Triton X-100, abbreviated as TX100 thereafter). They were used for the investigation of the phase behavior of the mixed solutions with HMHEC. They were chosen because their concentration could be easily detected by a UV spectrophotometer due to the presence of benzyl ring in their molecular structure. The critical micelle concentration (CMC) of TX114 and TX100 was 90 and 130 ppm, respectively, according to the manufacturer. Note that the surfactant hydrophilic head is not monodisperse according to the GC-MS chromatograms, the resolution of which is good enough to distinguish surfactant molecules with different numbers of ethylene oxide (EO) units. To illustrate, we show the molecular weight distribution for TX100 in Figure 2.3. The polydispersity index can then be determined.

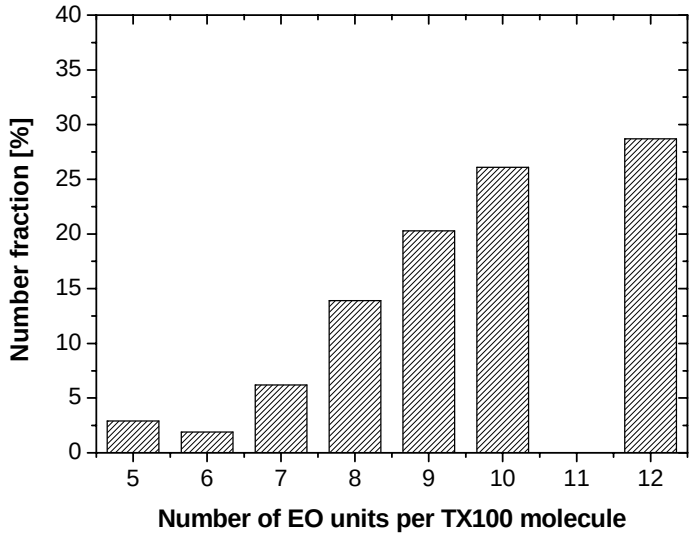

Figure 2.3: GC-MS results for the number fraction of TX100 molecules as a function of the number of ethylene oxide (EO) repeating units.

For the viscosity study, surfactants used were $C_{12}E_5$ (pentaethylene glycol monododecyl ether), $C_{12}E_6$ (hexaethylene glycol monododecyl ether) and $C_{12}E_9$ (nonaethylene glycol monododecyl ether). According to the manufacturer, they are highly monodisperse samples. Thus the effect due to the polydispersity of the surfactant hydrophilic moiety was eliminated. They were used without further purification. The surfactants used in this work are summarized in Table 2.1.

Table 2.1: Specifications of nonionic surfactants used in this work.

Surfactant	Molecular formula	M_w [a] g/mol	CMC [b] ppm	Polydispersity	Manufacturer
Triton X-114	4-(C_8H_{17})C_6H_4(OCH_2CH_2)$_{7.5}$OH	537	90	1.01 [c]	Sigma
Triton X-100	4-(C_8H_{17})C_6H_4(OCH_2CH_2)$_{9.5}$OH	625	130	1.02 [c]	Sigma
$C_{12}E_5$	$CH_3(CH_2)_{11}$ (OCH_2CH_2)$_5$ OH	406.5	27.6	1.00 [d]	Fluka
$C_{12}E_6$	$CH_3(CH_2)_{11}$ (OCH_2CH_2)$_6$ OH	450.6	30	1.00 [d]	Sigma
$C_{12}E_9$	$CH_3(CH_2)_{11}$ (OCH_2CH_2)$_9$ OH	482.8	46.6	1.00 [d]	Sigma

[a] Weight-averaged molecular weight provided by supplier;

[b] provided by supplier;

[c] determined by GC-MS;

[d] as provided by the supplier.

2.4 Experimental Methods

2.4.1 Sample Preparation

For the polymer HMHEC, a stock solution of 1 wt% or 1.2 wt% was prepared by dissolving the dry powder in deionized water purified through a Millipore MilliQ system. The solutions were magnetically stirred for 2 hr at 40 °C, and then cooled down to the room temperature before mixing with a proper amount of surfactant stock solutions to achieve a desired final composition. In the cases where the solution was already cloudy at room temperature, an ice-water bath was used to keep the solution clear. The prepared samples were then stored in a refrigerator for at least 24 hrs in order to complete hydration and interactions. All the samples were used within one week to avoid contaminations and degradations.

2.4.2 Cloud Point Measurement

The cloud point experiments were carried out in a water bath (Polyscience) equipped with a digital temperature controlled unit within 0.1 °C. The temperature

changing rate of the water bath is 1 ^{o}C /min. Each sample of approximately 10 ml placed in a screw-capped glass tube was heated in the water bath. The cloud point was determined by visual observation of the onset of an obvious turbidity change. Heating and cooling were regulated around the cloud point. The reproducibility of the CPT measurement was found to be good within 0.5 °C, and the average value was taken from triplicate measurements.

2.4.3 Phase Separation

Each sample of approximately 10ml was sealed off with a Teflon-lined screw cap in a flat-bottom test tube. Then the samples were placed in a thermostat water bath, set at a temperature slightly above the highest CPT of the batch of samples for the observation of their phase separation. For all the samples studied, two or three separated macroscopic phases with clear interfaces between them were obtained depending on the initial polymer and surfactant concentrations. However, the separation kinetics was generally slow (except for samples without HMHEC). For many samples, the heights of the phases hardly showed any change after 7 days, and were measured by a ruler for calculation of the phase volume fraction. The accuracy of the phase volume measurement is ~0.5mm in height. For some of them, an aliquot of each phase was carefully extracted by a syringe with a long needle and then diluted for subsequent composition analysis. Nevertheless, we did observe ongoing variation of the phases for a few samples even after 10 days.

2.4.4 Composition Analysis

The surfactant concentration was measured with a Shimadzu UV-Vis spectrophotometer for the absorption peak at either 223nm or 276nm, both due to the presence of the phenyl ring. At both wavelengths, no absorbance was seen for HEC or HMHEC.

The HEC concentration in the top phase after macroscopic phase separation was determined by gel permeation chromatography (GPC) using 0.1M $NaNO_3$ as the

mobile phase. Pure HEC solutions at known concentrations were run first to construct a calibration curve, which was then used by interpolation to determine the HEC concentrations in the top phase. The HMHEC concentration in the three-phase separation cases was indirectly determined from total carbon analysis (TOC-V, Shimadzu) by subtracting the contribution of the surfactant whose concentration had been measured with UV.

As will be discussed in Chapter 3, the TOC method for analyzing the HMHEC concentration suffered large uncertainties. Therefore a more accurate concentration determination method for HMHEC was later adopted: a colorimetric method using the anthrone reagent.[42-45] The procedure described by Snowden et al is adopted as follows.[42] The anthrone reagent was prepared by dissolving 0.15 g anthrone in 100 cm^3 of 76 wt% sulphuric acid with stirring, and was then stored in a refrigerator overnight before use. The reagent should be discarded after 1 day. A fixed volume of each sample (1 cm^3) was pipetted into a clean vial followed by addition of 9 cm^3 of the anthrone reagent with shaking. The vial was then placed in a boiling water bath for precisely 5 min, plunged into ice bath for 10 min, and then left to stand at room temperature for another 10 min. The absorbance spectrum of the resulting solution was recorded with a UV spectrophotometer, showing a peak at 626nm, because of the formation of furfural compounds in strong sulfuric acid.[45] The anthrone reagent is sensitive enough to detect a very low HMHEC concentration of ~10 ppm for a pure polymer solution.

However, it is interesting to note that the presence of surfactant indeed affects this anthrone reagent method, weakening the absorbance peak at 626 nm and rendering an additional peak at 504 nm. To the best of our knowledge, such interference has not yet been discussed in the literature. The chemistry for this interference is not clear, probably due to complexation between the surfactant and the formed furfural compounds. Despite the unexpected surfactant effect, the HMHEC concentration can still be determined by use of calibration curves as shown in Fig. 2.4, which plots the variation of the peak absorbance at 626 nm with TX100 concentration at four different HMHEC concentrations. Since the surfactant concentration can first

be measured independently by UV-Vis, the HMHEC concentration can then be determined easily by interpolation using Figure 2.4. This method is reliable as long as the HMHEC concentration is not too low.

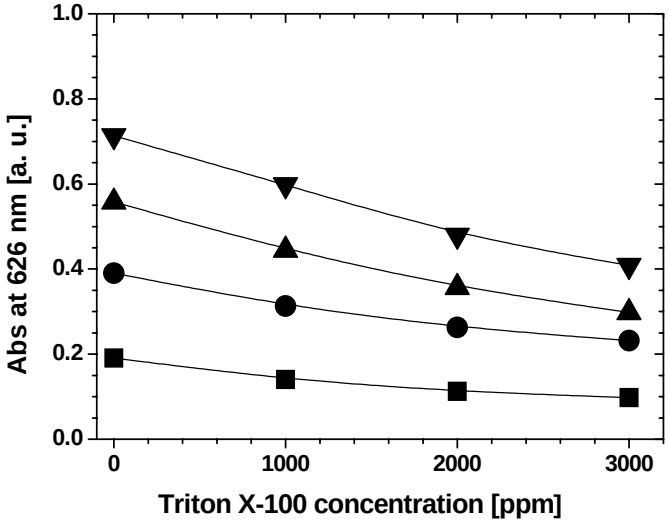

Figure 2.4: Calibration curves for the interference of Triton X-100 on the absorbance at 626 nm for HMHEC in the anthrone method. The HMHEC concentrations from bottom to top are 100, 200, 300 and 400 ppm, respectively.

2.4.5 Rheological Characterization

The solution viscosity was measured using a Haake RS75 rheometer with a DC50 temperature controller (water circulating bath). A double concentric-cylinder (DG41) geometry or a cone-and-plate (C60/4, cone diameter and angle are 60 mm and 4°) fixture was used to carry out the measurements, depending on the solution viscosity and shear rate range. To illustrate, diagrammatic representation of a cone-and-plate fixture and a double gap fixture[46] is shown in Figure 2.5 and Figure 2.6. After loading, each sample was kept at rest for 10 min before measurement to eliminate the mechanical history. It was found that a steady shear flow could be reached within 120 sec at each shear stress or shear rate. A thin silicone oil layer was applied to some samples, which required long measurement time, to prevent

evaporation.

For the dynamic oscillatory shear test, a stress sweep was conducted to ensure the linear viscoelasticity before the frequency sweep was started. To illustrate the oscillation test, we use the schematic representation of the cone-and-plate fixture shown in Figure 2.5 to present the very basic theory for the measurement. For the C60/4 fixture (cone diameter and angle are 60 mm and 4°), a gap distance of 0.14mm was fixed to carry out the measurements. This makes sure a constant shear rate at all points within the material, which is the most interesting feature of this geometry, especially when it comes to the study of highly non-Newtonian fluids such as high molecular weight polymers, as is our polymer of interest, HMHEC.[47]

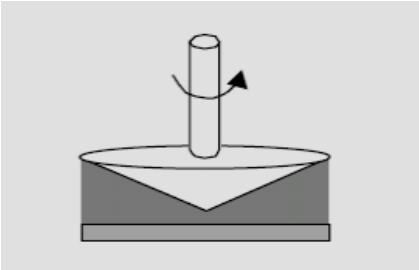

Figure 2.5: Diagrammatic representation of a cone-and-plate fixture used for rheological tests.

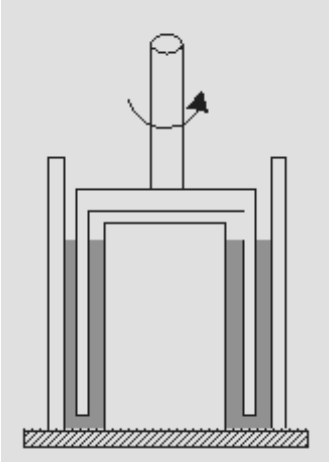

Figure 2.6: Diagrammatic representation of a double gap fixture used for rheological tests.

A sample volume of 4 ml was used. The test material is being held between a plate of radius R and a cone of angle α_0. Sample loading must be carefully done to

ensure the space between the cone and the plate is just filled up, without any spilling (see Figure 2.5). The dynamic oscillatory test is conducted by introducing a sinusoidal-wave of stress or strain. The resulting strain or stress should also be sinusoidal provided that the applied stress is well in the linear viscoelastic range, but a phase lag is expected for viscoelastic materials. The rheometer RS75 can only operate in the controlled stress mode for dynamic tests, and the corresponding principle, is illustrated as follows,

$$\sigma(t) = \sigma_0 \cos(\omega t) \tag{2.1}$$

where σ_0 is the amplitude of the stress, and ω is the angular frequency with the unit of rad/second. The resulting strain is measured by the rheometer and should also possess a sinusoidal form:

$$\gamma(t) = \gamma_0 \cos(\omega t - \varphi) \tag{2.2}$$

where γ_0 is the amplitude of the strain produced by the applied stress, and φ is the phase angle ranging from 0 to π/2.

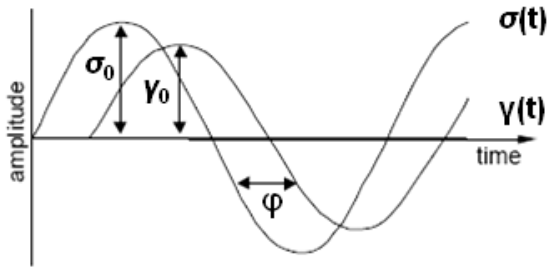

Figure 2.7: Sinusoidal wave forms for stress and strain functions in typical dynamic oscillatory shear test.

For a perfect solid, the strain $\gamma(t)$ is in phase with the stress $\sigma(t)$, thus φ =0. For a purely viscous liquid, in contrast, the stress is out of phase with the strain, but in phase with the strain rate $\dot{\gamma}$, which is the time derivative of the strain:

$$\dot{\gamma} = \frac{d\gamma(t)}{dt} = \frac{d[\gamma_0 \cos(\omega t - \varphi)]}{dt} = \omega\gamma_0 \cos(\omega t - \varphi + \frac{\pi}{2}) \tag{2.3}$$

Therefore the phase lag for a purely liquid is π/2. Since the behavior of a viscoelastic material is between these two extreme cases, the phase lag will lie in between 0 and π/2 at small strain or stress (to ensure within the linear viscoelatic range).

The ratio σ_0 / γ_0 and the phase angle φ are material properties, both of which depend on the applied oscillation frequency ω, a main feature of linear viscoelasticity. In other words, the viscoelasticity of a material describes how the two functions behave at different time scales. Because of the sinusoidal nature, it is more convenient to use a complex function to express the stress:

$$\sigma^* = \sigma_0 \exp(i\omega t) \tag{2.4}$$

and the corresponding complex strain will be

$$\gamma^* = \gamma_0 \exp[i(\omega t - \varphi)] = \gamma_0 \exp(i\omega t)\exp(-i\varphi) \tag{2.5}$$

where $i = \sqrt{-1}$. With the above expressions, the complex shear modulus $G^*(\omega)$ is defined as

$$G^*(\omega) = \frac{\sigma^*}{\gamma^*} = G'(\omega) + iG''(\omega) \tag{2.6}$$

where G' and G'' are the storage and loss moduli, associated with elasticity and viscosity of a material, respectively. Substituting (2.4) and (2.5) into (2.6) yields:

$$G^*(\omega) = \frac{\sigma^*}{\gamma^*} = \frac{\sigma_0 \exp(i\omega t)}{\gamma_0 \exp(i\omega t)\exp(-i\varphi)} = \frac{\sigma_0}{\gamma_0}\exp(i\varphi) \tag{2.7}$$

Therefore G*(ω) can be experimentally determined from oscillatory shear measurements by performing a frequency sweep, so can G' and G".

The experimental techniques and pitfalls in measuring and interpreting rheological properties are detailed in many classical texts, and are therefore not repeated here.[48-50]

2.4.6 Conductivity Measurement

Stock solutions of HMHEC and HEC were prepared following the same procedure as described in 2.4.1. Dialysis of the polymer solutions against pure water

for one week was found necessary to remove the inherent ions (the polymer powder contains ions due to the manufacturing process) to a negligible amount. Then the polymer concentration after dialysis was determined by a Total Organic Carbon (TOC) analyzer. The stock solution was then collected and diluted to various concentrations with a certain amount of salt stock solution to be mixed. The mixed solutions were stirred and left overnight to ensure they were well mixed. Conductivity measurement was then conducted at 25 °C by a Schott conductivity meter (Lab960 set).

CHAPTER 3 Clouding and Phase Behavior of Nonionic Surfactants in HMHEC Solutions

In this chapter, the thermodynamic properties, in particular, clouding phenomena and phase behavior of two nonionic surfactants, Triton X-114 and Triton X-100, in the presence of either hydroxyethyl cellulose or hydrophobically modified counterpart (HMHEC) were experimentally studied. The focus is on the effect of hydrophobic modification of HMHEC. We first present the results on how the CPT of surfactant is affected by the presence of both polymers, followed by the two-phase separation. An interesting three-phase separation phenomenon was reported for the first time in some HMHEC/Triton X-100 mixtures at high enough surfactant concentrations in the last section of the results in this chapter. Before the experimental results are presented, relevant literature is reviewed.

3.1 Early Investigations into the Phase Behavior

The foundations of today's activities on mixed polymer/surfactant systems were developed in work carried out in two separate areas. The first, in the 1940s and 1950s, involved protein (and, to a lesser extent, acidic polysaccharide) and synthetic ionic surfactant pairs. The importance of electrical forces of attraction was easy to recognize, with the interaction generally referred to as "binding" of the charged surfactant with the macromolecule and an awareness of changes in the conformation of protein molecules during the binding process was developed.[51] The second, in the 1950s and 1960s, involved water soluble synthetic polymers which were uncharged and surfactants which were charged. In the second case, the sites for binding of the surfactant molecules on such polymers were less easy to identify, but the notion of "binding" of the former persisted in this case also. In the last two decades, growing attention has been paid to the great importance of hydrophobic modification in the polymer in promoting interactions with surfactants.[52] The hydrophobic substitution entities can be as small as methyl groups, but usually they are C_{12} to C_{20} aliphatic

chains, as was discussed in the Introduction.

Despite numerous studies on the effect of hydrophobic interaction on CPT of nonionic surfactant/HMP mixtures, lesser attention has been paid to the properties of the separated macroscopic phases. There exists quite limited literature on the process and properties of macroscopic phase separation after the CPT is reached for mixtures of associative polymer and surfactant.

An HMP/surfactant mixture may undergo an associative phase separation into a phase enriched in both the polymer and surfactant and a very dilute water phase. Although the surfactant concentration in the latter phase is thought to be equal to or below its CMC, little experimental evidence has been reported in the literature. Unlike electrostatics for oppositely charged polymer and ionic surfactant, the attractive interaction responsible for the associative phase separation of a mixture of neutral HMP and nonionic surfactant is primarily of hydrophobic nature.

In contrast, a mixture of an unmodified neutral polymer and a nonionic surfactant usually segregates in two phases, each of which is rich in one of the solutes. Phase separation takes place at a temperature slightly above CPT, which can depend strongly on the mixture composition.[14] In a review article by Piculell and Lindman,[15] they proposed two terms, *segregative phase separation*, and its counterpart *associative phase separation*, to describe the existing experimental results on the phase separation behavior of polymer/surfactant mixtures. A wide range of studies supporting the proposed mechanism of phase separation could be found on charged HMP/surfactant mixtures[16-18] and also on neutral HMP/surfactant mixtures[19-20] in the last two decades.

3.1.1 Neutral Polymer/Surfactant Mixtures

The interactions between nonionic surfactant and neutral water soluble polymer are usually very weak or even nonexistent, except for the excluded volume effect. Examples of such polymers are poly(vinyl alcohol), PEO, poly(vinylpyrrolidone), and cellulose analogues.[21-22] However, these polymers at high concentrations do exert noticeable effects on lowering the cloud point of surfactants (oligoethylene glycol

ether, CxEy series).[23-24] The observed CPT decrease was explained by depletion flocculation because of the excluded volume interaction, leading to a segregative phase separation into a polymer-rich phase and a surfactant-rich phase. It should be noted that in the absence of surfactant, the above polymers, such like PEO and some cellulose analogues, in aqueous solutions can also turn turbid by heating.

The cloud point temperature (CPT) of a pure surfactant solution,[53] which in principle depends on the length of EO chain, the size and structure of hydrophobic tail. The cloud point temperature has been found to increase with increasing number of EO units, decreasing hydrocarbon tail and increasing degree of branching.[53] Also, the surfactant concentration can affect the cloud point. Right above the cloud point, the solutions will separate into a surfactant-lean and a surfactant-rich phase; the latter involves micellar aggregation.

3.1.2 Associative Polymer/Surfactant Mixtures

A different scenario arises for hydrophobically modified polymers. Attractive interaction between the surfactant hydrophobic tails and the hydrophobes of the polymers leads to unusual phase/clouding behaviors[5-8] and interesting rheological properties.[8-10] Thuresson and Lindman studied the phase separation behaviors of EHEC and HMEHEC with addition of $C_{12}E_5$ and $C_{12}E_8$.[5] They found that the CPTs of the nonionic surfactants were lowered in the presence of either polymer. The authors also measured phase volumes after phase separation at 25 °C, which indicated a segregative phase separation for EHEC, but associative separation for HMEHEC. Note that a pure HMHEC solution used here never turns cloudy upon heating up to 95 °C, unlike the HMEHEC, the CPT of which is found to be ~39 °C in Thuresson and Lindman's work.[5]

For hydrophobically end-capped polyethylene oxide (an uncharged telechelic HMP), Alami *et al*.[54] investigated the effect of addition of C_xE_y on the CPT of HMP. In their experiments, the HMP solution showed a clouding behavior, even in the absence of surfactant, owing to a phase separation into a dilute and a concentrated polymer solution. The latter contains an extended transient polymer network with

hydrophobic nodes. In addition, they found that the presence of nonionic surfactant can decrease the CPT of the HMP, and ascribed this behavior to the stabilization of the network and nodes. Appell *et al*.[55] also observed such a declination and attributed it to an additional intermicellar attraction due to chain bridging inferred from small angle neutron scattering. A schematic of the concept of chain bridging is shown in Figure 3.1.

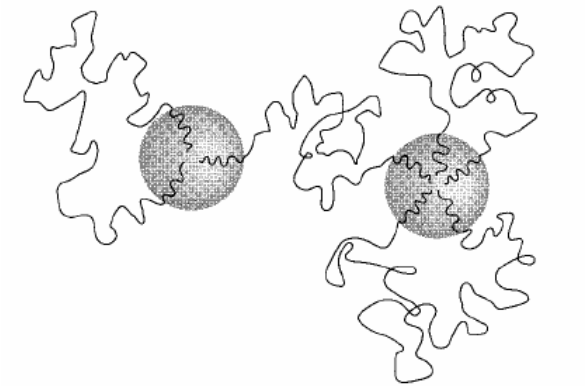

Figure 3.1: Schematic representation of the chains of PEO bridging two micelles. The spheres are the micelles (or the hydrophobic core).[55]

Robb et al.[19] studied the two-phase separation of hydrophobically modified hydroxyethyl cellulose (HMHEC)/4-(1,1,3,3-tetramethylbutyl) phenyl-polyethylene glycol (trade name as Triton X-100, abbreviated as TX100 thereafter) mixtures at room temperature and high surfactant concentrations (>15wt%). For such high TX100 concentrations, the hydrophobes of HMHEC were thought to be saturated with surfactant and thus behave like its unmodified analog, hydroxyethyl cellulose (HEC), leading to a segregative phase separation. It will be shown later in this chapter that the surfactant concentration for producing a three-phase separation must fall within a certain range.

For HMHEC with nonionic surfactant, the results in this chapter will show the HMHEC solution may separate into three macroscopic phases when the temperature is raised above the CPT. In addition to the water-rich phase and the cloudy phase, a bluish translucent phase emerges some time later as the bottom phase.

This interesting behavior is not fully clear, in particular with respect to the phase separation kinetics, the composition in each phase and the mechanism. To seek a better understanding, in the present chapter, we also carried our investigation on the three-phase separation behavior of HMHEC aqueous solutions in the presence of TX114 or TX100. We focused on the time evolution of phase volume fractions and the composition in each of the phases. The total organic carbon measurement was compared with the anthrone reagent method, which could obtain more accurate HMHEC concentrations. The details of this method have been given in Section 2.4.4 in Chapter 2.

The phase behavior of a mixture of charged hydrophobically modified polymer and nonionic surfactant and the corresponding rheology have also been investigated.[55-57] It was reported that the solution may undergo thermal gelation by heating and become very viscous, thanks to a transition to large vesicles bridged by the polymer chains.

3.2 Results and Discussion

3.2.1 CPT curves of nonionic surfactant with polymer

Figure 3.2 and Figure 3.3 plot the observed CPT *vs.* surfactant concentration. Since the lowest temperature investigated was 10 ^{o}C, some mixtures at low surfactant concentrations already turned cloudy at this temperature, and thus no data were shown. The addition of polymer lowers the CPT of the surfactant solution, similar to the observation in prior studies.[9, 58] The extent of CPT decrease, however, depends on the polymer species. When HEC is added, the CPT is decreased by at most 4 to 5 °C in the present study. This behavior is in remarkable contrast to that for the HMHEC cases, where the lowering of CPT can be as large as about 20°C for TX114 and 50°C for TX100 at low concentrations. Otherwise the magnitude of CPT decrease becomes comparable for both polymers.

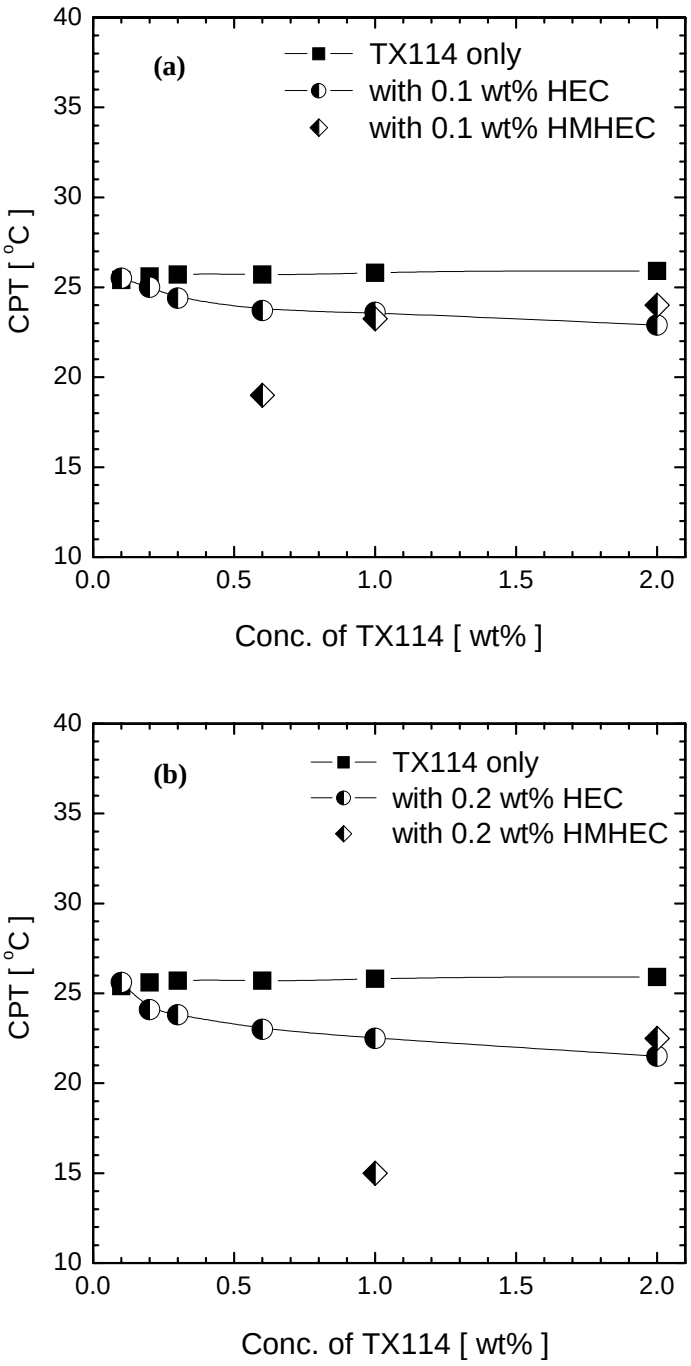

Figure 3.2: Cloud point temperature of TX114 with addition of (a) 0.1 wt% HEC or HMHEC; (b) 0.2 wt% HEC or HMHEC.

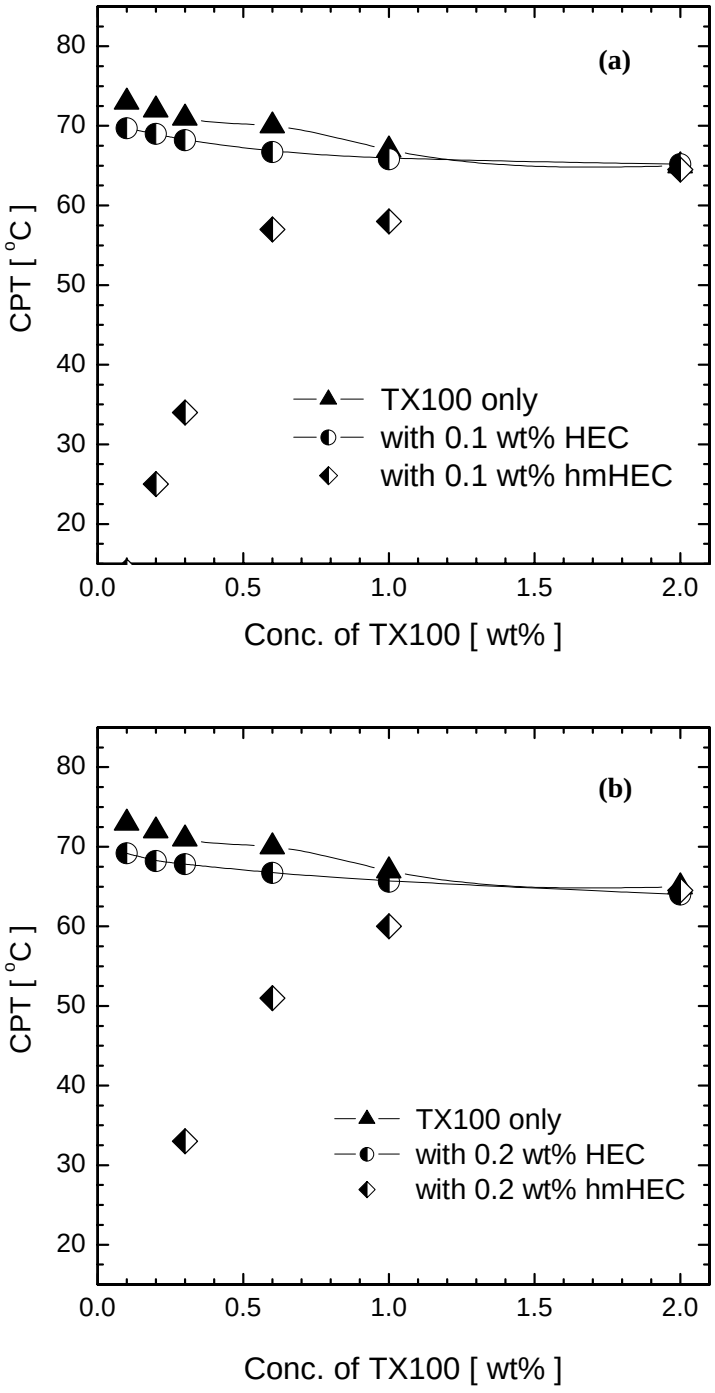

Figure 3.3: Cloud point temperature of TX100 with addition of (a) 0.1 wt% HEC or HMHEC; (b) 0.2 wt% HEC or HMHEC.

The parent polymer, HEC, has no strong molecular interaction with surfactant except for the excluded volume effect,[15, 59] thereby leading to a depletion flocculation for the micelles and a segregative phase separation.[60] In the present study, the CPTs

for both surfactant species are slightly lowered by HEC, since the polymer concentration is only 0.2 wt% and no strong effect can result. Piculell *et al*.[61] found that the weak short-ranged van der Waals interactions between the surfactant head groups and polymer backbone also influenced the segregative phase separation. This effect, however, is not expected in our case.

For the cases with added HMHEC, hydrophobic interaction plays a crucial role in the phase behavior.[6,22] Surfactant molecules can bind onto the hydrophobes of the polymers to form mixed micelles.[5,6,17, 62,63] Each mixed micelle contains several hydrophobes either from a chain or from different chains. At sufficiently low surfactant concentrations, nearly all surfactant molecules are associated with the polymer hydrophobes. At high enough surfactant concentration, such binding reaches a saturation point, beyond which free micelles are expected to coexist with the mixed micelles.

A dramatic decrease of CPT was previously reported by Appell *et al*.[7] for mixtures of $C_{12}E_6$ and hydrophobically end-capped PEO (see Fig. 2 in their paper). Below but near the cloud point, they detected an attractive interaction between micelles from small-angle neutron scattering (SANS) and attributed it to some of the polymer chains, each of which linked two mixed micelles on its ends. A similar bridging behavior can be expected for HMHEC as each chain contains about 10 hydrophobes. As a result, the solution can turn cloudy at a lower temperature. At the higher surfactant concentration (2 wt%), the free micelles greatly outnumber the mixed micelles, and therefore the CPT almost approaches the value of the pure surfactant solution at the same concentration.

3.2.2 Two-Phase Separation

Right at CPT, a pure TX100 solution became cloudy quite sharply, but no macroscopic phase separation could be seen immediately. Microscopically, the micellar coalescence was ongoing, leading to a size increase for the dispersed droplets of the second phase with a high surfactant concentration.[64-66] The consequent light

scattering gave rise to the cloudiness. After 2 to 3 hours, the droplets eventually formed a clear, bluish macroscopic phase below the water-rich phase. Using UV analysis, the measured TX100 concentration in each phase is shown in Table 3.1. To check the measurement accuracy, we assumed an equal density for both phases, and used the measured concentration in the top phase and phase volumes to calculate the concentration in the bottom phase. A comparison between the last two columns finds a good agreement. The measured TX100 concentration in the top phase is about an order of magnitude higher than the reported CMC (~130ppm), similar to the behavior reported by Maclay,[67] and by Strey for $C_{12}E_6$.[68]

Table 3.1: Surfactant concentration analysis for pure TX100 solutions after complete phase separation at 70 °C (98h).

TX100 [wt%]	bottom phase height [cm]	Total height [cm]	conc. $_{top}$ by UV [wt%]	conc. $_{bott}$ by UV [wt%]	Conc. $_{bott}$ [a] [wt%]
2	0.85	10.0	0.052±0.006	23.5±0.2	23.6±1.2
4	1.70	10.0	0.043±0.004	23.9±0.1	23.9±0.6

[a] The bottom phase concentration of TX100 is calculated from the measured surfactant concentration in the top phase using mass balance.

For the surfactant-HEC mixtures, we observed two macroscopic phases after 2 to 3 hours, when the temperatures were kept at 28 and 71°C for TX114/HEC and TX100/HEC, respectively. These temperatures were no more than 3°C above the highest CPT for the mixtures investigated here. After 24 hours, the volumes of the two phases remained constant, and were then measured. Figure 3.4a&b show the volume fraction of the bottom phase as a function of the total surfactant concentration. Note that the heavy phase was transparent but bluish, similar to the appearance of the surfactant-rich phase for a pure TX100 solution. When the total HEC concentration is doubled, the volume of the bottom phase hardly changes, because the segregative phase separation causes most of polymer molecules to locate in the light phase.

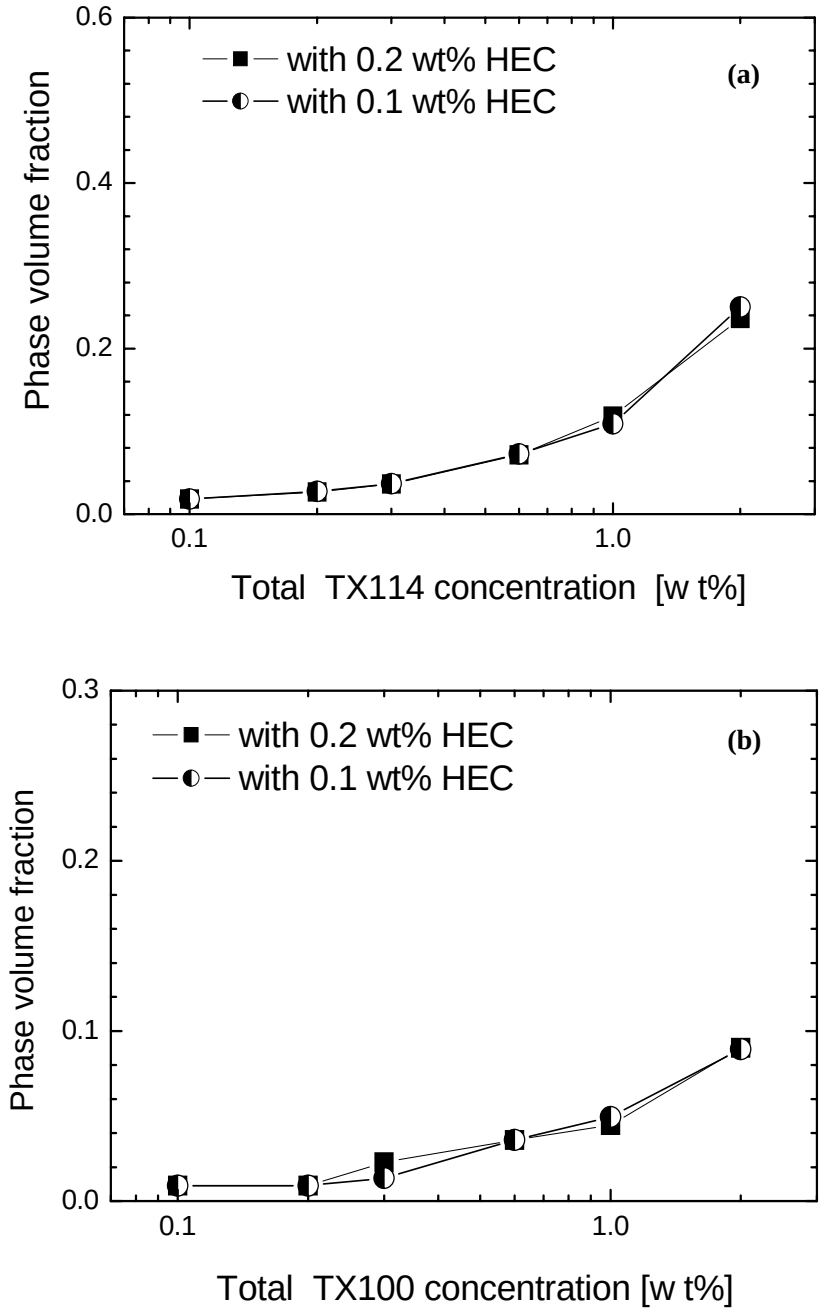

Figure 3.4: Volume fraction of the macroscopic heavy phase for (a) TX114 solutions, (b) TX100 solutions, in the presence of HEC.

The surfactant concentration in the upper phase was determined by UV spectrophotometry. The volume of the bottom phase at low total surfactant concentrations became very small and difficult to handle. Hence, its concentration was calculated instead on the basis of mass balance and an equal density for both phases. The surfactant concentrations in the two phases are plotted against the total

surfactant concentration in Figure 3.5a&b It can be found that the surfactant stays more favorably in the heavy viscous phase.

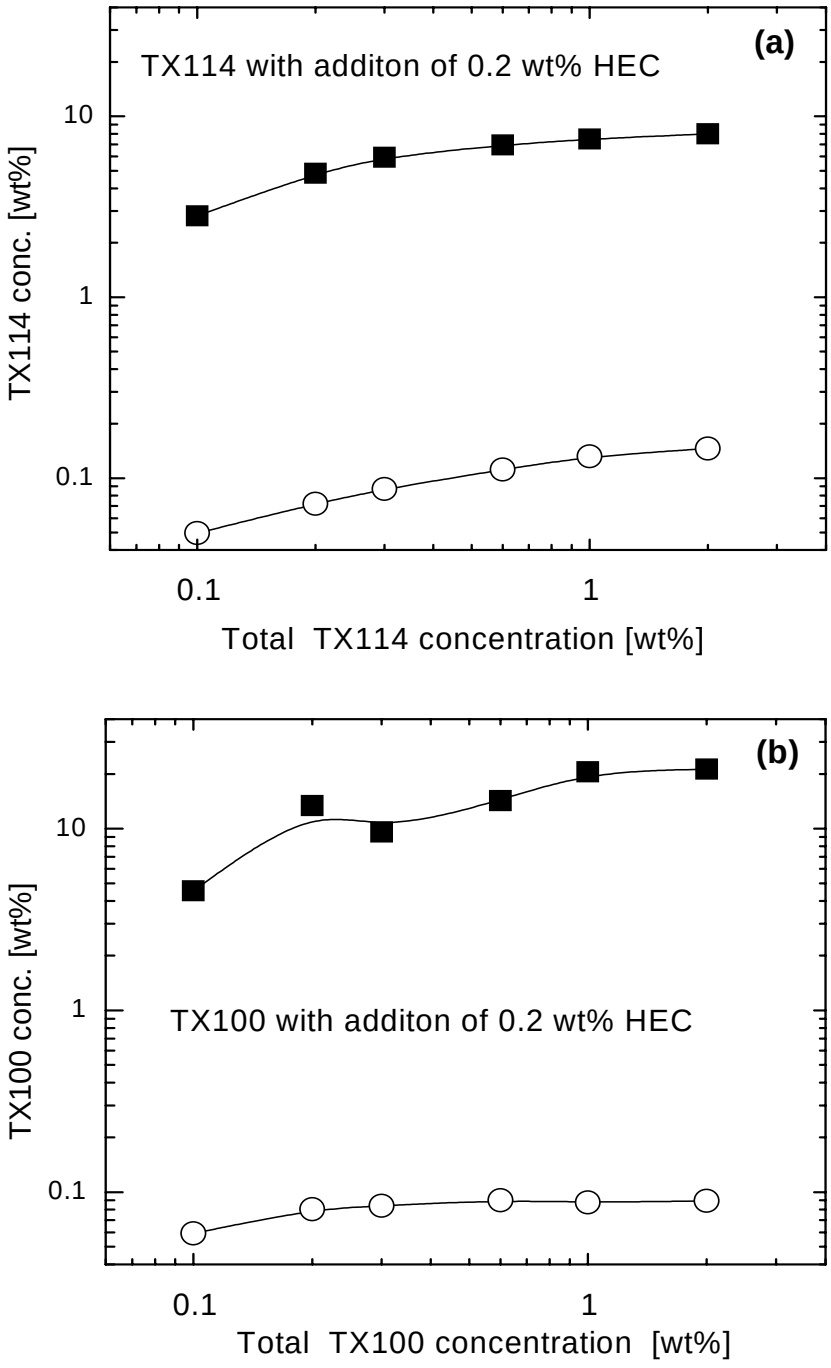

Figure 3.5: Concentration of surfactant in the top clear phase (open symbols) and the bottom clear bluish phase (closed symbols) after separation for mixtures with 0.2 wt% HEC; (a) TX114, (b) TX100.

The HEC concentration in the light phase is presented in Figure 3.6. The measured concentration is always close to or even higher than the total concentration. For the heavy phase, only two cases were attempted because of its small volume. On the basis of mass balance, the calculated HEC concentrations in the heavy phases are -0.04±0.05 wt% and 0.04±0.03 wt% for TX114 at total concentrations 1 and 2 wt%, respectively. The relatively big uncertainty and negative value comes mainly from: (a) a ±5% uncertainty in the measured HEC concentration in the top phase, (b) the inaccuracy in the bottom phase height readings, and (c) a minute quantity of HEC in the bottom phase. Nevertheless, such analyses along with the results in Figure 3.5 and Figure 3.6 suffice to suggest the occurrence of segregative phase separation.

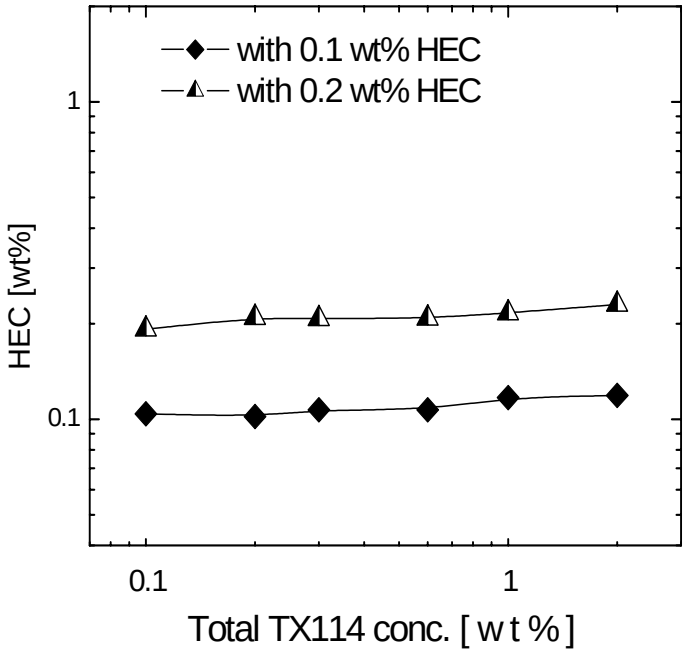

Figure 3.6: Concentration of HEC in the top phase for TX114 solutions with addition of HEC.

For HMHEC/surfactant mixtures, when the total surfactant concentration was no larger than 1 wt%, two bulk phases formed at a temperature slightly higher than CPT, and the phase volumes hardly changed after 24 hours. Interestingly, the heavy phase, in contrast to the HEC case, remained cloudy for up to 2 weeks, the maximum observation time in the present study.

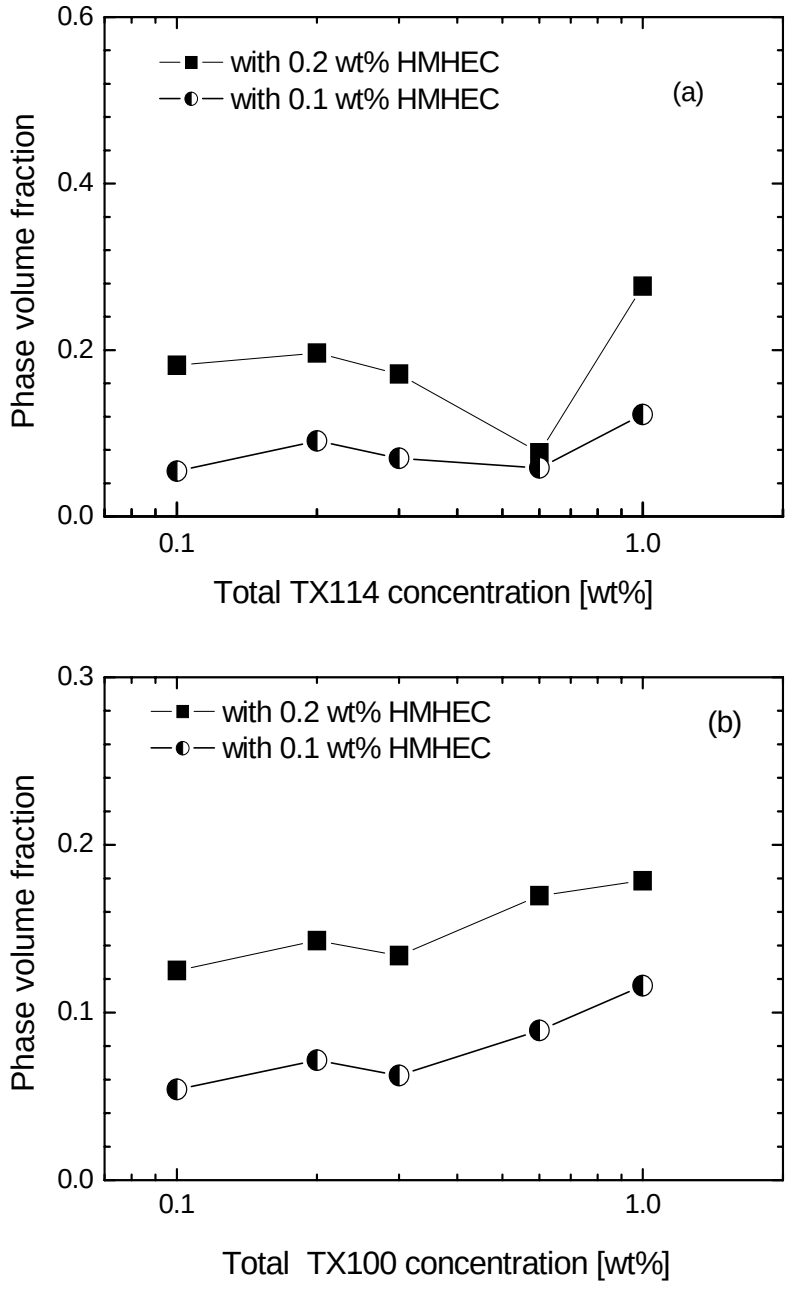

Figure 3.7: Volume fraction of the macroscopic heavy phase for (a) TX114 solutions; (b) TX100 solutions, in the presence of HMHEC.

The measured volume fraction of the heavy phase as a function of total surfactant concentration is presented in Figure 3.7. One can see that except one case, the volume of the bottom phase increases substantially as the HMHEC concentration is doubled, implying a considerable amount of HMHEC staying in the heavy phase.

Although the phase volume fractions shown in Figure 3.7 might not really represent the equilibrium values, they hardly changed during our observation period.

The persistent turbidity of the heavy phase manifests very slow droplet coalescence, because the heavy phase was very viscous, as opposed to the light clear phase having a low viscosity only about twice the value of water.[8] This finding further supports our thought that more HMHEC is in the heavy phase. It is interesting to note that the separated cloudy phase observed here is different from the stable colloidal phase for nonionic surfactant mixed with ionic surfactant, prior to the normal clouding, due to electrostatic repulsion.[64-66]

The results of surfactant concentrations for the HMHEC/surfactant mixtures with two coexisting macroscopic phases are shown in Figure 3.8. It is interesting to note that for TX114 in 0.2wt% HMHEC, the weak local maximum of TX114 concentration in the heavy phase seen in Figure 3.8a occurs at the total TX114 concentration equal to 0.6 wt%, for which an unexpected small volume fraction also results as shown in Figure 3.7a. Comparing the results in Figure 3.5 and Figure 3.8, we find that the partition of surfactant between the two phases is more uneven for HEC than for HMHEC; the surfactant concentration ratio of heavy to light phase for HEC is about an order of magnitude higher than for HMHEC.

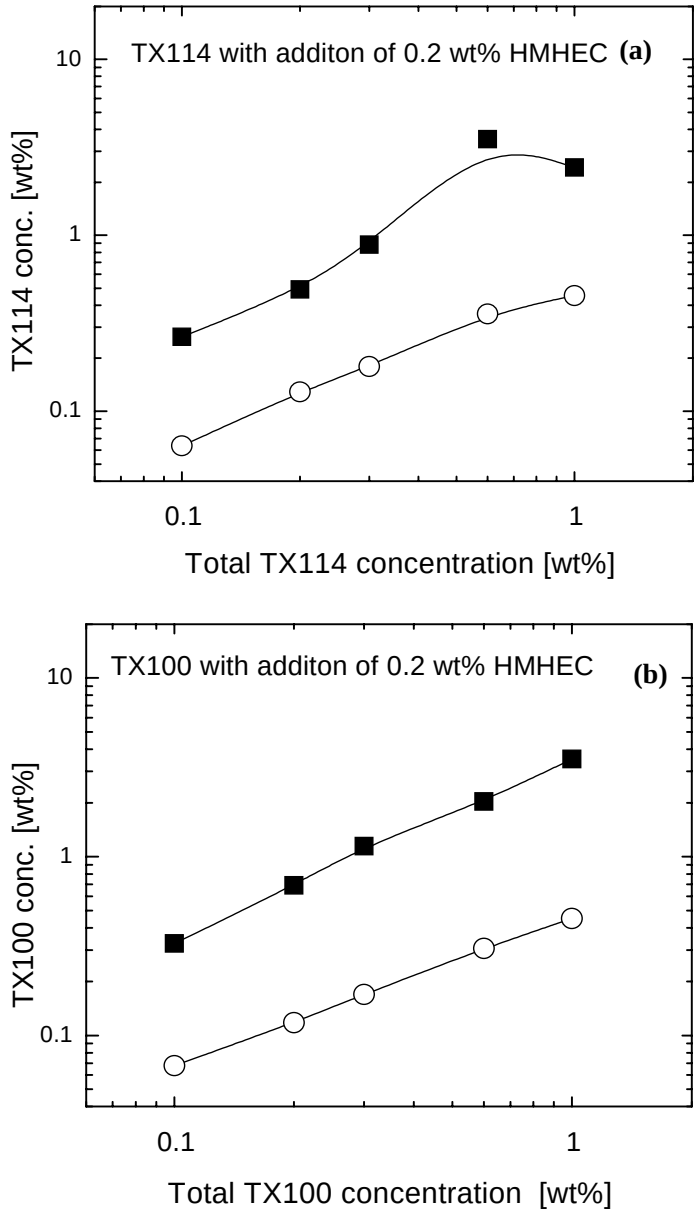

Figure 3.8: Concentration of surfactant in the top clear phase (open symbols) and the bottom cloudy phase (closed symbols) for 0.2 wt% HMHEC; (a) TX114, (b) TX100.

3.2.3 Three-Phase Separation

When the total TX100 concentration was 2 wt% or higher, a third phase, which appeared clear but bluish, started to emerge from the bottom of the test tube 2 to 3 hours after the formation of the two macroscopic phases. To our best knowledge, no similar observation has yet been reported in the literature. The new phase

continued to grow at the expense of the middle cloudy phase, until the phase volumes no longer showed any noticeable changes after 2 days, whereas the volume of the top clear phase only changed slightly towards its final value during this period. In fact, this 3-phase separation phenomenon was also observed for end-capped PEO/TX114 and HMHEC/TX114, despite no results shown here. Figure 3.9 shows a photo for a typical three-phase separation sample.

3.2.3.1 Composition analysis by TOC method

The composition results (by TOC method) for two cases 0.2wt% HMHEC + 2wt% TX100 and 0.2wt% HMHEC + 4wt% TX100 are shown in Table 3.2. It can be clearly seen that the bottom phase has the highest surfactant concentration, while the top phase has the lowest. Assuming a constant density for the three phases, the surfactant mass percentages in the three phases were estimated and presented in the fourth column. One can find that less than 10% of surfactant exists in the top phase. An indirect method was used to determine the polymer concentration in each phase from total carbon analysis (TOC) by subtracting the surfactant contribution obtained based on the UV measurement. For the middle and bottom phases, the results show quite a large uncertainty, arising primarily from the inherent large mass ratios of TX100 to HMHEC. This can be understood by the following analysis. With the average relative error in the TOC being about 6% determined from all of our measurements, the mean uncertainty in the total carbon concentration (around 70ppm) in the middle phase can be found to be 4ppm. Since the mass ratio of TX100 to HMHEC is about 7:1, the carbon concentration of HMHEC is 10±4ppm, leading to a large relative error in the calculated HMHEC concentration. The uncertainty gets even worse in the bottom phase because of a larger TX100-HMHEC mass ratio. In fact, the calculated negative HMHEC concentrations together with the clear bluish phase imply that there should exist very little or virtually no polymer in the bottom phase.

Table 3.2: Composition analysis of two samples showing three phase separation.

	height [cm]	TX100 [a] [wt%]	distribution	HMHEC [b] [wt%]
0.2wt% HMHEC + 4wt% TX100				
Top phase	6.6±0.1	0.21±0.04	4%	0.19±0.01
Middle phase	1.5±0.1	5.9±0.1	24%	1.0±1.4
Bottom phase	1.4±0.1	18.1±0.4	72%	-0.02±0.4
0.2wt% HMHEC + 2wt% TX100				
Top phase	7.5±0.1	0.25±0.01	9%	0.10±0.01
Middle phase	1.4±0.1	6.4±0.3	45%	0.7±0.5
Bottom phase	0.6±0.1	15.0±1.8	46%	-0.41±1.2

[a] The surfactant concentration was determined by UV.

[b] The polymer concentration in each phase was measured by total carbon analysis, subtracting the contribution from the surfactant.

Figure 3.9: A photo showing the three coexisting macroscopic phases for the sample of 0.2 wt% HMHEC+4 wt% TX100.

In the cloudy phase, free micelles coexisted with the mixed micelles. Some of the free micelles appeared to gradually separate from the cloudy phase to form the clear phase at the bottom of the test tube, while the polymer remained in the middle phase in the form of mixed micelles. The later emergence of the third phase implies that the free micelles diffuse very slowly through and away from the cloudy viscous phase. The

actual mechanism is unclear yet. It must be pointed out that the three-phase compositions do not necessarily represent the true equilibrium positions, because the observation time was one week for the two samples studies here.

3.2.3.2 Phase Separation Kinetics

In this study, the concentration range for HMHEC is 0.05-0.5 wt%, while that for surfactant is 1-6 wt%. We find that at a given HMHEC concentration, separation into three macroscopic phases can occur when the surfactant concentration is high enough. Note that without HMHEC, there are only two phases formed after separation. Figure 3.10 and Figure 3.11 show the phase separation kinetics for four samples at different HMHEC concentrations with 6 wt% TX100 and 6 wt% TX114, respectively. These results were experimentally obtained by measuring the height of the separated macroscopic phases with a ruler, at different time points up to a maximum of 10 days. We find that the bottom phase emerges some time after the formation of the top and middle phases, and the time lag is substantial at high HMHEC concentrations. The phase heights (or equivalently the volume fractions) hardly change to a measurable extent after 7 days for all the samples except for two with 6wt% TX114 and HMHEC at 0.3 and 0.5 wt%, respectively. The bottom phase volume of the latter case has not yet even reached a constant value after 10 days. It is noted that the temperature driving force within the batch of 4 samples differs because the CPT is different. However the trend of the separation kinetics is not affected since the sample with higher HMHEC concentration separated rather slower. In light of the slowness of phase separation at high HMHEC concentrations, we limit the polymer concentration to be no higher than 0.5 wt%.

The clouding phenomenon and the ensuing phase separation have been attributed to substantial aggregation of free and mixed micelles,[64-65] leading to the formation and growth of droplets, which are rich in surfactant and polymer and big enough to scatter light strongly. The slow phase separation observed in this work is thought to arise from the high viscosity of HMHEC solutions because the droplets must diffuse to encounter each other and get coalesced so as to gradually become a continuous phase. Figure 3.12 presents a photo of the separated phases of the

solutions with 6 wt% TX114 and various HMHEC concentrations. The picture was taken against a black background in order to achieve good contrast. The middle phase appears persistently cloudy even after two weeks, resembling the appearance of the cloudy phase for the case of two-phase separation of HMHEC/TX114 mixture at lower surfactant concentration. The bottom phase, which is clear and bluish, has a similar appearance to the surfactant-rich phase obtained from a pure surfactant solution above its CPT. The top phase is a water-like phase. Although the phase heights after 7 days appear to remain constant for the cases with lower global HMHEC concentrations, these phases may not represent the true thermodynamic equilibrium state, implied by the persistent cloudiness of the middle layer.[14] Also, the species polydispersity and heterogeneity could lead to fractionation into more phases for a longer time. In our study, some samples were indeed observed even up to three months, and the relative phase volumes still remained unchanged.

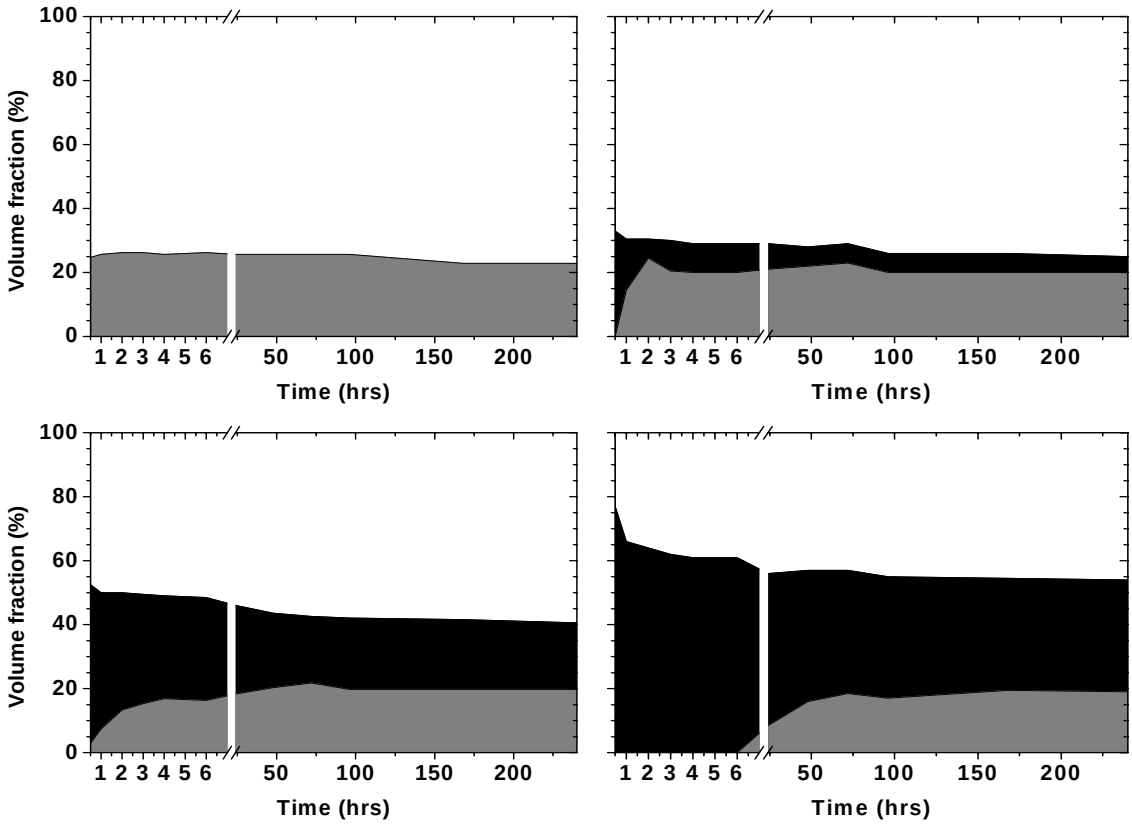

Figure 3.10. Evolution of phase volume ratio for four samples at 6 wt% TX100 and different HMHEC concentrations: 0.0 wt% (top left), 0.1wt% (top right), 0.3wt% (bottom left), 0.5wt% (bottom right). The temperature is 70 °C.

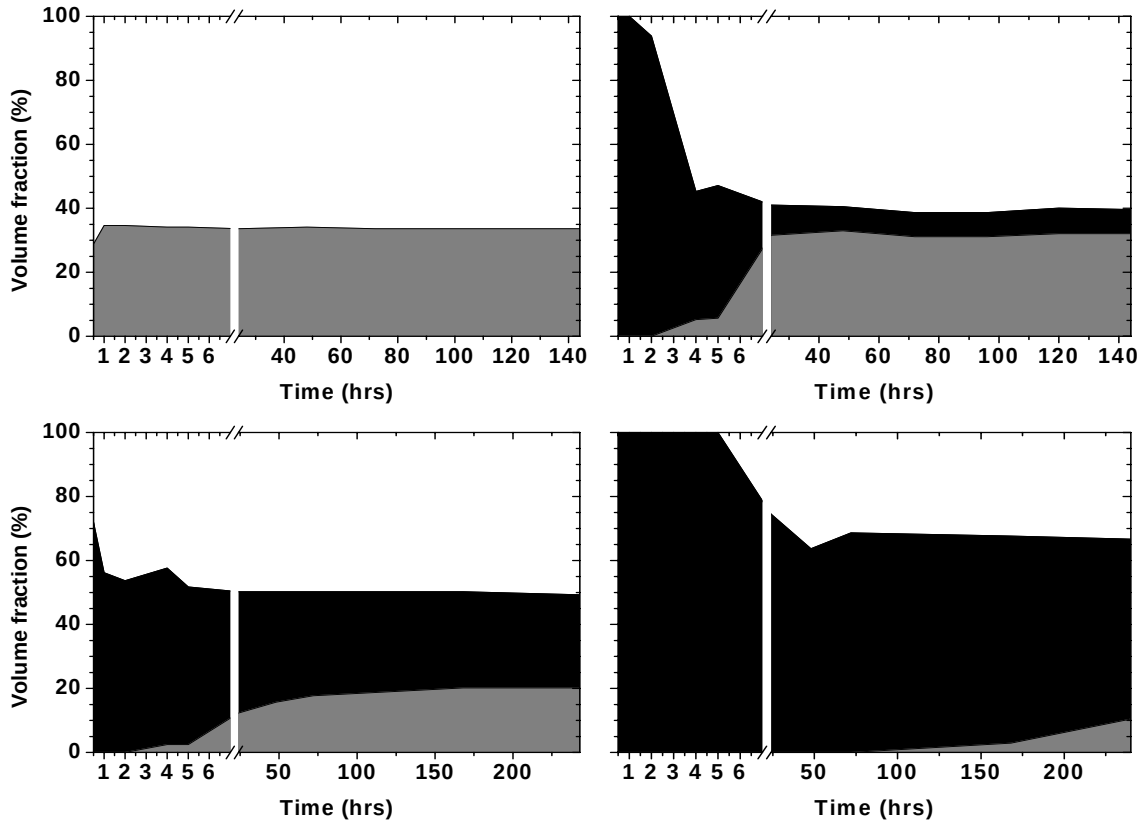

Figure 3.11: Evolution of phase volume ratio for four samples at 6 wt% TX114 and different HMHEC concentrations: 0.0 wt% (top left), 0.1wt% (top right), 0.3wt% (bottom left), 0.5wt% (bottom right). The temperature is 35 °C.

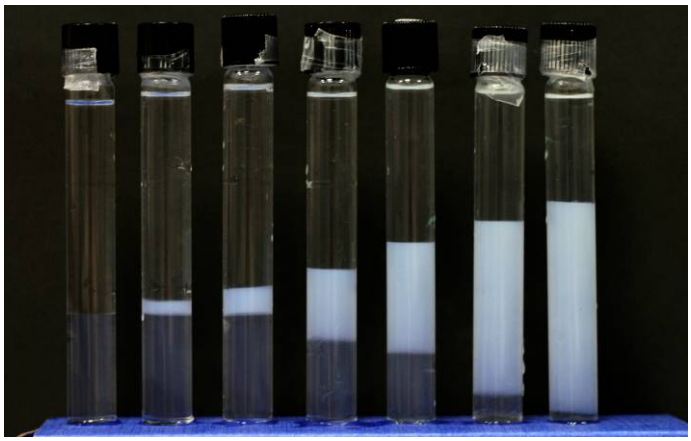

Figure 3.12: A photo of the three-phase separation for 6 wt% TX114 and HMHEC at various concentrations: 0, 0.05, 0.1, 0.2, 0.3, 0.4, and 0.5 wt% (from left to right). The picture was taken after 7 days at 35 °C, when the individual phase heights no longer changed (except for the first two samples from the right).

3.2.3.3 Phase Volume Fraction

It is interesting to observe from Figure 3.12 a certain relation between the phase heights and the global HMHEC concentration. Our previous study on two samples (0.2 wt% HMHEC with addition of 2 wt% TX100 and of 4 wt% TX100, respectively) has found that the global surfactant concentration affects the volume of the bottom phase, but not the middle.[14] To systematically explore the possible correlations, we plot the volume fractions of the middle and bottom phases against the normalized global surfactant concentration for the cases of TX100 and TX114 at several global HMHEC concentrations on the 7th day of phase separation in Figure 3.13 and Figure 3.14, respectively. We find from Figure 3.13a and Figure 3.14a that at each of the global HMHEC concentrations, the volume fraction of the bottom phase changes linearly with the global surfactant concentration, with the slope being similar to that for the corresponding case of pure surfactant solutions without polymer. Also, all the slopes in the figures fall within a narrow range (4~5), where the global surfactant concentration has been normalized by the 100-fold CMC, implying that the bottom

phase volume could be primarily determined by the micelle concentration.

As mentioned earlier, a three-phase separation requires a high enough surfactant concentration. The critical concentration can indeed be estimated from the intersection of the curves with the abscissa in Figure 3.13a and Figure 3.14a, depending on the HMHEC concentration. For the middle phase, we can see from Figure 3.13b and Figure 3.14b that its volume fraction appears nearly independent of the global surfactant concentration when the global HMHEC concentration is fixed.

Figure 3.15 and Figure 3.16 plot the volume fractions of the bottom and middle phases versus the global HMHEC concentration at 6 wt% TX100 and TX114, respectively. A striking feature can be noticed that the volume fraction of the middle phase increases linearly with the HMHEC concentration, whereas that of the bottom phase decreases with polymer concentration, more significantly for TX114 than for TX100. The trend of the phase volume fractions shown in Figures 3.13~3.16 together with the observed phase appearances suggests a strong likelihood that a majority of polymer stays in the middle phase, while most of surfactant exists in the bottom phase.

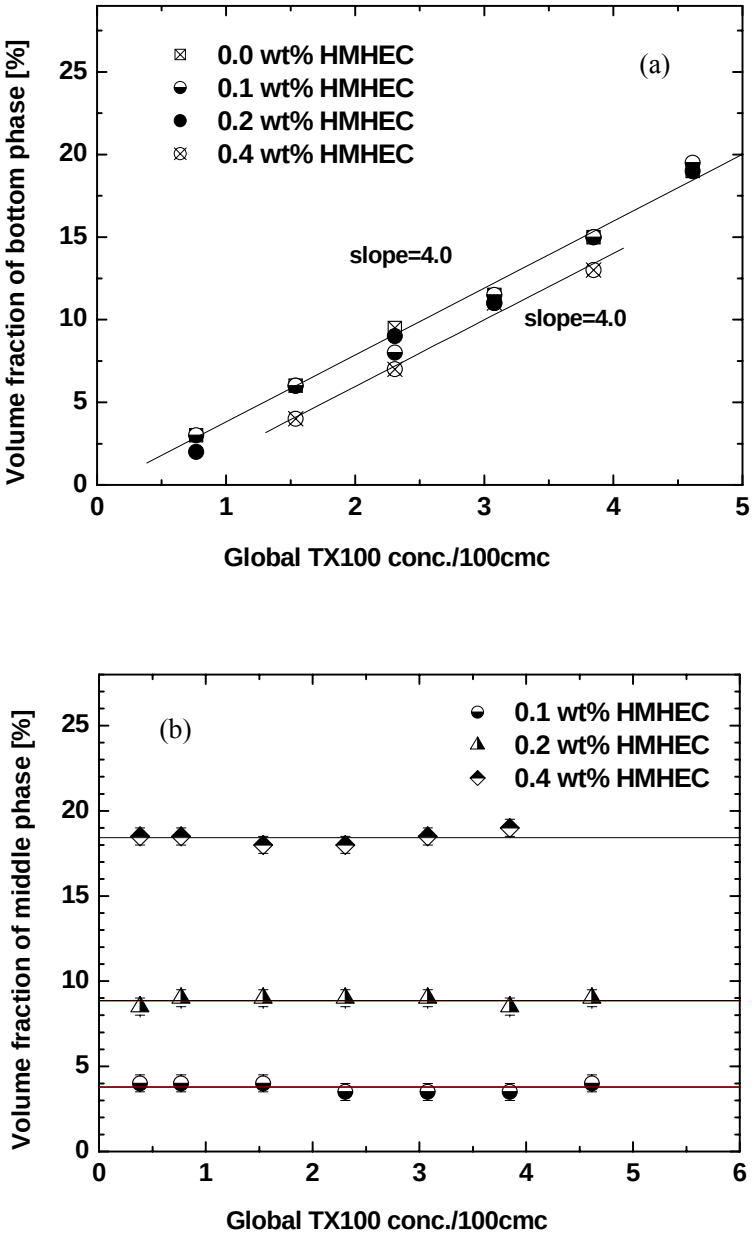

Figure 3.13: The volume fraction of (a) the bluish (bottom) phase and (b) the cloudy (middle) phase versus the global surfactant concentration normalized by the surfactant's cmc for HMHEC/TX100 mixtures at 75 °C after 7 days. The volume fraction of the bluish phase for the pure surfactant solutions after phase separation was also included for comparison.

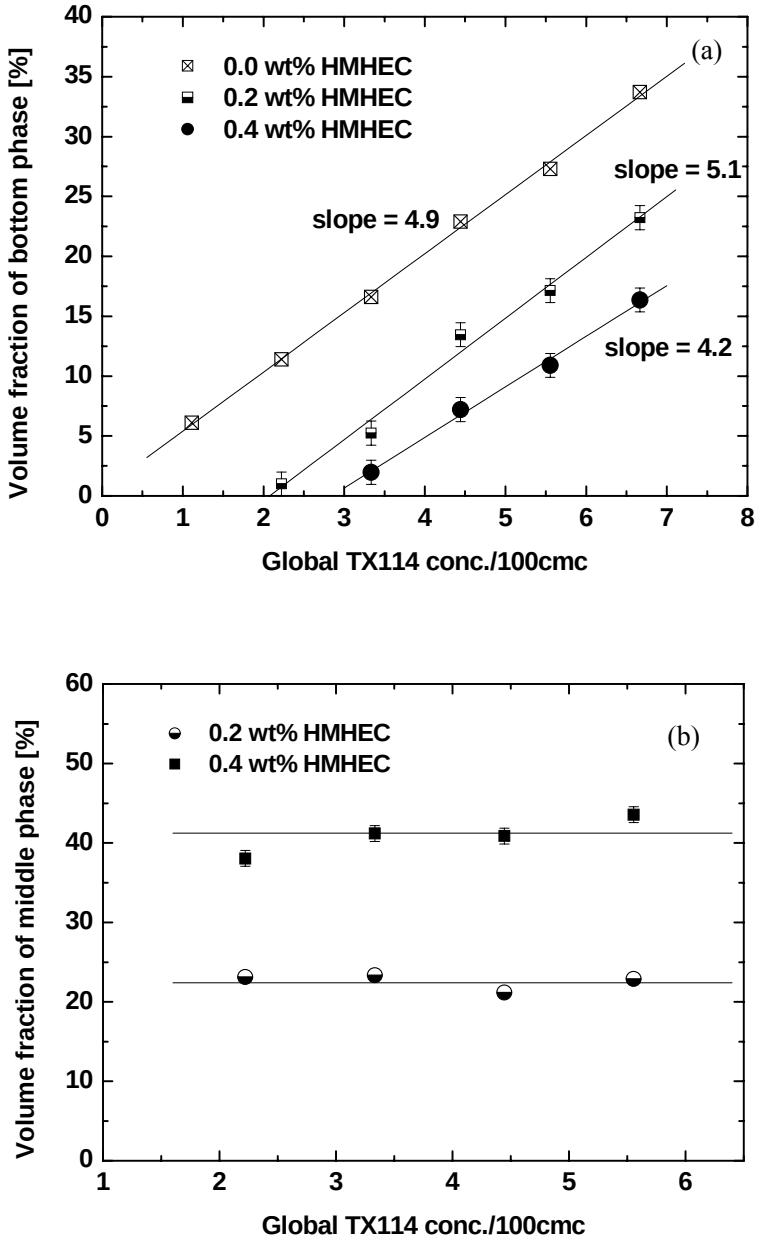

Figure 3.14: The volume fraction of (a) the bluish (bottom) phase and (b) the cloudy (middle) phase versus the global surfactant concentration normalized by the surfactant's cmc for HMHEC/TX114 mixtures at 35 °C after 7 days. The volume fraction of the bluish phase for the pure surfactant solutions after phase separation was also included for comparison.

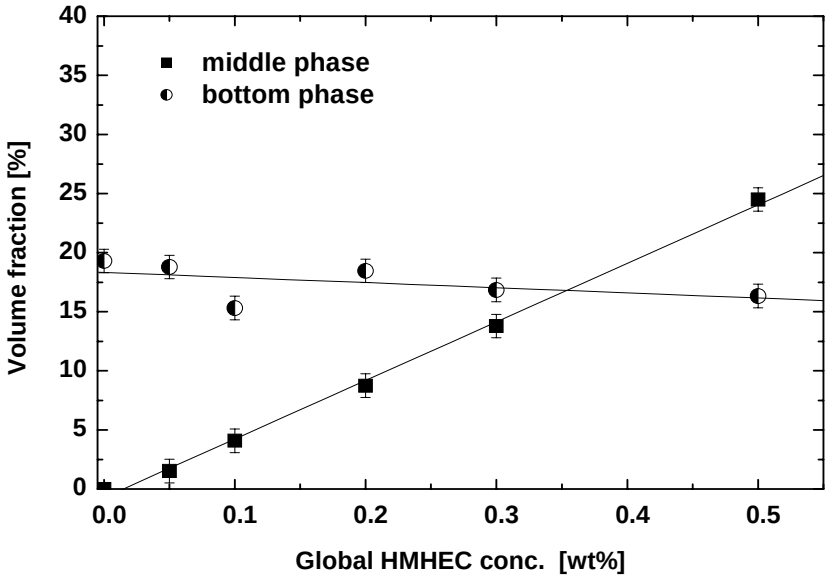

Figure 3.15: The volume fractions of the bluish (bottom) phase and the cloudy (middle) phase versus the global HMHEC concentration for 6 wt% TX100 at 75 °C after 7 days.

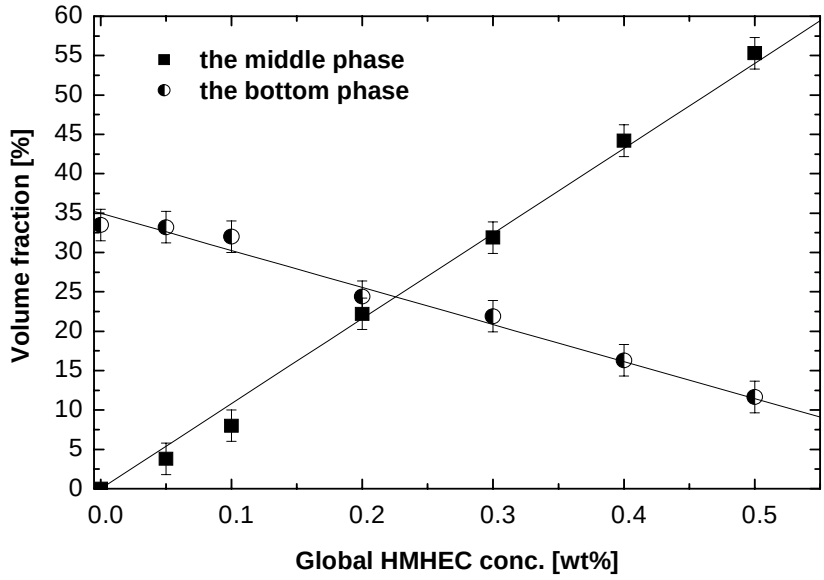

Figure 3.16: The volume fractions of the bluish (bottom) phase and the cloudy (middle) phase versus the global HMHEC concentration for 6 wt% TX114 at 35 °C. The measurement was done after 7 days except for the two samples at 0.4wt% and 0.5wt% HMHEC, which were analyzed on the 10th day due to their slower separation process.

3.2.3.4 Composition Analysis by Anthrone Method

To verify the above argument, it is necessary to determine the composition in each phase. In 3.2.3.1, we used UV-Vis spectrophotometry to first determine the surfactant concentration, which was then used together with total organic carbon (TOC) analysis to indirectly calculate the HMHEC concentration. Unfortunately, the obtained polymer concentration in the bottom phase could become negative and was thus not as accurate. Here, we adopt the anthrone reagent method, which has been very successful in determination of cellulose concentration in the absence of surfactant.[42-44] The data of both species from the composition analysis are shown in Table 3.3 for HMHEC/TX100 mixtures at 70 °C.

It is found that the surfactant and polymer concentrations are the highest in the bottom and the middle phase, respectively. In the middle layer, the HMHEC falls within the range of 1.03-1.25 wt% (1.1 wt% on average), while the surfactant concentration ranges from 5.1 to 5.9 wt% (5.5 wt% on average). We note that the low HMHEC concentration in the bottom phase cannot be determined precisely due to the high surfactant concentration (~23.6 wt%). The value of 0.1 wt% shown in Table 3.3 is an estimated upper limit. The difficulty and limitation of the anthrone reagent method will be elaborated as follows.

As mentioned in Experimental Methods Section in Chapter 2, we find in the course of composition analysis that the presence of surfactant changes the UV-Vis spectrum of HMHEC when using the anthrone reagent method. The absorbance peak at 626 nm representing the HMHEC, due to the formation of furfural compounds in strong sulfuric acid,[45] is weakened, while a second peak comes out at 504 nm. The latter emerges only when the solution contains both HMHEC and surfactant. This interference problem has never been reported in the literature prior to the present study.

In order to accurately determine the HMHEC concentration, we calibrated the weakening effect of the surfactant on the 626nm peak of the polymer at various surfactant concentrations, as shown in Figure 2.4. However, when the surfactant concentration becomes very high and the HMHEC concentration becomes very low

such like on the order of 100ppm, the HMHEC peak can be suppressed substantially, making the concentration determination very difficult. Moreover, to analyze the bottom phase, an aliquot extracted must be diluted at least 20 times to avoid the interfering scattering of UV/Vis by free surfactant micelles since the surfactant concentration before dilution is too high (~23.6 wt%). Such a dilution renders the HMHEC concentration too low to be detected. The upper limit for HMHEC concentration shown in Table 3.3 is estimated by (1) preparing several mixture solutions at a surfactant concentration comparable to that in the bottom phase after dilution (~1 wt%), with gradually decreased low polymer concentrations, and (2) testing these solutions to see if the HMHEC signal remains detectable. Since measuring the polymer concentration using the anthrone reagent method involves several steps, only three solutions were analyzed in this study with the results shown in Table 3.3.

Table 3.3: Composition analysis for samples of HMHEC/TX100 mixtures that show three-phase separation at 70 °C.

0.2%hmHEC+4%TX100	Height [cm]	HMHEC [wt%]	TX100 [wt%]
Top phase	7.3	0.10±0.01	0.20
Middle phase	1.3	1.03±0.07	5.9
Bottom phase	1.4	< 0.1 [a]	23.4
0.3%hmHEC+6%TX100			
Top phase	6	0.13±0.01	0.31
Middle phase	1.9	1.23±0.11	5.1
Bottom phase	2	< 0.1[a]	23.9
0.4%hmHEC+4%TX100			
Top phase	6.2	0.16±0.02	0.33
Middle phase	2.6	1.12±0.12	5.1
Bottom phase	1.2	< 0.1 [a]	23.5

[a] Estimated upper limit. (Details on how it is estimated are described in the text Section 4.2.3)

Because of a comparatively small quantity of surfactant in the top phase as shown in Table 3.3, the critical concentration at the x-axis intercept in Figure 3.13a and Figure 3.14a mentioned earlier also reflects the amount of surfactant present in

the middle phase, which is associated with the surfactant-to-polymer ratio in the mixed micelles. We find that the surfactant mass in the middle phase is higher for TX114 than for TX100. This could be explained by the difference in aggregation number for mixed micelles. Around the cloud points, the aggregation number for TX114 is supposed to be larger than for TX100, due to the smaller hydrophilic head of TX114 and its higher sensitivity to temperature.[69-71] Namely, it is easier for TX114 molecules to pack themselves around hydrophobes.

Figure 3.17 plots the effect of the global HMHEC concentration on the surfactant concentrations in the individual separated phases for TX114 with its global concentration kept at 6 wt%. For pure TX114 solutions, the bottom phase after separation is bluish, translucent, and contains 17.9 wt% TX114, representing a surfactant-rich micellar solution, according to the phase diagram of TX114 reported in the literature.[72] In contrast, the top phase is a clear surfactant-lean phase with about 0.02 wt% TX114, which is still higher than the CMC.[14,67-68] In the presence of HMHEC, the surfactant solutions show a three-phase separation with a cloudy phase in the middle when compared to the case of a pure surfactant solution.

As can be seen from Figure 3.13, the volume fraction of the middle phase is small when the global HMHEC concentration is low, and thus it is not easy to take out a sufficient amount for analysis. In view of this difficulty, we analyzed the middle phase only for three samples. It can be found from Figure 3.17 that the surfactant concentration in the middle phase lies between 7.1 and 9.8wt%, while the bottom phase has a nearly constant surfactant concentration, similar to the value of 17.9 wt% for the case of a pure surfactant solution. In contrast, the top phase is surfactant lean, where the surfactant concentration increases with the global polymer concentration. Note that the top phase is a dilute polymer solution with the concentration dependent on the global polymer concentration (see Table 3.3). It may indicate occurrence of polymer fractionation as pointed out by Tsianon et al.,[73] who studied the segregative phase separation behavior of a mixture of ethyl hydroxyethyl cellulose (EHEC) and

its modified counterpart HMEHEC, and reported significant fractionation of HMEHEC into the EHEC rich phase due to its polydispersity and heterogeneity. A similar situation could happen to our HMHEC sample with polydispersity index~4.5. The nearly linear increase of the surfactant concentration in the top phase with the global polymer concentration can be accounted for by a constant amount of surfactant bound to each polymer molecule.

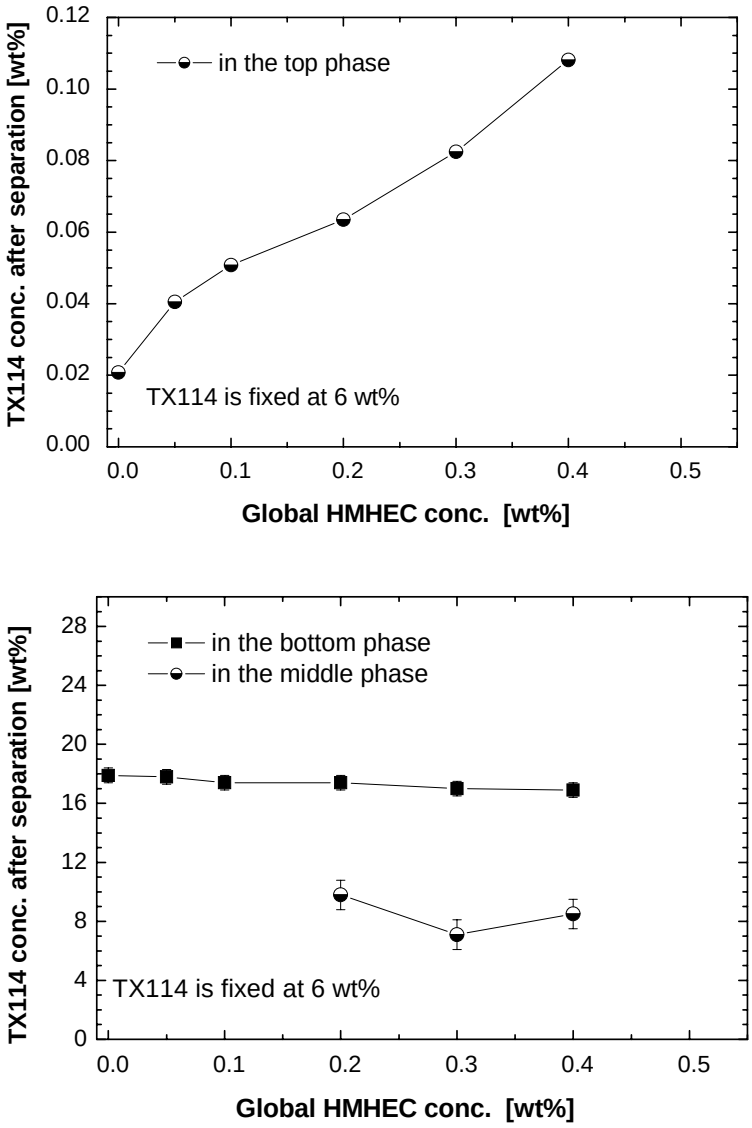

Figure 3.17: TX114 concentrations in the separated phases versus the global HMHEC concentration for the global TX114 concentration fixed at 6 wt%. The analysis was done at 35 °C after 7 days, except for the sample of 0.4wt% HMHEC done after 10 days. For 0.05 wt% and 0.1 wt% HMHEC, the middle phases were too small to be extracted for analysis.

The considerable surfactant concentration in the middle phase can be explained by the association between HMHEC and surfactant. The hydrophobes ($-C_{16}H_{33}$) attached to the backbone of HMHEC can attract the hydrophobic tails of nonionic surfactants to form mixed micelles.[5, 74] The binding between the surfactant molecules and the hydrophobes can reach a saturation point, beyond which any further addition of surfactant to the HMHEC solution leads to formation of free micelles.

When CPT is reached, the solution undergoes an associative phase separation. Our results have found that a majority of HMHEC stays in the cloudy phase, and therefore must take up a considerable amount of surfactant to form mixed micelles. When the global surfactant concentration is high enough, a portion of surfactant originally staying in the cloudy phase in the form of free micelles will aggregate and diffuse away slowly, and hence the new phase (bottom phase) emerges some time later. It can be explained by existence of saturated HMHEC which enhances free micelle aggregation and thus leads to a segregative phase separation.[19] The diffusion is very slow due to the presence of HMHEC, giving rise to a high viscosity in the middle phase. From Table 3.3, the surfactant-to-hydrophobe ratio is estimated to be about 450 in the middle phase for TX100/HMHEC mixtures at 70 °C. For comparison, the aggregation number for micelles in pure TX100 solution at 10mM (or 0.63 wt%) is about 100 at room temperature,[75] and should increase with temperature.[76] Since the surfactant and HMHEC concentrations do not vary much in the middle phase as shown in Table 3.3 and Figure 3.17, we can justify why the middle phase volume fraction increases almost linearly with increasing global HMHEC concentration with a fixed global surfactant concentration, as shown in Figure 3.15 and Figure 3.16. On the contrary, the volume fraction of the bottom phase decreases with increasing global HMHEC concentration because more surfactant is taken up by the middle phase. In view of the slow diffusion of free micelles away from the middle phase, we do not know whether any free micelles remain trapped at the end of the observation period.

For a truly ternary system at constant temperature and pressure, the maximum number of coexisting phases is three, according to the Gibbs phase rule. As such, the

compositions of all three phases are fixed because of no degree of freedom left. Changing the global composition can only lead to changes in the phase volumes. The mixtures investigated in this study are not a truly ternary system because of species polydispersity and heterogeneity, and thus fractionation is highly likely to occur. However, according to the composition analysis in Table 3.3 and the linear behavior shown in Figures 3.13 ~3.16, they behave rather similarly to a ternary system.

3.3 Conclusions

Nonionic surfactant shows different clouding and phase separation behavior, depending on the added polymer species. Compared with HEC, HMHEC can strongly lower the cloud point temperature of nonionic surfactants at low surfactant concentrations. A chain bridging effect is responsible for the larger decrease of the CPT by HMHEC, while added HEC exerts a much weaker effect on CPT via depletion flocculation. The composition analyses in various formed macroscopic phases suggest a segregative phase separation for HEC, while an associative phase separation occurred for HMHEC.

A macroscopic three-phase separation has been reported for the first time in some mixtures of HMHEC/TX100. This new phenomenon was systematically studied. Within the surfactant concentration range investigated in the present study, the three-phase separation is found to occur when the surfactant concentration is high enough. The interesting phase behavior can be accounted for by an initial associative phase separation responsible for the formation of the clear and cloudy phase, followed by the occurrence of a segregative phase separation in the cloudy phase, leading to the ensuing emergence of the bluish bottom phase. The three phases can persist for some time at least as long as 14 days. Our composition analysis finds that most of polymer remains in the middle cloudy phase with nearly constant concentration, while the bottom phase is surfactant rich also at almost constant concentration. In view of species polydispersity and heterogeneity, the possibility for fractionation of species into various phases cannot be ruled out.

To gain a better understanding and mechanistic interpretation of the 3-phase separation, one can explore the microstructure of each phase to find out how micelle growth affects phase separation. For the nonionic surfactant-polymer mixtures, Piculell et al. have studied the effect of the micellar size on the segregative phase separation.[61] They found that the two-phase area increases with increasing micellar size and polymer molecular weight. In the present study, the micellar size is expected to grow with increasing surfactant concentration and temperature for TX114 and TX100. Our observation that the emergence of the third phase requires a sufficiently high surfactant concentration implies a necessity of sufficient micellar sizes for the possible ensuing segregative phase separation. It is worth investigating microscopic details and mechanisms for this system in the future. Possible experimental techniques are small angle neutron scattering and fluorescence.

CHAPTER 4 Nonionic Surfactant and Temperature Effects on the Viscosity of Hydrophobically Modified Hydroxyethyl Cellulose Solutions

After gaining a knowledge of the phase behavior of mixtures of HMHEC and nonionic surfactant in Chapter 3, the viscosity behavior of HMHEC solutions were subsequently investigated experimentally, focusing on nonionic surfactant and temperature effects in this chapter. The nonlinear rheology is then addressed in the next chapter.

4.1 Literature Review

The main feature of a hydrophobically modified polymer, or associative polymer, is association between hydrophobes, which can be either interchain or intrachain. At sufficiently high polymer concentration, a dramatically high viscosity can be attained because of the formation of a gel-like structure arising from the dominant intermolecular association.[2] The hydrophobic association may be enhanced or weakened by an imposed flow, depending on the flow strength and polymer concentration.[3] The hydrophobic association is also affected by the presence of surfactant via interactions of various kinds, such as the hydrophobic interaction, and the electrostatic interaction. For a mixture of uncharged HM polymer and nonionic surfactant, the most important interaction is hydrophobic binding between the HMP hydrophobes and the surfactant tails to form so called “mixed micelles”.[4]

At low surfactant concentration, this binding enhances the interchain association for gel-like HMP solutions, leading to an increase in viscosity.[25-28] Further addition of the surfactant can result in an increased number of mixed micelles, each of which however contains hydrophobes in a decreased number[25-28]. As a result, the viscosity will reach a maximum and then decrease. With excess surfactant, each hydrophobe will eventually be masked by a mixed micelle, leading to disappearance of the

hydrophobe links and formation of free micelles. This behavior is reflected by a nearly constant viscosity since the HMP has been saturated with surfactant and the free micelles exert a very small effect on the viscosity (if the free micelles are still spherical, not wormlike). For ionic surfactant, the electrostatic repulsion between the mixed micelles can affect the polymer conformation and the corresponding gel microstructure, thus the viscosity behavior.[26-28]

The temperature effect on the flow dynamics of a charged HMP-surfactant mixture was examined by Tirtaatmadja et al.[77] While the viscosity showed an Arrhenius behavior in their work, a recent study from our lab on mixtures of hydrophobically modified hydroxyethyl cellulose (HMHEC) and a nonionic surfactant Tergitol 15-S-7 found that the viscosity may slightly increase with temperature.[10]

In this chapter, we examine the effects of nonionic surfactant and temperature on the viscosity behaviors of HMHEC, which was related to the phase behavior, in an attempt to seek the correlation between molecular interactions and flow behavior.

4.2 Results and Discussion

4.2.1 Temperature Effect on Pure HMHEC Solutions

We first examine the behavior of surfactant free HMHEC solutions. Using the same HMHEC as in this study, Maestro et al.[2] measured the interfacial tension of polymer water solutions and toluene to deduce a very low critical aggregation concentration (CAC) of about 0.0004 g/dL, or 4ppm. They also measured the reduced viscosity of HMHEC at various concentrations and found that the reduced viscosity exhibited a sharp increase at about 0.15 g/dL, which is comparable to the value reported for shorter HMHEC (Mw = 300,000 g/mol) by Nishikawa et al.[78] For dilute solutions (<0.15 g/dL), Nishikawa et al. also carried out fluorescence probe experiments to conclude that the aggregation number of HMHEC micelles should be on the order of 10 or less. It can thus be inferred that when the HMHEC concentration is between 0.0004 g/dL and 0.15 g/dL, small aggregates, each of which consists of a few polymer chains, are formed due to hydrophobe linking/hydrophobic interaction,

somewhat similar to the flower micelles of a telechelic HMP (such as HEUR). At 0.15 g/dL, the aggregates start to associate to form a gel (network), analogous to the loop-to-bridge transition of a telechelic HMP. [78]

Figure 4.1 plots the viscosity of 0.4 wt% HMHEC solutions against shear rate at various temperatures. Note that this concentration is higher than 0.15 g/dL, implying a certain extent of gelation in the absence of flow. Typically, the viscosity at a given shear rate is found to decrease with increasing temperature. It can also be seen that weak shear thickening takes place at moderate shear rates, followed by shear thinning. A similar behavior was also observed for 0.35 wt% and 0.5 wt% solutions from our experiments, although the results are not shown here. The intriguing shear thickening phenomenon of HMHEC at intermediate shear rates, which was previously noticed by Maestro *et al*. for 0.5 wt% solution,[3] is attributed to the shear enhanced interchain association of hydrophobes as the imposed flow elongates and aligns the polymers to promote the intermolecular bridging via the hydrophobic interaction. The shear thickening of HMHEC will be discussed in great detail in the next chapter.

In a stronger flow, however, the links can be disrupted and thus the solution becomes shear thinned. It can be found from Figure 4.1 that the thickening behavior shifts to lower shear rates at lower temperatures. Since hydrophobes possess a lower thermal energy at a lower temperature, a weaker flow suffices to promote interchain association and also the hydrophobes involved are more unlikely to escape the resulting associate.

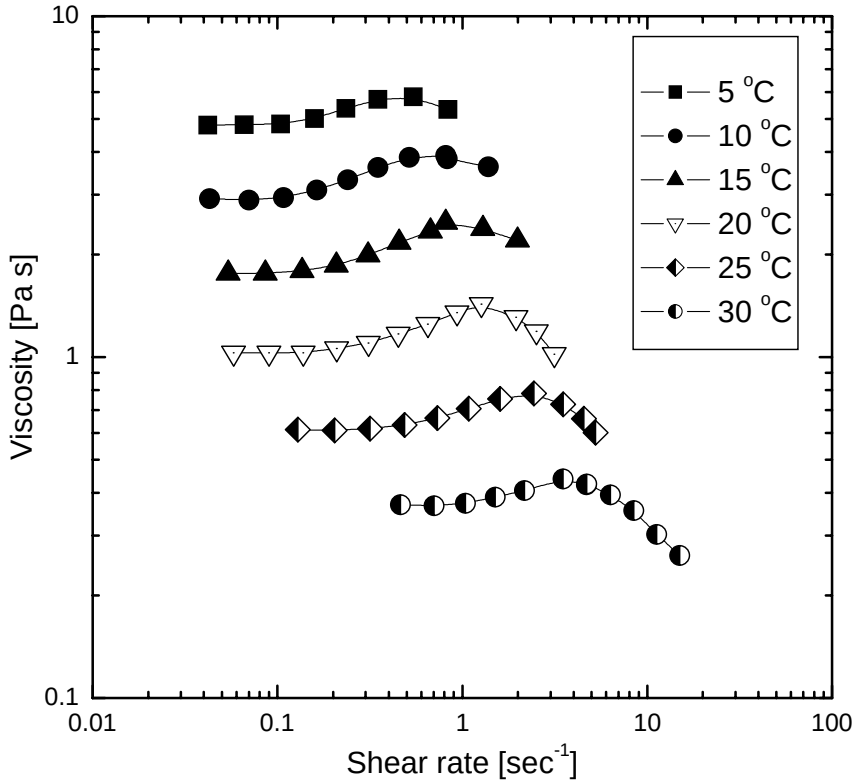

Figure 4.1: Steady-state flow curve of pure 0.4 wt% HMHEC at various temperatures.

Figure 4.2 plots the flow curves of 1wt% HMHEC solutions at various temperatures. In contrast to the behavior of 0.4wt% solutions, no shear thickening is observed in the shear rate range investigated. The different behavior can be understood because at high enough concentrations, HMHEC molecules already entangle substantially, leading to a considerable degree of interchain association as reflected by a much higher viscosity than that of 0.4 wt%. Therefore, the molecular elongation caused by an imposed external flow can hardly give rise to noticeable enhancement in the chain bridging for the formation of a stronger network. Instead, the flow at high enough shear rate simply disrupts the existing hydrophobe associates and results in the significant shear thinning. The slopes of the curves in Figure 4.2 are all around one at high enough shear rates, typical of a gel behavior that the viscosity dramatically drops associated with the gel-sol transition at a critical stress.[25]

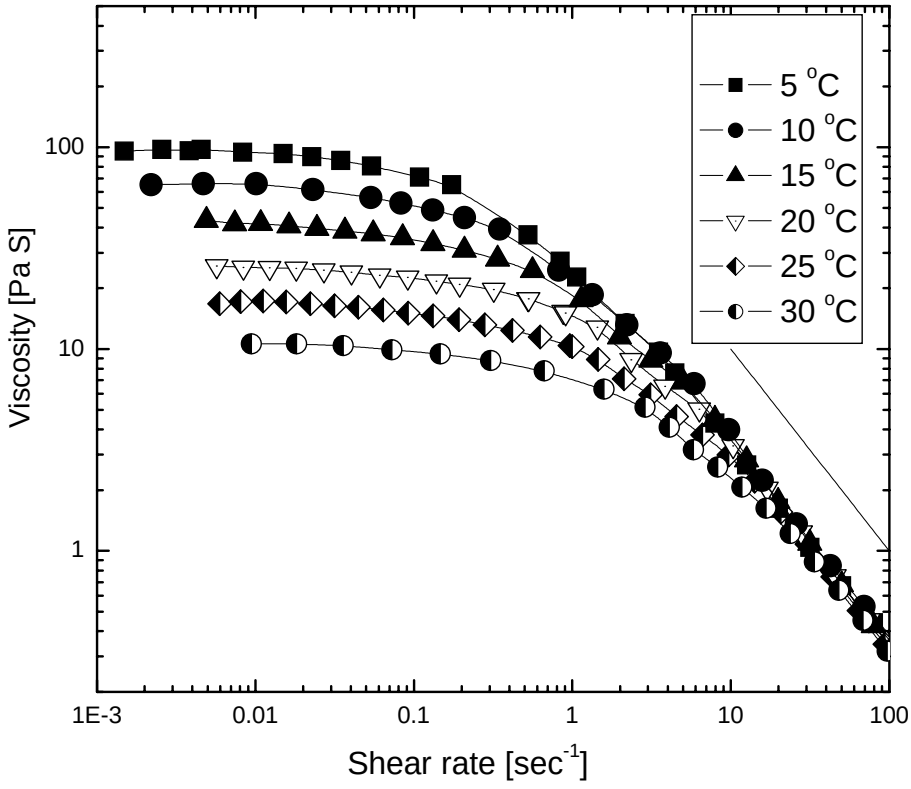

Figure 4.2: Steady-state flow curves of pure 1 wt% HMHEC solutions at various temperatures.

The logarithm of zero-shear viscosity is plotted against the reciprocal temperature in Figure 4.3. The good linear fit seen in the figure indicates that the zero-shear viscosity of the HMHEC solution exhibits an Arrhenius behavior. The activation energies of dissociation determined from the fitting lines are 62.1 kJ/mol and 71.2 kJ/mol for 1% and 0.4% solutions, respectively, comparable to the estimate of 60 kJ/mol by Maestro *et al*. from the relaxation time.[2]

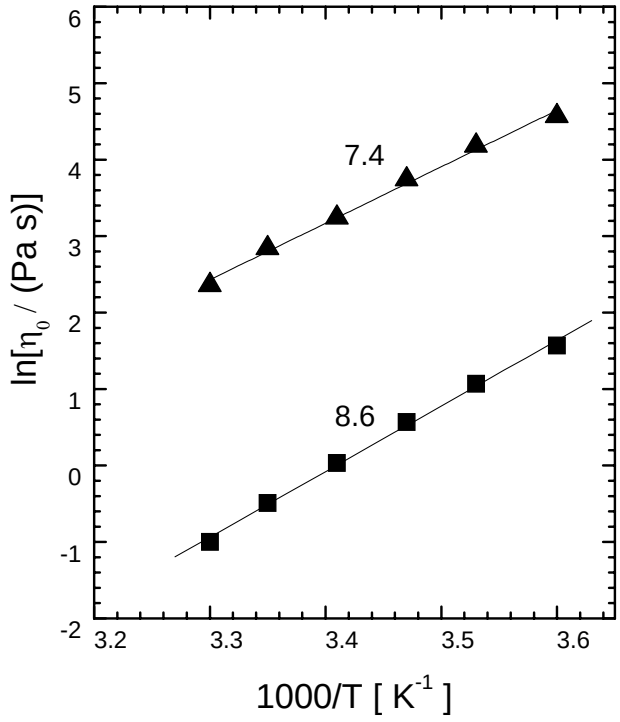

Figure 4.3: Arrhenius plots of zero-shear viscosity of pure 0.4 wt% (square) and 1 wt% (triangle) HMHEC solutions. The slopes of the fitting lines are shown as well.

4.2.2 Clouding Behavior of HMHEC-Surfactant Solutions.

For the HMHEC solutions, we also conducted cloud point experiments from 20 ^{o}C to 95^{o}C, but did not observe any clouding phenomenon. For pure surfactant solutions, the turbidity at cloud point arises from the formation of a surfactant-rich phase due to the micellar flocculation. It is associated with the breakup of hydrogen bonds between the hydrophilic heads and water molecules. As mentioned in Section 3.1.1, CPT depends on the sizes of hydrophilic and hydrophobic moieties. In this regards, our observation indicates that up to 95 ^{o}C, the increased thermal energy is not sufficient to break hydrogen bonds between the HMHEC backbone and water molecules so as to make clouding or phase separation occur. The explanation to this behavior is twofold. First, the alkyl hydrophobes are not sufficient both in length and quantity. Second, the existence of the hydroxyl groups of HMHEC gives rise to stronger hydrogen bonding with water.

We now investigate the effect of HMHEC on the CPT of non-ionic surfactants, $C_{12}E_5$ and $C_{12}E_6$ that possess the same hydrophobic moiety, in an attempt to relate it to the viscosity behavior of the mixtures.

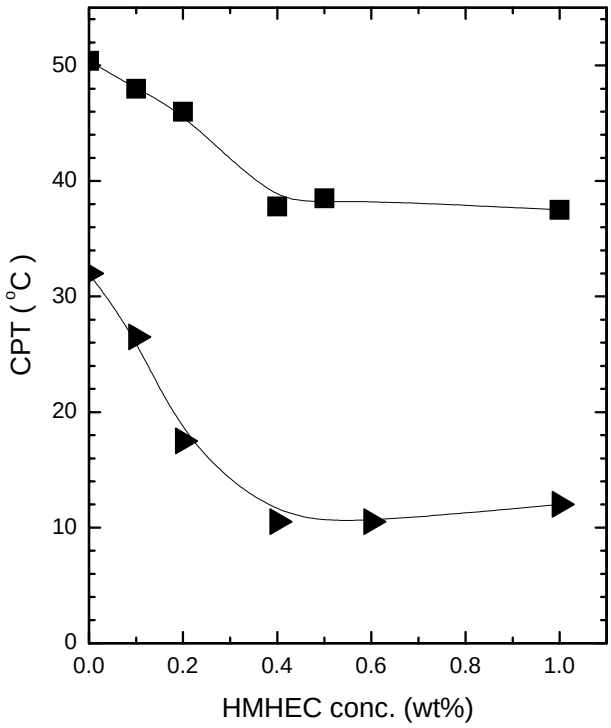

Figure 4.4: Cloud point temperature of 1 wt% surfactant solutions with addition of HMHEC; $C_{12}E_5$ (triangles), $C_{12}E_6$ (squares).

Figure 4.4 shows the variation of CPT with HMHEC concentration for 1 wt% surfactant solutions. When the HMHEC concentration exceeds 1 wt%, the solution becomes quite viscous and difficult to be handled. Also the solution appears slightly turbid, which may affect the accuracy in the CPT determination for the mixture cases. Therefore, in this study, the maximum concentration of HMHEC is limited to 1 wt%.

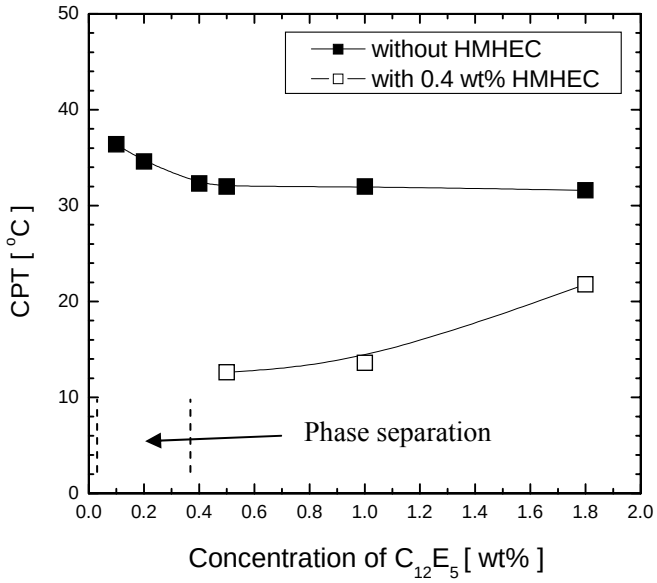

Figure 4.5: Cloud point temperature as a function of $C_{12}E_5$ concentration without HMHEC and with 0.4 wt% HMHEC. For the latter, macroscopic phase separation occurred even at 2 °C (lowest temperature investigated) in the region between the dashed lines.

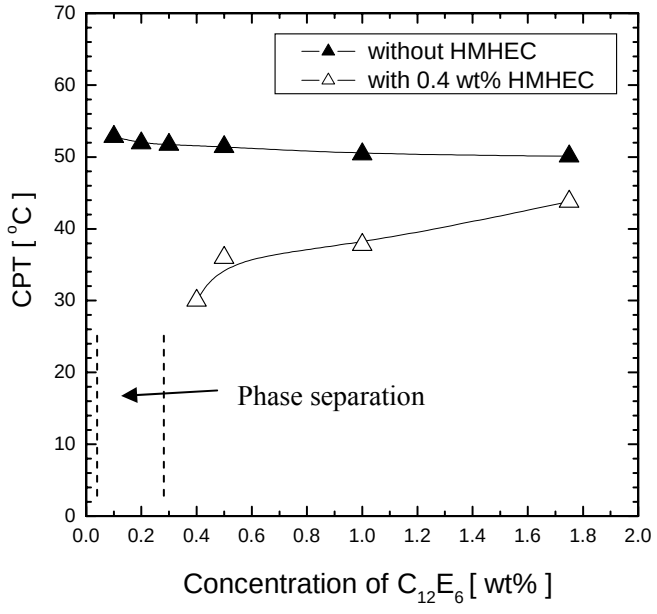

Figure 4.6: Cloud point temperature as a function of $C_{12}E_6$ concentration without HMHEC and with 0.4 wt% HMHEC. For the latter, macroscopic phase separation occurred even at 2 °C (lowest temperature investigated) in the region between the dashed lines.

Figure 4.5 and Figure 4.6 present the variation of CPT with the surfactant concentration for cases without and with presence of HMHEC at 0.4 wt%. Note that 2 °C is the lowest temperature investigated in this study. It can be found from Figs. 4.4 ~4.6 that the presence of HMHEC lowers CPT as compared to that for the corresponding pure surfactant solution. It is worth pointing out that in the presence of 0.4wt% HMHEC, the solutions at low enough surfactant concentrations have already phase separated even at a temperature as low as 2 °C, and thus no corresponding CPT data are seen in Figure 4.5 and Figure 4.6. After separation into two macroscopic phases, the viscosity of the dense phase that appears white is very viscous, while the light phase is clear and has a viscosity about twice the value of water. Generally, the phase behavior observed here is quite similar to that shown in Chapter 3.

4.2.3 Viscosity Behavior of HMHEC-Surfactant Solutions

To understand the clouding behavior of the mixture, we must examine the interactions between HMHEC and the surfactant. It has been well known that surfactant molecules may bind onto the hydrophobes of the polymers to form mixed micelles. Each mixed micelle may contain several hydrophobes either from a chain or from different chains. At sufficiently low concentrations, there exist no free micelles since nearly all surfactant molecules are associated with the polymer, enhancing the hydrophobic association. The enhancement strengthens the network when the HMHEC concentration exceeds the critical value for gelation. This is evidenced by the increase of zero-shear viscosity with the increasing surfactant concentration as shown in Figure 4.7 and Figure 4.8 for 1 wt% and 0.4 wt% HMHEC, respectively. Beyond the viscosity maximum, a progressive increase in surfactant concentration reduces the average number of hydrophobes in each mixed micelle, which eventually becomes a small single-digit value. At this concentration, the hydrophobes are masked by excess surfactant, and the binding between surfactant and polymer is deemed saturated. Hence a further increase in surfactant concentration can give rise to the formation of free micelles.

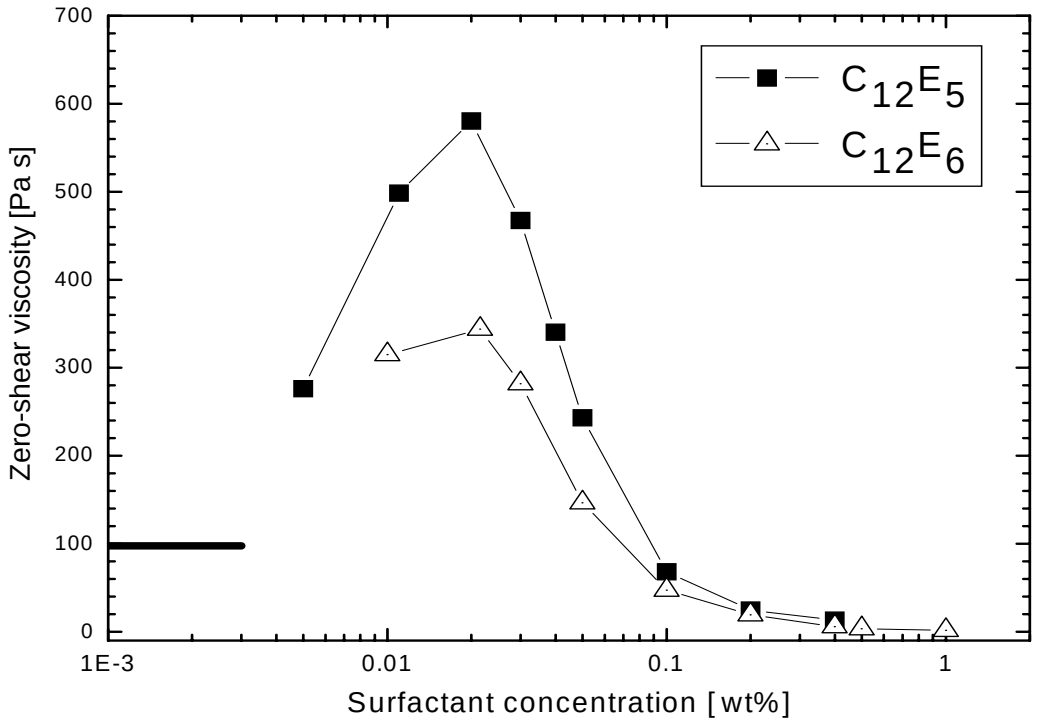

Figure 4.7: Cloud point Zero-shear viscosity of 1.0 wt% HMHEC with addition of nonionic surfactant as a function of surfactant concentration at 5 °C. The short horizontal line indicates the value in the absence of surfactant.

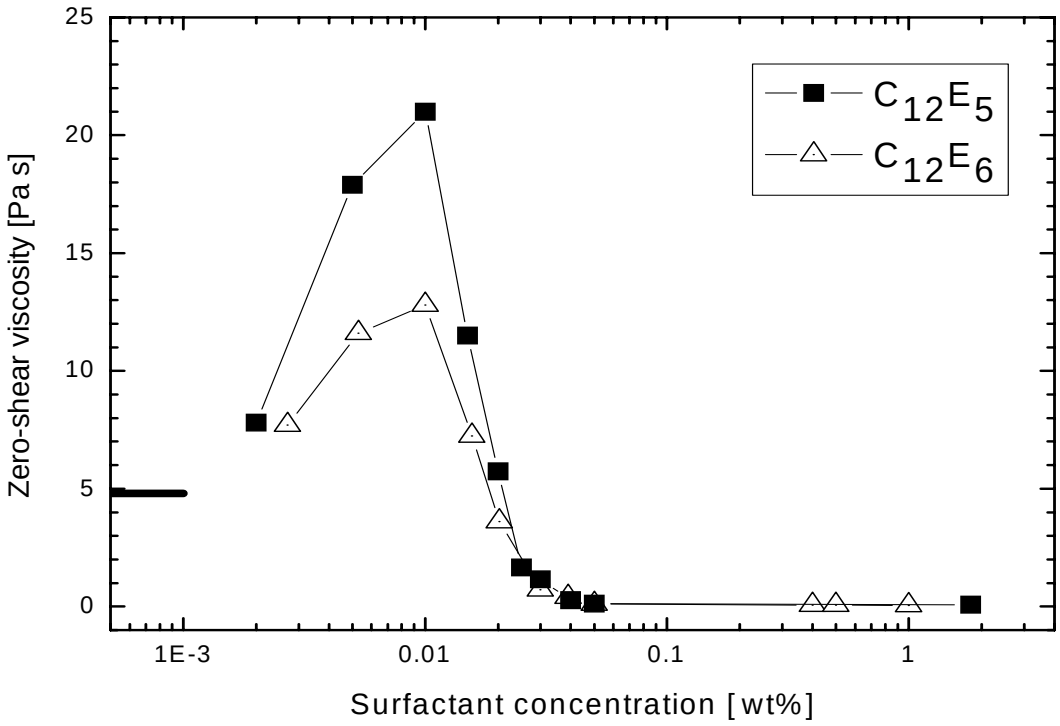

Figure 4.8: Zero-shear viscosity of 0.4 wt% HMHEC with addition of nonionic surfactant as a function of surfactant concentration at 5 °C. The short horizontal line indicates the value in the absence of the surfactant.

This behavior is indeed reflected by the viscosity decrease towards a constant as seen in Figure 4.7 and Figure 4.8. It should be noted that phase separation takes place in 0.4 wt% HMHEC solutions with surfactant concentration ranging from 0.1 to 0.3 wt%, and hence no viscosity data are available. The asymptotic viscosity at high surfactant concentrations is even lower than the value of HMHEC alone. When the surfactant concentration exceeds the saturation value, the intermolecular association is disrupted substantially, thereby leading to an increased ease of deforming the material. The saturation concentration can be crudely estimated by the concentration at which the viscosity becomes nearly a constant. From Figure 4.7 and Figure 4.8, the surfactant concentrations for saturation are found to be about 0.2 wt% and 0.04 wt% for 1 wt% and 0.4 wt% HMHEC, respectively. These results indicate that the CPT results shown in Figs. 4.4 ~4.6 are all under the condition that the hydrophobes have been masked by the surfactant.

For $C_{12}E_6$ solutions with addition of hydrophobically end-capped PEO at small amount, Appell et al.[7] observed a reduction of cloud point temperature. Below but near the cloud point, they detected an attractive force between micelles from small angle neutron scattering, and attributed this force to some polymer molecules, each of which links two mixed micelles. A similar bridging behavior can be expected for HMHEC as each chain contains more than two hydrophobes. With sufficient addition of surfactant, there exist both free and mixed micelles. Since the mixed micelles on a same polymer are indeed linked together, their aggregation at elevated temperatures due to weakened hydrogen bonding is enhanced.[7] As a result, the solution can turn cloudy at a lower temperature than in the absence of HMHEC. It can be seen from Figure 4.5 and Figure 4.6 that the declination of cloud point temperature is less substantial for higher surfactant concentrations. This behavior can be explained by the comparatively large amount of free micelles, on which the polymer chains exert no direct effect, as opposed to coexisting mixed micelles. As can be seen in Figure 4.4, at a fixed surfactant concentration, a smaller drop in CPT occurs for lower HMHEC concentrations. When the mixed micelles greatly outnumber the free micelles, the

linking effect of HMHEC can indeed result in phase separation at very low temperatures, as shown in Figure 4.5 and Figure 4.6. A dramatic reduction of CPT was also reported by Appell et al. for mixtures of $C_{12}E_6$ and end-capped PEO. [7]

We now examine the temperature effect on the viscosity of HMHEC solutions with added surfactant. Figure 4.9 plots the viscosity for the cases with $C_{12}E_5$, while Figure 4.10 and Figure 4.11 present the results for $C_{12}E_6$. The CPTs for various cases are indicated in the figures. It can be found that the temperature dependence of the solution viscosity no longer follows the Arrhenius behavior, as opposed to pure HMHEC solutions. For the case of $C_{12}E_6$, Figure 4.10 shows that the mixture viscosity first decreases, reaches a local minimum and then increases till around the cloud point temperature. The viscosity can rise by a factor of two with respect to the local minimum. For $C_{12}E_5$, to the contrary, the viscosity increases right from the lowest temperatures investigated till about the cloud point. The viscosity increase can be even threefold as shown in Figure 4.9. The viscosity increase is more significant than for HMHEC+Tergitol 15-S-7 in our previous study. [10] It should be noted that the viscosity data beyond the cloud point shown in these figures are the values measured 5 min after each temperature is reached. For these cases, the solution stability will be discussed in detail later.

The interesting temperature dependence below the cloud point can be explained by a competition between Arrhenius behavior and micellar aggregation. At low enough temperatures, hydrogen bonding between the hydrophilic moiety of $C_{12}E_6$ and water is strong. Therefore, aggregation between micelles is unlikely and the viscosity simply shows an Arrhenius behavior. At higher temperatures, the thermal energy weakens the hydrogen bonds considerably, thereby leading to micellar aggregation. Some aggregation involves mixed micelles on different chains, and can directly give rise to interchain association. Even the aggregation between mixed micelles on a same chain can bring polymer molecules closer because the involved mixed micelles may have already been linked with other chains. Both account for the viscosity rise till the cloud point. Since the number of EO units in the hydrophilic head is lower for

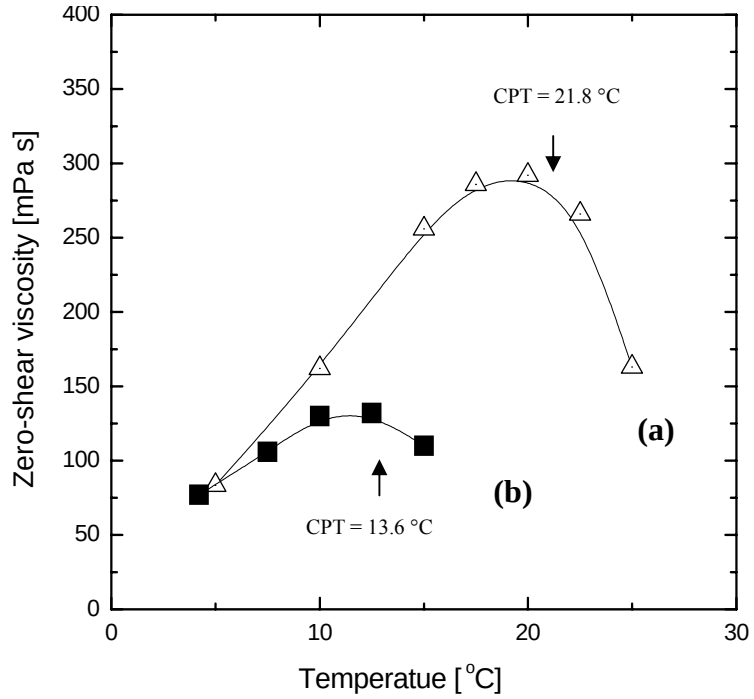

Figure 4.9: Temperature dependence of zero-shear viscosity for (a) 0.4wt% HMHEC +1.8 wt% $C_{12}E_5$, and (b) 0.4wt% HMHEC+1.0 wt% $C_{12}E_5$.

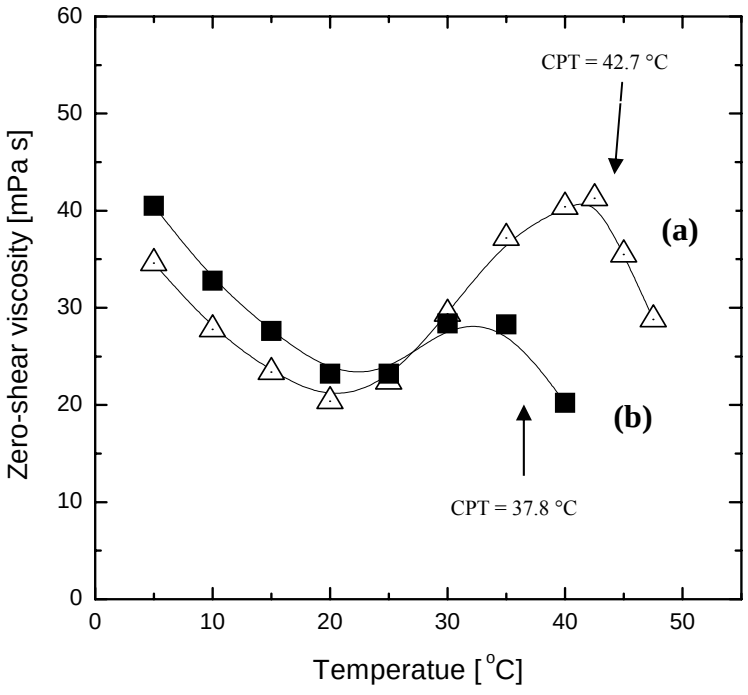

Figure 4.10: Temperature dependence of zero-shear viscosity for (a) 0.4 wt% HMHEC +1.8 wt% $C_{12}E_6$, and (b) 0.4 wt% HMHEC+1.0 wt% $C_{12}E_6$.

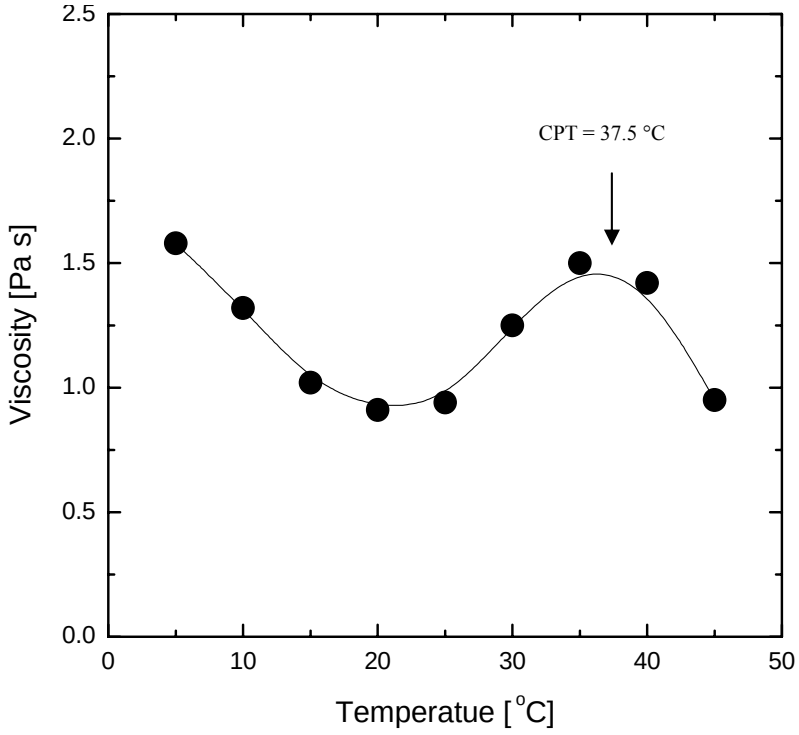

Figure 4.11: Temperature dependence of viscosity at 0.2 s^{-1} for 1.0 wt% HMHEC + 1.0 wt% $C_{12}E_6$.

$C_{12}E_5$ than for $C_{12}E_6$, the micellar aggregation can take place at lower temperatures for $C_{12}E_5$, and this explains why the viscosity increase is seen at comparatively low temperatures.

When the cloud point is reached, the HMHEC-surfactant solution becomes turbid, and a second phase starts to form as droplets. To observe the phase evolution, in this study, the cloudy solutions were placed in the water bath at a temperature slightly higher than the cloud point temperature to stand for some time. We find that for 0.4 wt% HMHEC, the phase separation took hours to days to be complete, resulting in two macroscopic phases: a supernatant above a white viscous phase. The viscosity of the supernatant is only about two times as high as water viscosity, indicating that most of the polymer and surfactant form complexes and stay in the white phase (c.f. Section 3.2.2 for more details). For 1 wt% HMHEC, however, the solution remained cloudy and we could not obtain two macroscopic phases even after two weeks.

This slow process is attributable to the high solution viscosity as droplets must

diffuse to encounter each other and get coalesced so as to gradually become a continuous phase. Since the solution becomes biphasic above the CPT and the phase separation is ongoing, the solution viscosity is essentially time dependent. To illustrate such a behavior beyond the cloud point, we plot the solution viscosity as a function of time for 0.4 wt% HMHEC+1.8 wt% $C_{12}E_6$ in Figure 4.12. At each temperature, the viscosity was measured as a function of time for a period of 1 min and the second measurement was conducted 3 min later. It can be clearly seen that at 42.5 ^{o}C (slightly below CPT), the viscosity is independent of time. At 47.5 ^{o}C, in contrast, the solution becomes unstable showing a fluctuating viscosity, and the viscosity even differs in the two measurements. It is clearly indicative of a time dependence of viscosity. In this regards, the viscosity trend above CPT shown in Figs. 4.9 ~4.11 should be taken with caution, in particular for 0.4 wt% HMHEC since the phase separation is comparatively fast.

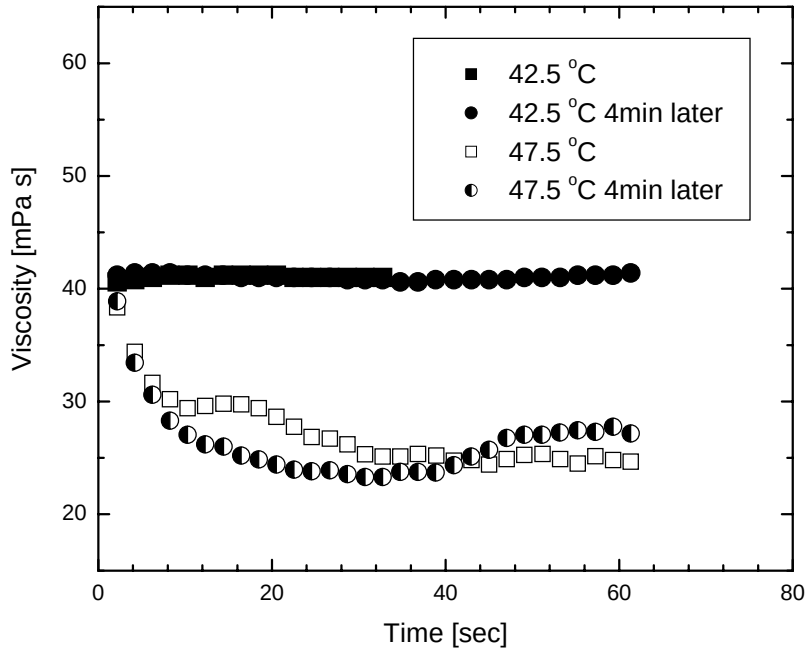

Figure 4.12: Viscosity of 0.4wt% HMHEC+1.8wt% $C_{12}E_6$ as a function of time at 2 s^{-1} (low enough for the Newtonian plateau) with temperature fixed at 42.5 °C (slightly below the CPT) and 47.5 °C (4.8 °C above the CPT). Note that at each temperature, the second measurement was conducted 4 min after the starting time of the first.

4.2.4 Comparison with the System of Charged HMP

It is interesting to compare the behavior of our system, which is mixture of hydrophobically modified neutral polymer and nonionic surfactant, with that involving charged HMP and C_xE_y in the prior works.[55-57] It has been reported that by heating, a C_xE_y solution with small enough y undergoes a consecutive phase transition in such an order: a single micellar phase, a micellar biphase, and a lamellar phase which may coexist with a water phase. In the presence of charged HMP, the electrostatic repulsion between polymer segments suppresses the aggregation of mixed micelles and thus stabilizes a single micellar phase. As a result, the micellar biphase has a shrinking temperature range or even disappears in the phase diagram when the concentration of charged HMP is sufficiently high.[55-56] For the latter case, the authors observed a local viscosity maximum at a certain temperature and attributed it to reversible thermal gelation associated with the transition from a micellar phase to a lamellar phase. In the lamellar phase, the surfactant forms large vesicles bridged by the polymer chains due to the dissolved hydrophobes in the vesicle bilayer. The corresponding viscosity for some cases could become ten times as large as the value for the single micellar phase.

In our study where there is no electrostatic repulsion for HMHEC, the solution viscosity increases with temperature prior and near to the cloud point, and appears to have a local maximum around the cloud point. Unlike the formation of a monophasic solution of bridged lamella, the phase separation in our system inhibits a further increase in viscosity with temperature. In the work of Iliopoulos and Olsson,[55] the effect of added salt that screened out the electrostatic repulsion between charged HMP was also investigated. They found that with sufficient salt addition, a biphasic solution could exist over a considerable temperature range and the temperature for the transition to the biphase is lowered as compared to the case of pure surfactant. This finding indeed agrees with our observation using the neutral polymer HMHEC. However, a further comparison cannot be made since no viscosity result was reported by them for the case of added salt.

4.3 Conclusions

We have conducted an experimental study on the influences of surfactant and temperature in the phase and viscosity behaviors of HMHEC that contains randomly distributed hydrophobes. For surfactant free HMHEC solutions at moderate concentrations, shear enhanced hydrophobic association can take place at intermediate shear rates, in particular for low temperatures. For HMHEC-surfactant mixtures, the cloud point temperature is decreased by the presence of the polymer owing to an additional attractive interaction between mixed micelles arising from chain bridging. The variation of viscosity at sufficiently high temperature shows an interesting correlation with the enhanced interchain association caused by the aggregation of mixed micelles prior to the cloud point.

CHAPTER 5 Nonlinear Rheology of Aqueous Solutions of HMHEC with Nonionic Surfactant

In this chapter, shear thickening and strain hardening behavior of HMHEC solutions were experimentally examined. We focused on the effects of polymer concentration, temperature and addition of nonionic surfactant.

5.1 Early Investigations Relevant to this Study

Ma and Cooper [79] observed shear thickening for HEUR polymer solutions at 0.05 M sodium dodecyl sulfate (SDS, an ionic surfactant). At lower SDS concentrations, the solution behavior became unclear because of the onset of flow instabilities. The incipient shear thickening occurs at the same reduced shear rate as in the corresponding solution without SDS (see Figure 10 of their paper). This finding supported the free path model of non-Gaussian chain stretching,[36] predicting that the critical reduced shear rate depends only on the polymer molecular weight. One can also find from that figure that the degree of shear thickening was hardly changed upon the addition of 0.05 M SDS, although it was not pointed out by the authors.

For comblike HMP, Talwar *et al.* recently examined the low-shear flow behavior of HASE+nonylphenol ethoxylate surfactant (NPe series, nonionic), and reported that the presence of surfactant affected the relaxation time and plateau modulus of the network structure[80]. For HMHEC, however, Maestro *el al.* found that addition of $C_{12}E_4$ (polydisperse Brij30) affected only the relaxation time[81]. To date, there exists no study on how nonionic surfactants can affect the nonlinear flow behavior of HMHEC.

In this work, we experimentally investigate the shear thickening and strain hardening behavior of HMHEC, focusing on the effects of concentration, temperature and added nonionic surfactant on the nonlinear rheology. It is aimed at seeking a better understanding of flow behavior of comblike HMP.

5.2 Results and Discussion

5.2.1 Absence of Surfactant

5.2.1.1 Steady Shear Behavior

First we examine the shear thickening behavior of pure HMHEC solutions. Figure 5.1 plots viscosity against shear stress for various HMHEC concentrations at 10 ^{o}C. The flow curves normalized by the zero-shear viscosities are presented in Figure 5.2. Although the Newtonian plateau cannot be very accurately determined for 0.2-0.4 wt% HMHEC (see Figure 5.1) because of the limitation of our rheometer, the trend shown in Figure 5.2 is not affected. In the concentration range from 0.15 to 0.5 wt%, shear thickening takes place at intermediate shear rates, followed by substantial shear thinning.

Although the shear thickening of HMHEC was previously observed by Maestro *et al.*[3], no systematic studies were conducted to investigate this interesting behavior in their paper. To quantify the thickening behavior, we define a shear thickening index as the maximum normalized viscosity. When shear thickening is absent, the index is unity. One can see from Figure 5.2 that 0.25 wt% HMHEC solution showed the highest shear thickening index of about 2.2 at 10^{o}C. In comparison, this highest value is larger than ~1.3 for the end-capped PEO (HEUR) having a molecular weight 20k with C_{18} hydrophobes (at 2 wt%) at the same temperature, as reported by Ma and Cooper[31]. Examining similar polymers with C_{16} under steady shear at 24.5^{o}C, Jenkins [29] found the highest index ~1.9 for 1 wt% polymer of an average molecular weight 34k, while it was about 1.5 for a number averaged molecular weight of 51k (also at 1 wt%) as studied by Xu et al[82]. From the comparison, we can conclude that the extent of shear thickening depends on the chemical species, molecular weight, hydrophobic segments, concentration and temperature.

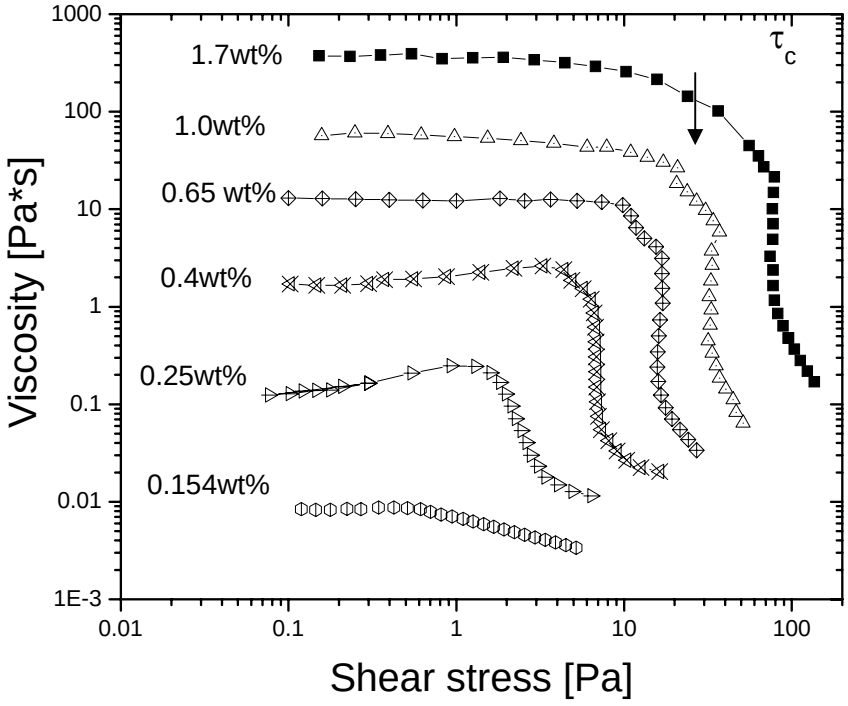

Figure 5.1: Viscosity versus shear stress for pure HMHEC solutions of different concentrations at 10 °C. The arrow indicates the critical shear stress τ_c for 1.7 wt% HMHEC solution.

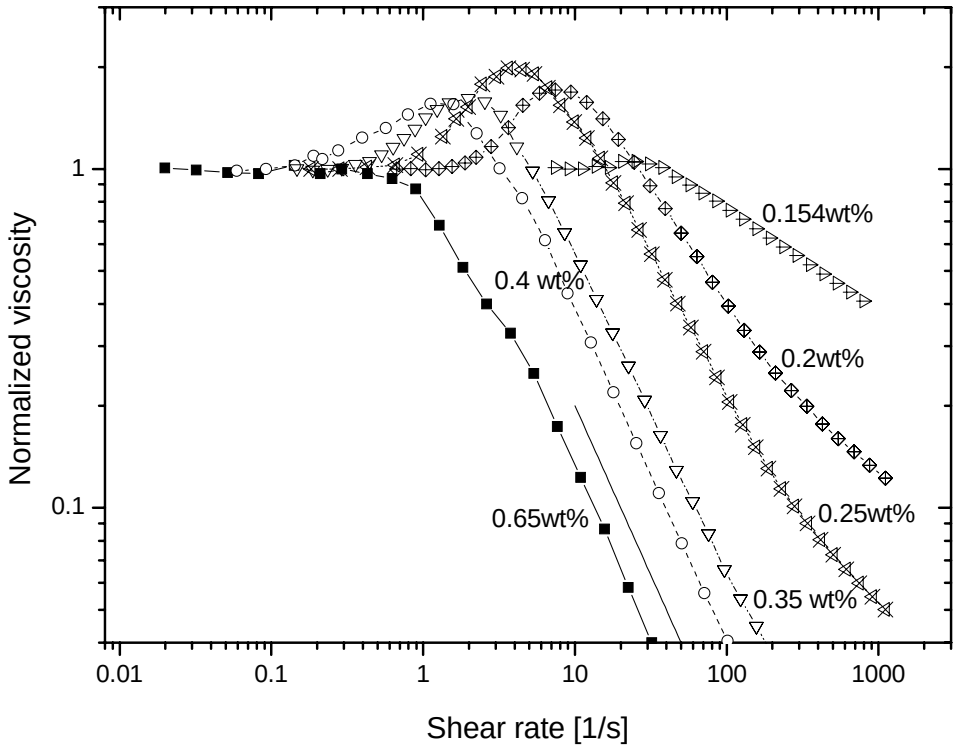

Figure 5.2: Normalized viscosity versus shear rate for pure HMHEC solutions of different concentrations at 10 °C. The black line has a slope of -1 and is shown only for comparison purpose.

In view of the difference in flow behavior, three concentration regimes could be identified: a dilute regime (c < 0.15 wt%), a semidilute or shear thickening regime (0.15 wt% < c < 0.5 wt%), and a concentrated regime (c > 0.5 wt%). In the dilute regime, the solution is nearly Newtonian because of the absence of a network structure. Indeed, HMHEC starts to form discrete aggregates at a very low concentration (a few ppm), evidenced by surface tension measurement.[2] The aggregates start to overlap and associate with one another at around 0.15 g/dL (c^*, the overlap concentration of a polymer solution which is defined as the point where the polymer chain coils just start to touch each other), deduced from the turning point for a sharp increase in the reduced viscosity against concentration curve [2]. Above c^*, interchain association leads to substantial linking of aggregates, similar to the loop-to-bridge transition for telechelic HMP[83].

Interestingly, this overlap concentration tallies with the concentration for the incipient shear thickening observed in our experiment. In the shear thickening regime, we find from Figure 5.1 and Figure 5.2 that the shear rate for the strongest thickening (or the onset) appears to decrease with increasing HMHEC concentration, while the corresponding shear stress shows a reverse trend. Shear thickening of HMP has been accounted for by shear enhanced association and cooperative non-Gaussian chain stretching. [31,35,37,40] However, it still remains controversial as to which mechanism dominates.

Different behaviors for different concentration regimes can also be seen from the concentration dependence of zero-shear viscosity η_0 as plotted in Figure 5.3: the exponent is 5.7 ($\eta_0 \sim c^{5.7}$) in the shear thickening regime, in contrast to 3.5 ($\eta_0 \sim c^{3.5}$) in the concentrated regime. The stronger concentration dependence in the shear thickening regime suggests an ongoing development of interchain association promoted by raising the polymer concentration. Occurrence of shear thickening within a certain concentration range has been observed for telechelic HEUR[38] and comblike HASE[39]. In the shear thickening regime for HASE, English *et al.*[39] reported a much stronger concentration dependence ($\eta_0 \sim c^{7.9}$), partly because the HASE backbone is charged at high pH. Weakened dependence at two higher concentrations

can be seen from their Figure 9, but they attributed it to heterogeneity formed when solubilizing the HASE latex.

For comblike polymer, the absence of shear thickening at high concentrations was thought to be due to the topological entanglements that dominate over the hydrophobic interactions[31]. This explanation is not applicable to HEUR, whose molecular weights are usually below the critical entanglement value.[84]

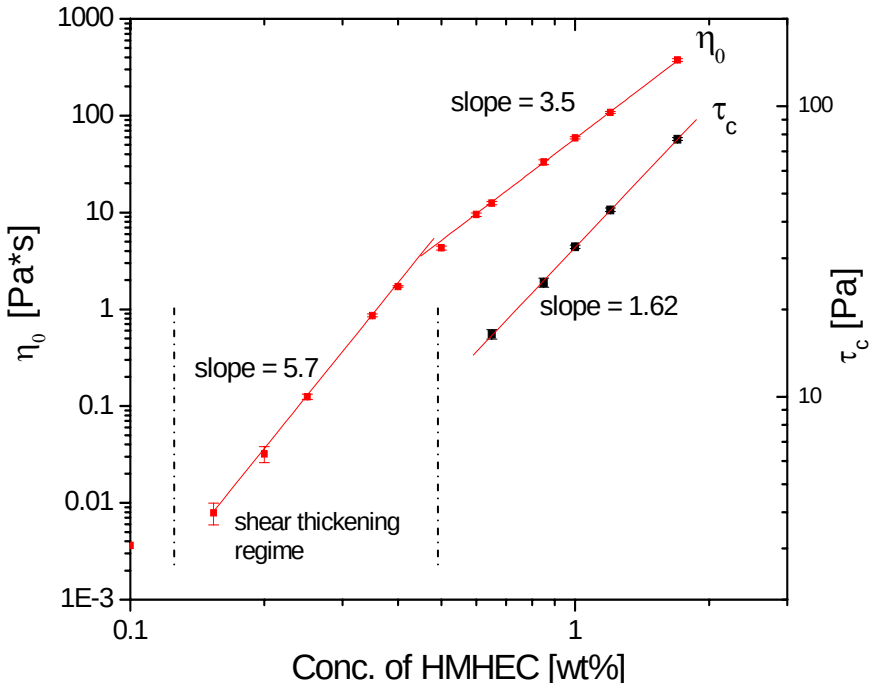

Figure 5.3: Zero-shear viscosity and critical shear stress versus concentration for pure HMHEC solutions at 10 °C.

In the concentrated regime, the abrupt decline in viscosity shown in Figure 5.1 In the concentrated regime, the abrupt decline in viscosity shown in indicates that the viscosity scales with shear rate as $\eta \sim \dot{\gamma}^{-1}$ when the solution becomes strongly shear thinned. When the concentration is high enough in the semi-dilute regime, a substantial decrease in viscosity can also be seen, although it is not as abrupt and prominent. The abrupt decline in viscosity was previously observed for comblike HM hydroxypropyl guar (HMHPG) by Aubry and Moan.[85] They regarded the discontinuity as the critical shear stress τ_c for complete destruction of the transient network, and reported the scaling law $\tau_c \sim c^{1.7}$ for concentrations ranging from 0.5 to

1.5 wt% (within the concentrated regime). Our data for HMHEC shown in Figure 5.3 finds $\tau_c \sim c^{1.62}$ from 0.6 to 1.7 wt%. The similar behavior implies the likelihood of a universal scaling law for comblike HMPs. For HASE, however, English *et al.* [39] reported a much stronger dependence $\tau_c \sim c^5$ for concentrations higher than 0.7 g/dL. The difference may be due to: (1) the critical shear stress defined by English *et al.* is the value for the onset of shear thinning, different from that used by Aubry and Moan, [85] at which the solution shows $\eta \sim \dot{\gamma}^{-1}$, and (2) HASE is a polyelectrolyte mentioned earlier. As for extensively studied HEUR, there is no report yet on whether it exhibits a similar scaling behavior.

5.2.1.2 Dynamic Oscillatory Shear Behavior

To further understand the flow behavior of HMHEC solutions, we examined the strain dependence of the storage modulus G' and loss modulus G'' via dynamic tests under an oscillatory shear flow. The normalized moduli at 1 Hz and 10 °C for various HMHEC concentrations are shown in Figure 5.4. As seen, linear behavior remains until the strain reaches about 0.5. When the strain exceeds this value, considerable strain hardening for both moduli, followed by strain softening at higher strains. This behavior is observed for semidilute solutions as well as for some concentrated samples, which do not show shear thickening in a steady flow. The degree of strain hardening for G' or G'' reaches its highest value at a certain concentration. The onset of a decrease in G' occurs at a smaller strain than that of G''. The observed behavior of HMHEC is qualitatively similar to those of HASE [39-40, 86-88] and HEUR[87]. It has been widely accepted that the sharp decreases in the moduli at large enough strains arise from network breakdown.[86] However, the mechanism for strain hardening for G' is controversial.

To get more clues about the mechanism, we plot in Figure 5.5 the normalized moduli against strain for 0.85 wt% HMHEC at two frequencies: 0.0215 and 1 Hz. The former is lower and the latter is higher than the crossover frequency (0.0417 Hz) determined from the frequency sweep for the same polymer solution within the linear

regime. It can be clearly seen that the strain hardening of G' almost vanishes at the lower frequency, in contrast to the behavior at the higher frequency.

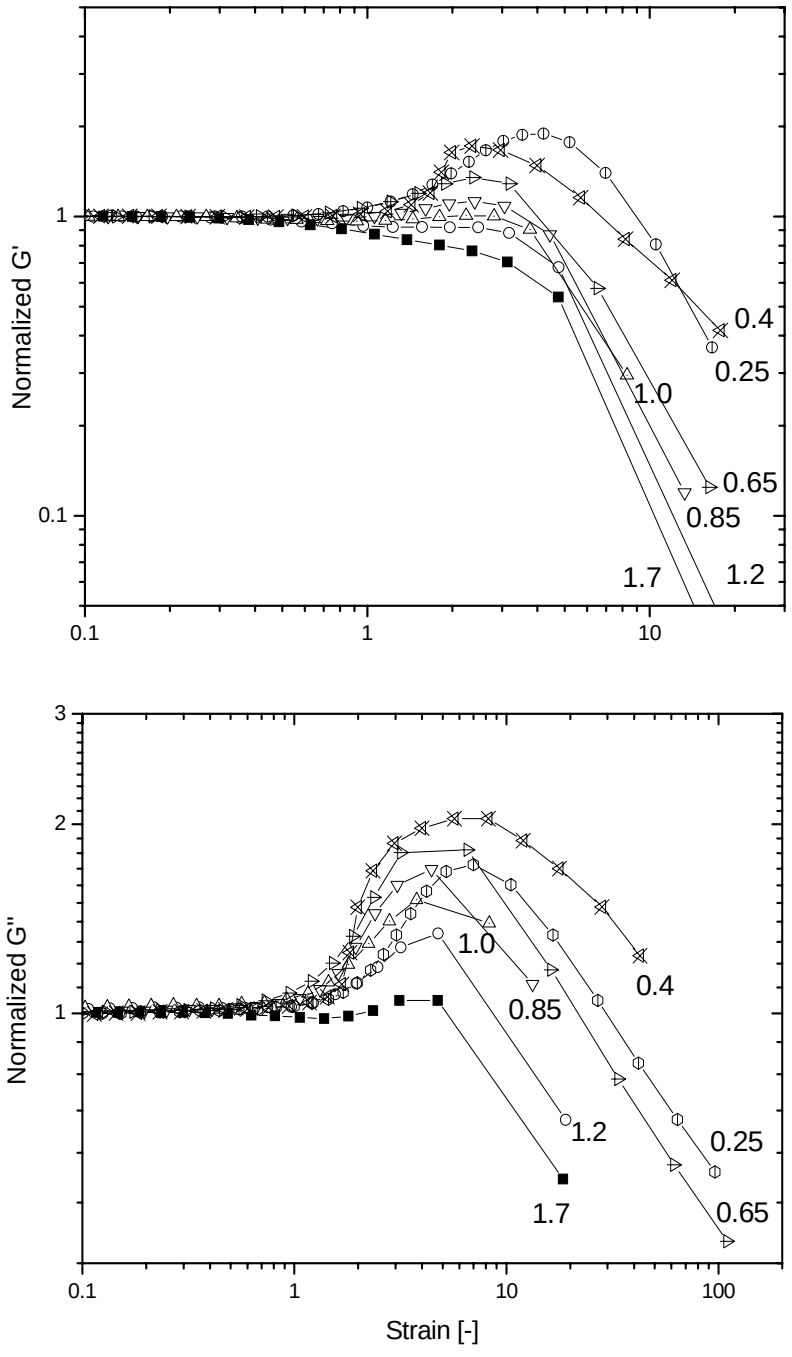

Figure 5.4: Normalized storage modulus (a) and loss modulus (b) versus strain for HMHEC solutions of different concentrations (numbers indicated in wt%) at 10 °C. The frequency is 1 Hz.

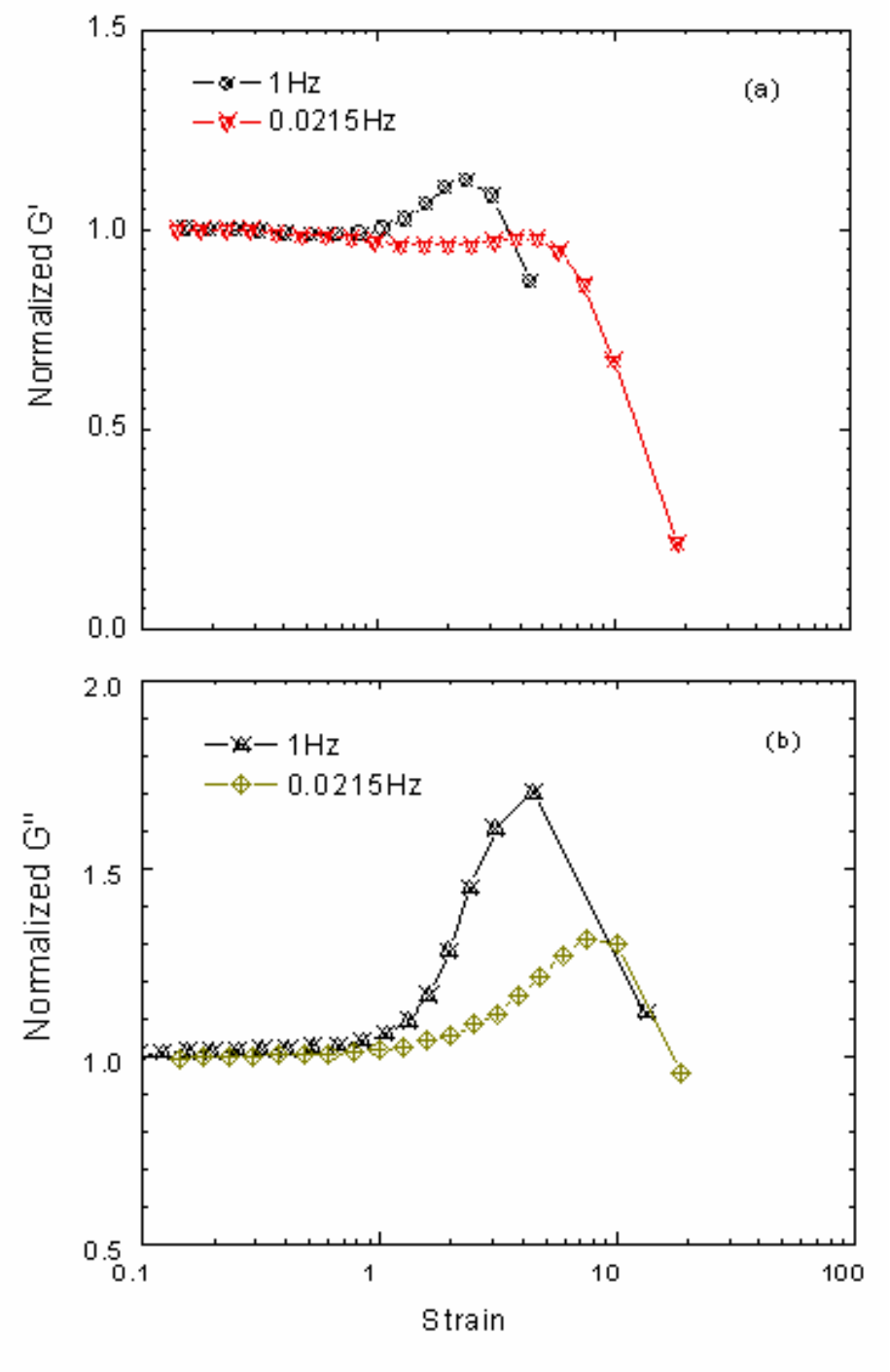

Figure 5.5: Normalized storage modulus (a) and loss modulus (b) versus strain for 0.85 wt% HMHEC at 10 °C at two different frequencies: one higher and the other lower than the crossover frequency (0.0417 Hz). Lines are added only to guide the eye.

At low frequencies, the network could have sufficient time to rearrange its configuration to avoid overstretching. It implies that the non-Gaussian chain stretching occurs at sufficiently high frequencies, contributing considerably to strain hardening.[87] Examining fluorinated HEUR with a very long relaxation time (~56 sec), Serero *et al.*[89] conducted step-strain experiments to calculate the modulus in the short-time limit, which shows strain hardening. Their finding provides evidence of nonlinear stretching, because it is very unlikely for an instantaneous increase in the network junction density within a time interval, far shorter than the network relaxation time.

5.2.1.3 Temperature Effect on Shear Thickening

The temperature effect on the flow curve is presented in Figure 5.6, which plots the normalized steady-shear viscosity again shear rate for 0.2 wt% HMHEC solution at various temperatures. It can be seen that the shear thickening is reduced with increasing temperature, and completely disappears when the temperature reaches 25 °C. Also, the shear rate for the maximum viscosity increases with increasing temperature. This behavior is similar to that of HEUR observed by Ma and Cooper [31].

The temperature dependence of the shear thickening index of HMHEC observed here is, however, different from the behavior of fluorinated HEUR designated as F-HEUR by Berret et al. [90] because its shear thickening index is around 1.3 at both 25 and 35 °C (cf. Fig. 3 in that paper). To analyze the data, we use the shear rate for the maximum viscosity as a characteristic rate $\dot{\gamma}_c$, to provide an indication of the dynamics of the shear-induced transient network. Some researchers adopt the shear rate at the onset of the nonlinear behavior for this purpose [31]. However, the two definitions are thought to provide the same qualitative trend [36]. The reciprocal of $\dot{\gamma}_c$, reflecting the characteristic relaxation time, is found to follow the Arrhenius law, allowing us to determine the activation energy E of the relaxation process. We obtain E = 75 kJ/mol, which is quite close to 70 kJ/mol calculated from the temperature dependence of the zero-shear viscosity. The activation energy values

obtained here are also in excellent agreement with the value obtained by Maestro *et al*.[3] for the same polymer HMHEC, and is also comparable with that of HEUR with the same hydrophobes (C_{16}) by Annable *et al* [30]. The agreement indicates that the relaxation during shear thickening is still associated with the disengagement of a hydrophobe from a junction. The hydrophobe disengagement can be enhanced by raising the temperature, i.e., providing a higher thermal energy. According to the free path length model of Marrucci *et al.* for telechelic HMPs [36], the shear thickening index is proportional to *E/kT*, where *kT* is the thermal energy. This model was formulated on the basis of cooperative non-Gaussian chain stretching and partial relaxation of an escaped chain before joining a new junction [36]. A plot of the index versus *E/kT* for our data (inset of Figure 5.6) appears to be a straight line with slope equal to 0.57, indicating applicability of the free path length model to the shear thickening of comblike HMHEC.

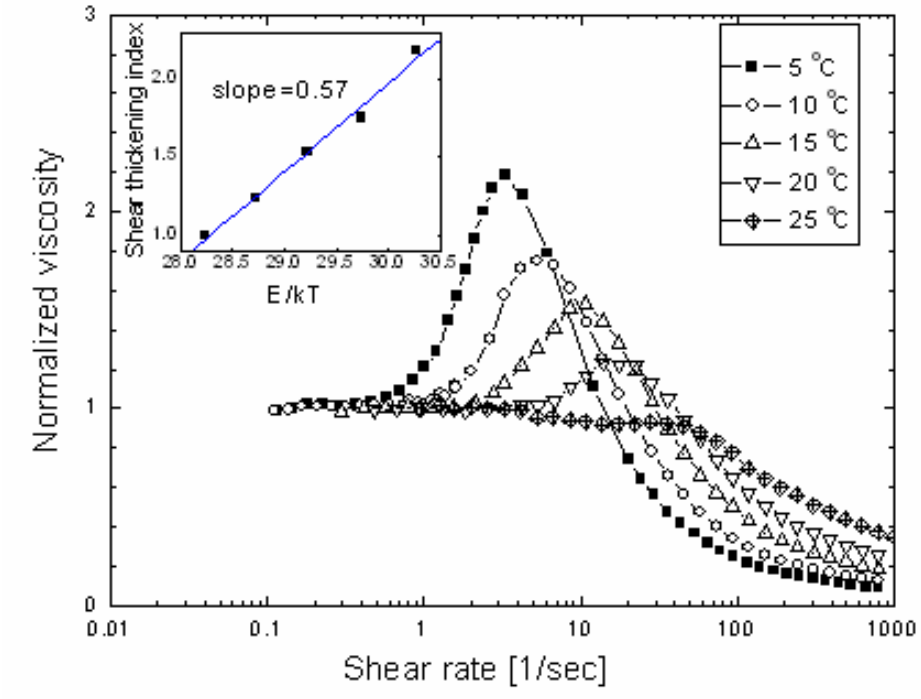

Figure 5.6: Normalized viscosity versus shear rate for 0.2 wt% HMHEC at different temperatures. The inset shows the temperature dependence of the shear thickening index.

5.2.2 Presence of Nonionic Surfactant

The effects of nonionic surfactant $C_{12}E_5$ and $C_{12}E_9$ on the shear thickening behavior of HMHEC solutions were studied in this work. We chose 0.2 and 0.4 wt% HMHEC solutions because they showed strong shear thickening in the absence of surfactant. Figure 5.7 presents the viscosity versus shear rate for 0.2 wt% HMHEC at various $C_{12}E_5$ concentrations. Figure 5.8 plots the viscosity versus shear stress for the same data as in Figure 5.7. The effect of $C_{12}E_5$ on the variation of the normalized viscosity with shear rate is shown in Figure 5.9. The effect of $C_{12}E_5$ on the variation of the normalized viscosity with shear rate is shown in Figure 5.10. The shear rates for both the inception of the nonlinear behavior and the maximum viscosity are found to gradually shift to lower values with the addition of surfactant until the concentration reaches 60 ppm, beyond which the shear thickening is weakened dramatically. In contrast, the corresponding shear stress appears to shift monotonically to lower values, as seen in Figure 5.8. When the $C_{12}E_5$ concentration exceeds 100ppm (corresponding to ~69 surfactant molecules per polymer molecule or ~7 surfactant molecules per hydrophobe), the shear thickening behavior completely disappears. We find from Figure 5.9 that prior to the large drop in the shear thickening index, the zero-shear viscosity has reached the maximum at about 60ppm $C_{12}E_5$, which is about 2.5 times higher than that in the absence of surfactant. In contrast, the shear thickening index only increases by 20% at most. The zero-shear viscosity and shear thickening index start to decrease at about the same surfactant concentration. Note that since the presence of HMHEC can lower the $C_{12}E_5$ CMC, small mixed micelles may form at 20 ppm.

Although there have existed numerous studies examining the surfactant effect on zero- or low-shear viscosities of polymers.[9,25,26,28,91] The present work, for the first time, reports the correlation of the effects of nonionic surfactant on the zero-shear viscosity and shear thickening. Also, the behavior is dominated by the hydrophobic interaction between surfactant and HMHEC, unlike the case with ordinary polymer.[92]

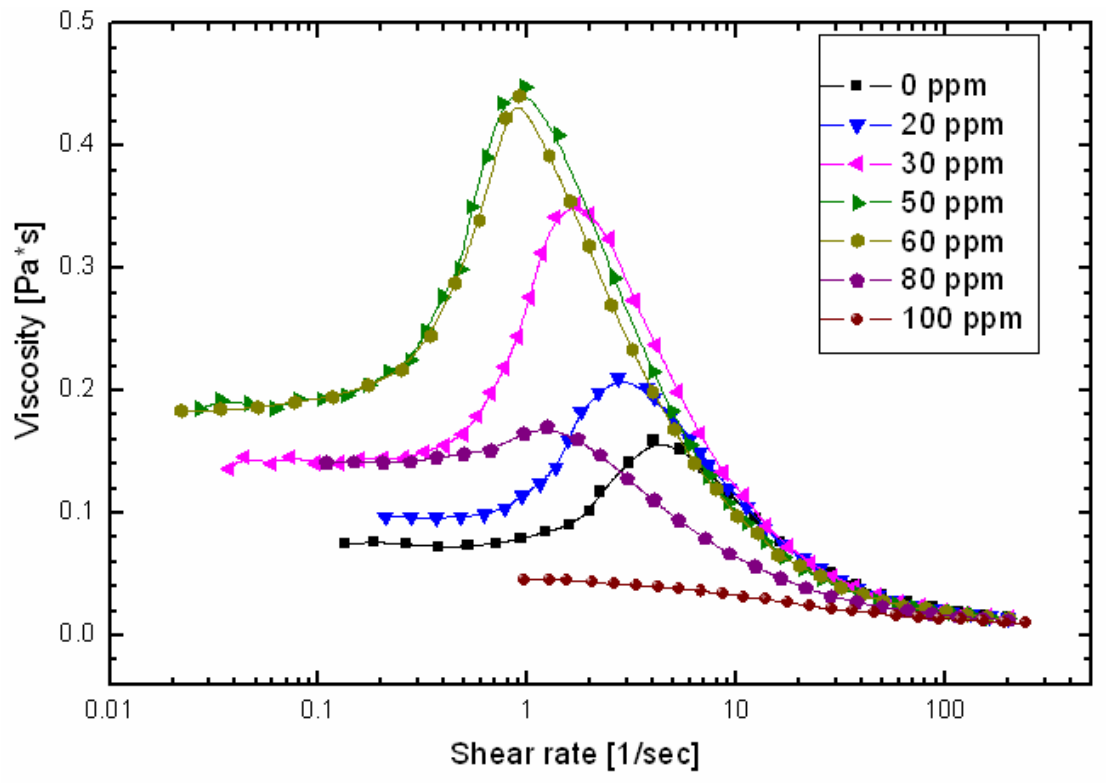

Figure 5.7: Apparent viscosity versus shear rate for 0.2 wt% HMHEC with added $C_{12}E_5$ of various concentrations at 5 °C.

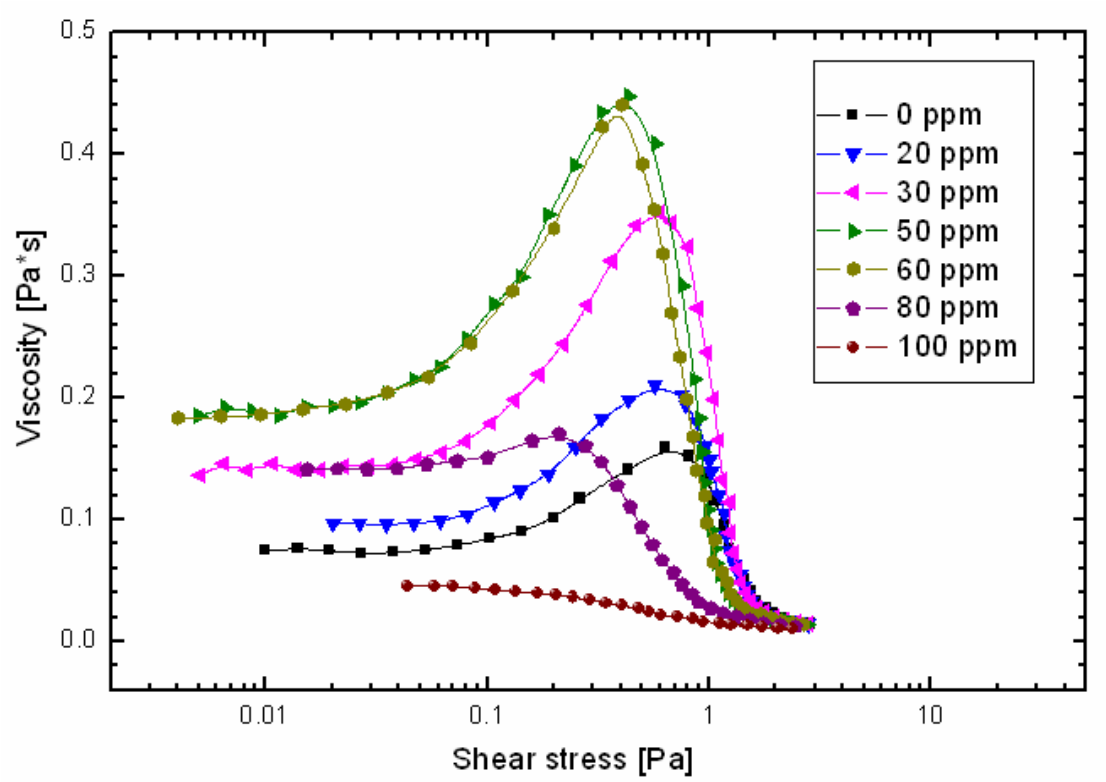

Figure 5.8: Apparent viscosity versus shear stress for 0.2 wt% HMHEC with added $C_{12}E_5$ of various concentrations at 5 °C.

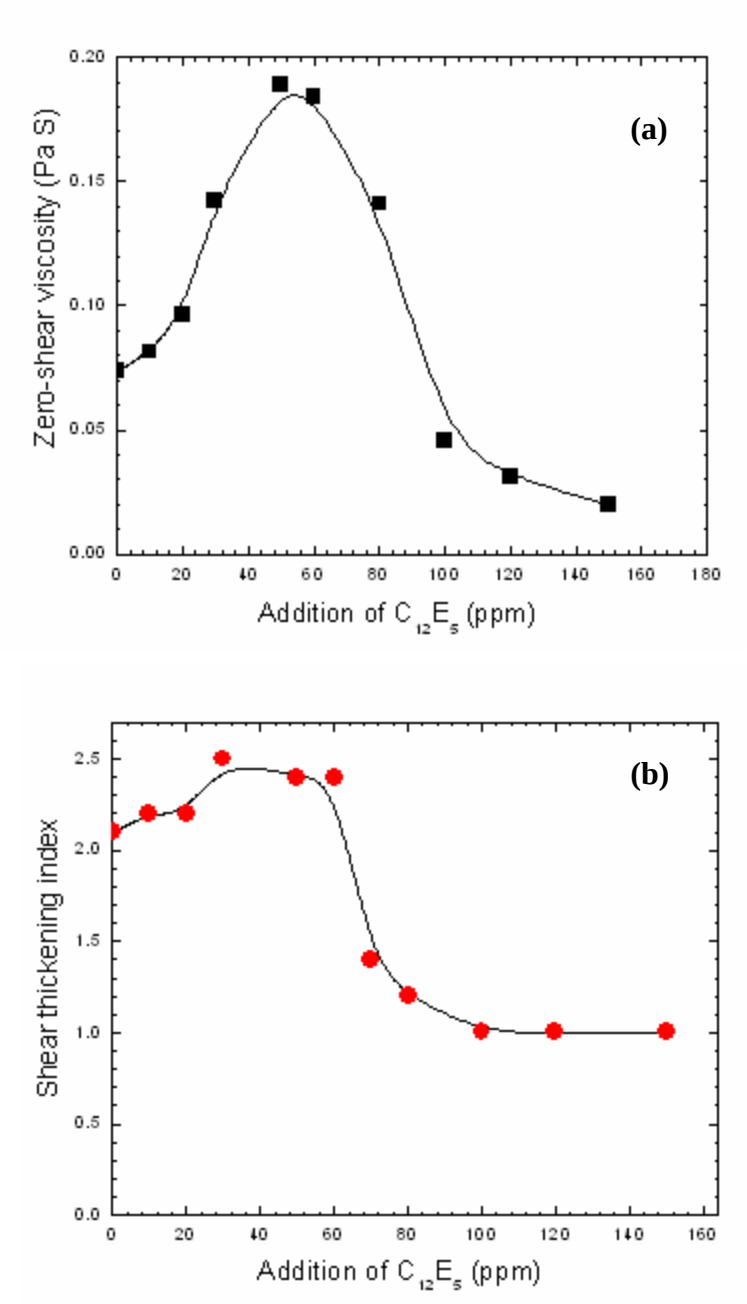

Figure 5.9: Zero-shear viscosity (a) and shear thickening index (b) of 0.2 wt% HMHEC solution as a function of $C_{12}E_5$ concentration at 5 °C.

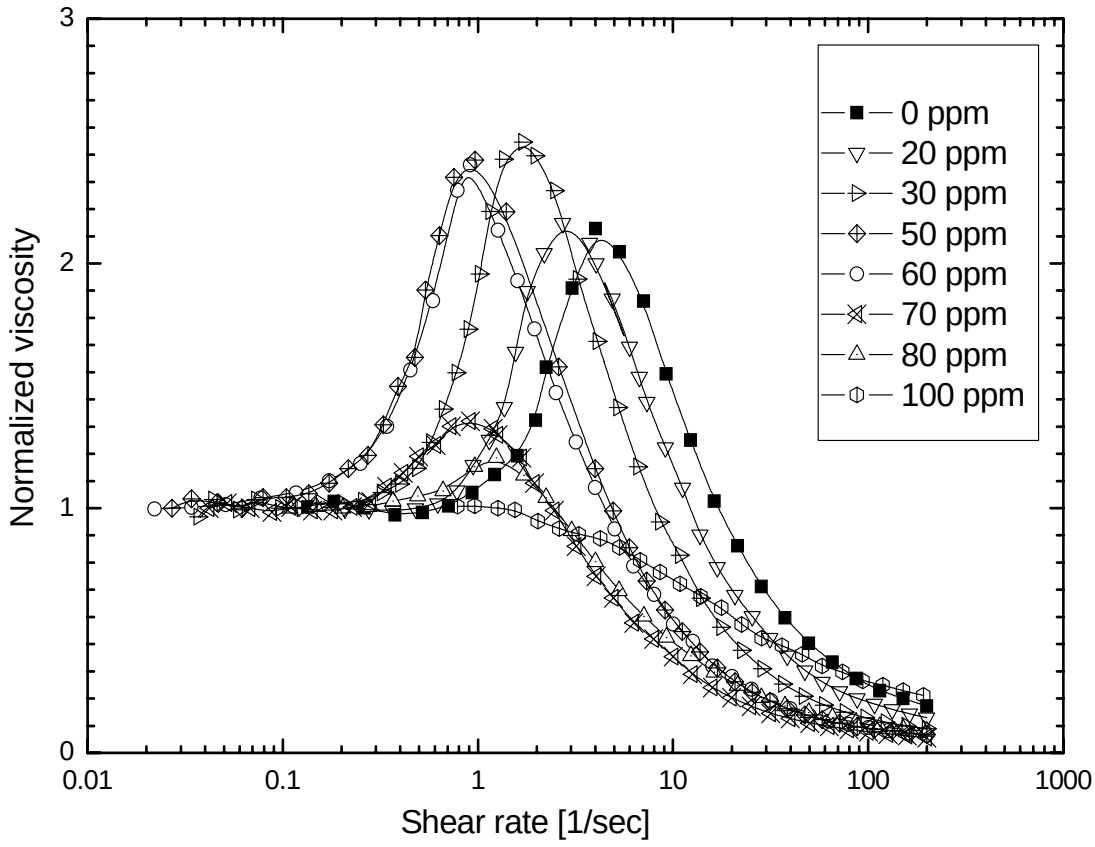

Figure 5.10: Normalized viscosity versus shear rate for 0.2 wt% HMHEC with added $C_{12}E_5$ of various concentrations at 5 °C.

From Figure 5.9, one can find that when the $C_{12}E_5$ concentration exceeds about 100 ppm, the zero-shear viscosity becomes lower than that in the absence of surfactant. This can be explained by masking of the polymer hydrophobes saturated with the surfactant through the formation of mixed micelles.[9,26,28 91] When the $C_{12}E_5$ concentration is below 60 ppm, the surfactant molecules in the form of mixed micelles strengthen the network. In this concentration range, we find from Figure 5.7 that the critical shear rate for the maximum viscosity or for the onset of nonlinear behavior progressively shifts to lower values, upon addition of the surfactant. It implies that the increase of the zero-shear viscosity is likely due to an increase in life time of the hydrophobic junctions[80-81]. Interestingly, only within this surfactant

concentration range, does the shear thickening index of HMHEC solutions maintain its high value ~2.2 (~120% increase than the zero-shear viscosity). The effect of $C_{12}E_9$ on the shear thickening of HMHEC solutions was also investigated, and exhibited a similar trend, although the data are not shown. A schematic representation of the transient polymer network adsorbed with surfactant molecules is shown in Figure 1.1.

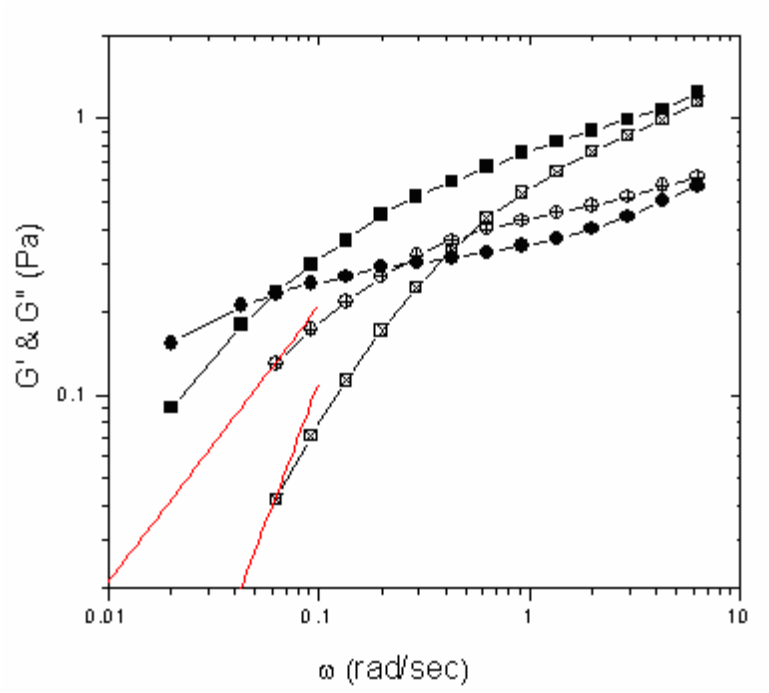

Figure 5.11: Storage and loss moduli versus frequency for two samples, 0.4 wt% HMHEC (open) and 0.4 wt% HMHEC + 100ppm $C_{12}E_5$ (filled symbols) at 5 °C. Lines are added only to guide the eye.

It is difficult to attain a quantitative explanation for the behavior of comblike HMPs with addition of surfactant, because the presently available transient network theories proposed by Marrucci *et al.*[36], Tanaka and Edwards[93], and Jenkins[29] are all for telechelic polymers, mostly in the absence of surfactant. To better understand the flow behavior in the linear regime, we plot in Figure 5.11 the typical mechanical spectra for two investigated samples, 0.4wt% HMHEC and 0.4 wt% HMHEC + 100 ppm $C_{12}E_5$. The crossover between the two moduli shifts to a lower angular frequency for the case with addition of 100 ppm $C_{12}E_5$, analogous to that for HMHPG + Triton X100.[25] These moduli could not be fitted to a unimodal or bimodal Maxwell

expression, in agreement with the earlier studies on HMHEC.[2,28,.91] Also, the terminal region showing the plateau elastic modulus at high frequencies cannot be reached within the accessible frequency range.

In an attempt to analyze the data, we adopt the method of Piculell *et al.* [28] to determine a characteristic modulus G_c and time t_c, only using the crossover point. It should be pointed out that the obtained G_c and t_c have no clear physical meanings, because of a distribution of relaxation times for the HMHEC/surfactant mixtures. The tendencies for the two parameters presented in Table 5.1 reveal qualitatively how the network dynamics and microstructure vary with the surfactant concentration; G_c decreases monotonically with surfactant concentration, whereas t_c increases first and then decreases.

To analyze the results, we employ the Green-Tobolsky rubber network model[94], $\eta_0 = G_0 \tau = vkT\tau$ with G_0 and τ being the plateau modulus and relaxation time. The applicability of this model is supported by the nearly constant ratio shown in the last column of Table 5.1. On the basis of this theory, one can find that the enhancement of zero-shear viscosity at low $C_{12}E_5$ concentrations is dominated by an increase in the characteristic relaxation time, similar to that for HEUR with sodium dodecyl sulfate at high concentrations.[95] From Table 5.1, we also find that the zero-shear viscosity and the relaxation time show a similar variation with the surfactant concentration. It implies that the attraction and association between hydrophobes is reinforced by formation of larger mixed micelles when the surfactant concentration is increased but remains low enough. In comparison, addition of $C_{12}E_4$ to HMHEC causes the relaxation time to increase and then decrease slightly, but does not lead to a noticeable change in the plateau modulus, as reported by Maestro *et al.*[81], who conducted experiments at 30 ^{o}C. It should be noted that since this temperature is already higher than the cloud point of a pure $C_{12}E_4$ solution at sufficient concentrations, it should exceed the cloud point of the mixture with HMHEC[14], making the situation more complicated than that for HMHEC/ $C_{12}E_5$ studied in the present work.

Table 5.1: Rheological data of 0.4wt% HMHEC with addition of $C_{12}E_5$ at 5 °C.

$C_{12}E_5$ [ppm]	ω_c [rad/sec]	G_c [Pa]	t_c [sec]	G_c*t_c [Pa s]	η_0 [Pa s]	$\eta_0/(G_c*t_c)$
0	0.52	0.381	1.92	0.73	2.5	3.41
20	0.309	0.339	3.24	1.10	3.6	3.28
50	0.097	0.257	10.31	2.65	9.2	3.47
100	0.061	0.231	16.39	3.79	12.3	3.25
150	0.071	0.197	14.08	2.77	9	3.24
200	0.135	0.174	7.41	1.29	4.46	3.46

Finally, the effect of nonionic surfactant $C_{12}E_5$ on the strain hardening of 0.4wt% HMHEC is shown in Figure 5.12, which plots the normalized moduli against strain at 1 Hz. The use of this frequency ensures that the flow process is at least 10 times faster than the characteristic relaxation of the mixture (cf. Table 5.1). Note that when the shear stress exceeds 20 Pa, G' for all the samples tested becomes too small to be measured by the rheometer, so we only show data for stress up to 20 Pa for G'. It can be found that at this frequency, the addition of surfactant progressively weakens the strain hardening of HMHEC except for the $C_{12}E_5$ concentrations lower than 20ppm. The strain hardening of the storage modulus eventually disappears at 200 ppm $C_{12}E_5$.

Despite showing a similar trend, the shift of the strain for the onset of strain hardening is less significant than that of the critical shear rate for shear thickening. The degree of strain hardening is only slightly changed by adding surfactant up to about 50 ppm. The weak variation in shear thickening and strain hardening for low surfactant concentrations could be explained partly by the decrease in the number of junction with increasing surfactant concentration, causing the bridging chain segments longer and looser, and hence lesser nonlinear stretching.

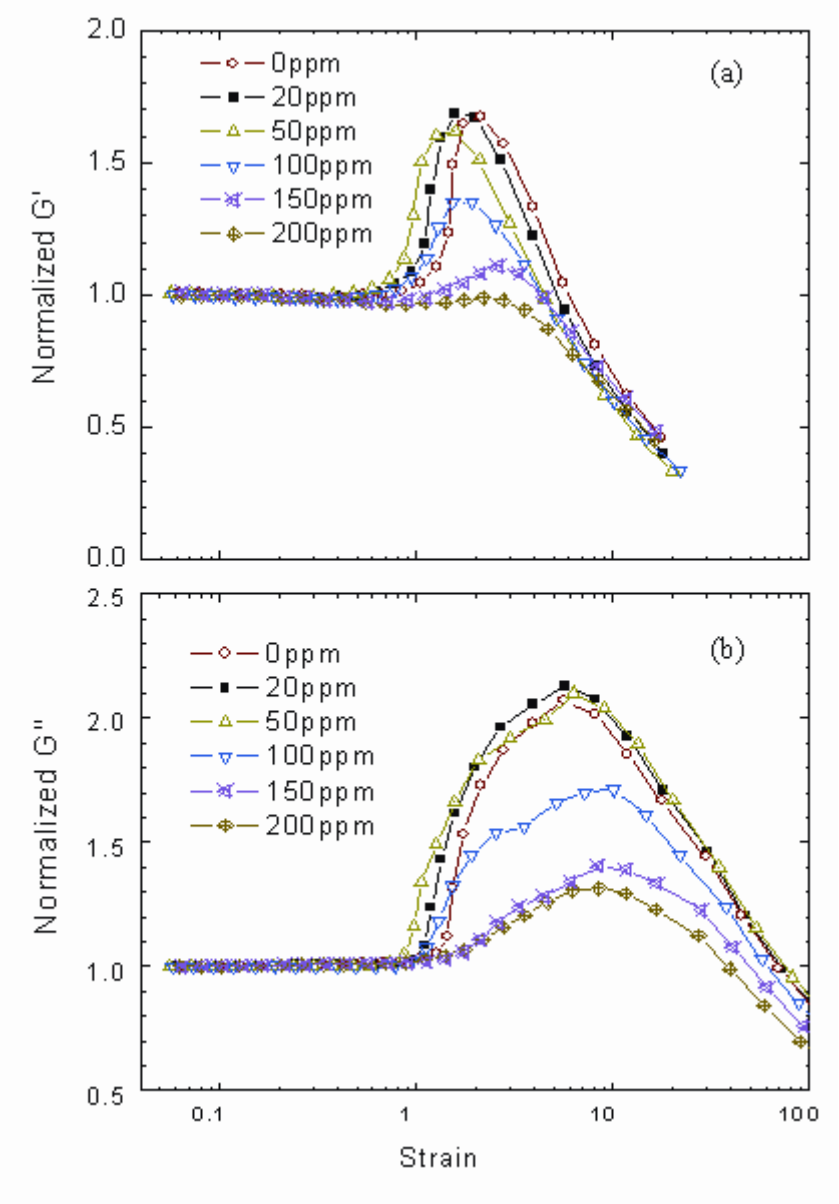

Figure 5.12: Storage and loss moduli versus frequency for two samples, 0.4 wt% Normalized storage (a) and loss (b) moduli versus strain in oscillatory shear for 0.4 wt% HMHEC with different concentrations of added $C_{12}E_5$ at 5 °C. Lines are added only to guide the eye. The frequency is 1Hz.

5.3 Conclusions

We have carried out an experimental investigation on the shear thickening of HMHEC solutions with/without nonionic surfactant. The shear thickening can take place at intermediate shear rates only within a certain polymer concentration range. At 10^{o} C, the shear thickening index of HMHEC can be as large as 2.2, which is higher

than that of HEUR. The degree of shear thickening decreases with increasing temperature, and almost diminishes at room temperature. In the concentration regime where shear thickening occurs, we have reported for the first time that the zero-shear viscosity shows an obviously stronger concentration dependence ($\eta_0 \sim c^{5.7}$) than that in more concentrated regime. This feature provides an additional, important insight into the enhancement of hydrophobic association by introducing more hydrophobes to a solution. By comparing our results with those in the literature, we conclude that the extent of shear thickening depends in general on the chemical species, hydrophobic modification, concentration and temperature.

We have also found that gradual addition of nonionic surfactant to the polymer solution can slightly enhance shear thickening and cause the shear rate for maximum viscosity to shift to lower values until a certain surfactant concentration is reached, beyond which the shear thickening is weakened or even disappears. The dynamic tests reveal that with addition of surfactant, the increase in the zero-shear viscosity of HMHEC solutions is due to an increase in the strength of the junctions instead of the number. Compared to the variation of zero-shear viscosity with surfactant concentration, the weaker concentration dependence of shear thickening and strain hardening could be attributed partly to the decrease in the junction number, leading to longer and looser bridging chain segments and hence reduced nonlinear chain stretching. This new, interesting finding is not only crucial to advance our understanding of how surfactant molecules interact with HMP to influence the flow properties, but also lends support to the mechanism of nonlinear stretching. Moreover, it could be practically useful to better design daily care products, which usually contain both polymer and surfactant, and involve flows in nonlinear regime during manufacturing.

CHAPTER 6 Microrheology of HMHEC Aqueous Solutions

Chapters 4 and 5 have investigated the macroscopic/bulk viscosity behavior of HMHEC solutions, which characterizes the material properties of the solution in the limit of a continuum fluid. It is known that the microviscosity of a polymer solution may significantly differ from its bulk viscosity.[96-97] Here we are interested in probing the microrheology of HMHEC aqueous solutions by measuring the conductivity of small ions through the polymeric network, in the hope that it could provide us further information on the microstructure of the network.

6.1 Literature Review

One of the traditional methods for determining the viscosity of a polymer solution is the falling ball viscometer. The viscosity of the polymeric medium is determined by measuring the migration time of a heavy particle (normally a metal ball) through the microscopically inhomogeneous solution due to gravitational force. The underlying assumption for this method is that the particle must be far larger than the characteristic length (or correlation length) corresponding to the inhomogeneity of a polymer solution. In this limit, the particle essentially feels a homogeneous medium during the "fall" inside a viscometer, and thus the Stokes-Einstein relation, which links the diffusivity of the particle to the bulk medium viscosity, is generally valid.[98-99]

However, when the particle size, becomes comparable to or even smaller than the characteristic length, of the polymer solution, the particle can experience the inhomogeneous microstructure. Under this condition, the Stokes-Einstein relation can no longer hold true. The bulk viscosity in the equation should be replaced by the effective viscosity (microviscosity), which is generally smaller than the macroscopic viscosity in aqueous solutions.[96,97] The microviscosity was defined by Lin and Phillies more than 2 decades ago,[100-101] reflecting the behavior of the medium over a smaller

distance. The microviscosity η_c, can be experimentally measured as

$$\eta_c/\eta_0 = \mu_0/\mu \tag{6.1}$$

where η_0 is the solvent viscosity, and μ_0 and μ the mobilities of the particle in the absence and presence of polymer, respectively.

For charged particles in neutral flexible polymer solutions, the mobility has been determined by applying an external electric field. The measured mobility of the particle can be well described by the stretched exponential function[102-103]

$$\mu/\mu_0 = \exp(-\alpha c_p^{\nu}) \tag{6.2}$$

where both the prefactor α and the scaling exponent ν were found to vary with the particle size and the polymer molecular weight.[102-103] Unlike the bulk viscosity, the microviscosity of a polymer solution could not be completely determined by its own.

Recently, Wang and Tsao[96] came up with an idea to use small ions migrating through a neutral flexible polymer (PEG) solution under an electric field, and measured the electric conductivity. Their experiment corresponds to a limiting case, where the particle size is small compared to the polymer solution's mesh size. They found that the microviscosity could be described by a simple exponential function, with the value of the microviscosity deviating significantly from the bulk viscosity of the polymer solution. In dilute PEG solutions, the conductivity reduction was found to be a linear function of the polymer weight concentration, independent of the polymer molecular weight and the initial salt concentrations.

In this work, we intend to look into the microviscosity of a hydrophobically modified neutral polymer HMHEC and compare it with the bulk viscosity as studied in the previous chapters. The unmodified parent polymer HEC was also tested for comparison with HMHEC.

6.2 Results and Discussion

6.2.1 Absence of Polymer

Figure 6.1 presents the electric conductivity of a NaCl aqueous solution as a function of its concentration. The slope value of the fitting line is also indicated. When the concentration of sodium chloride in the solution is increased, it is not surprising that the conductivity of the solution increases too. This is because by increasing the salt concentration, more ions are present in the solution. In the dilute electrolyte solutions, the electric current is purely the sum of the current carried by individual ions, provided that the ion-ion interaction is ignored. This is known as Kohlrausch's law of independent migration of ions. Consequently, the electric conductivity of an electrolyte solution κ based on the aforementioned additivity is given by

$$\kappa = \sum_{\pm} \kappa_i = \sum_{\pm} z_i e \mu_i c_i \tag{6.3}$$

where z_i is the valency of species i and c_i is its number concentration, and $e = 1.6 \times 10^{-19}$ C. The mobility μ_i is defined as the ratio of ion velocity to the imposed electric field. According to the above equation, the conductivity is proportional to ion number concentrations in dilute solution.

A linear growth of conductivity with salt concentration indicates that, the ion-ion interaction can be ignored and the electrolyte solution is considered dilute. In other words, if the curve starts to deviate from a straight line, the ion-ion interaction must be taken into account. In our experiment, the ion-ion interaction is kept weak, so that the reduction of the electric conductivity will be attributed to the hindrance effect of the polymer. Therefore, Kohlrausch's law of independent migration of ions is obeyed. From Figure 6.1, we have chosen salt concentrations of 3, 5 and 10 mM for our experimental investigation of the conductivity reduction by the polymer.

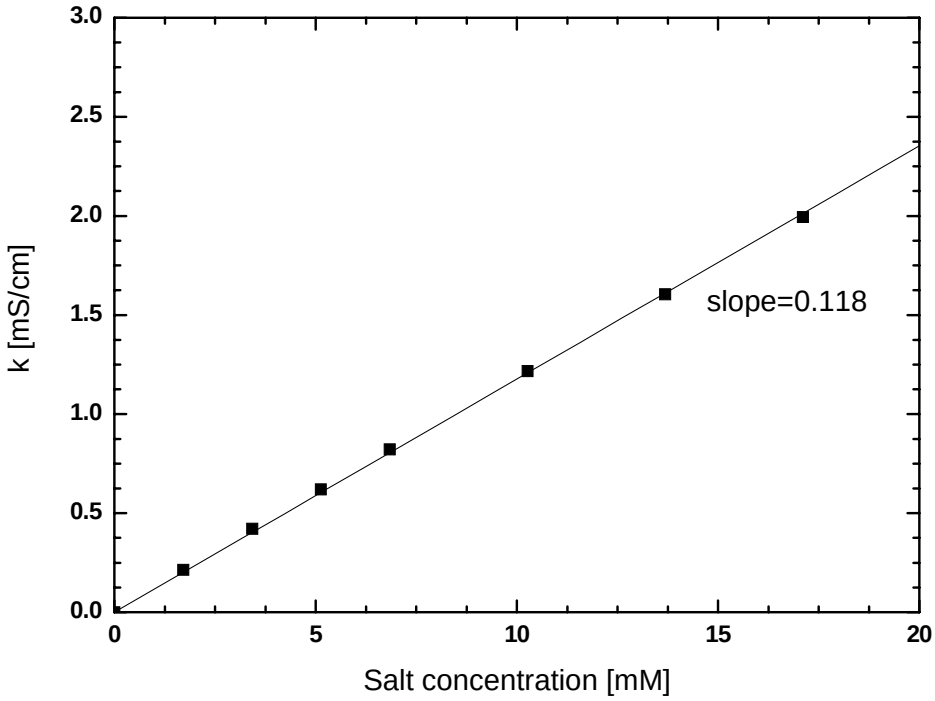

Figure 6.1: Plot of the electric conductivity of NaCl aqueous solutions against its concentration. The slope value from a linear fitting is indicated.

6.2.2 Presence of Polymer

According to de Gennes[104] and Langevin and Rondelez,[105] they mentioned that when the particle size is much smaller than the correlation length, representing the average mesh size of the fluctuating polymer network, the particle is able to move at ease, experiencing essentially just the solvent viscosity. In contrast, if the particle is much greater than the correlation length, the particle motion is affected by the bulk viscosity. The correlation length of a polymer solution depends on the concentration.

Figure 6.2 presents the raw electric conductivity data of NaCl against the polymer concentration. Figure 6.3 presents the normalized conductivity with respect to that of a polymer-free solution. The linear fit of the data is also shown in the figures. As can be seen, the fitting describes the data quite well for both polymers investigated in this study. We can observe that the conductivity declines as the concentration of the two polymers increases. This finding is similar to Wang and Tsao's observation by using PEG of different molecular weight.[96] The conductivity reduction appears to be affected by the polymer weight concentration rather than the type of polymer, either

neutral or hydrophobically modified. When the polymer concentration increases, the number of polymer segments increases, leading to higher hydrodynamic resistance to the motion of the probe ions that no longer move as freely. Since the conductivity is proportional to the mobility of ions, according to Eq. 6.3, the conductivity of the solution is decreased.

Previous studies by Stojilkovic *et al.*[97], Foster *et al.*[106], and Bordi *et al.*[107] show that the polymer effect on the electric conductivity of simple ions depends mainly on the amount of PEG added into the solution and very weakly on the PEG molecular mass. Comparing the results shown in Figure 6.3a and b, it is also observed that the two very different polymers (differing in both molar mass and hydrophobic modification) exerts roughly the same resistance to the conductivity of NaCl (i.e., the slopes of both fitting lines are quite close to each other). Our observations suggest that the microviscosity of a polymer solution is a rather weak function of the polymer molar mass (c.f. Eq. 6.1), in great contrast to the bulk viscosity, which strongly depends on the polymer molecular mass.[108] This means violation of Walden's rule, which relates the conductivity, κ, and the bulk viscosity, η_0, of a polymer solution by:

$$\frac{\kappa\eta_0}{n_{electrolyte}} = \text{const} \tag{6.4}$$

where $n_{electrolyte}$ is the number concentration of the electrolyte. The contribution of this work is that we showed the hydrophobic modification of HMHEC did not affect the microviscosity.

From Figure 6.3, we can also see that the reduced conductivity data for the three different salt concentrations collapse into a single line. This again indicates that the mobility hindrance experienced by the ions is solely due to the polymer segment concentration. Previous studies done by Radko and Chrambach on the electrophoretic migration of charged particles through solutions of entangled polymers showed that the measured mobility of the particle can be well described by the stretched exponential function (Eq. 6.2).[102-103] Measuring the conductivity of small ions in PEG

solutions, Wang and Tsao[96] showed that the conductivity reduction followed a simple exponential function of the polymer concentration for both dilute and semidilute regimes:

$$\frac{\kappa}{\kappa_0} = \exp(-[\kappa]c_p) \tag{6.5}$$

where [κ] is the intrinsic attenuation factor, independent of c_p, the polymer number concentration. In the dilute limit, the reduced conductivity curve can be well described by a linear relationship with the polymer concentration: $\kappa/\kappa_0 = 1-[\kappa]c_p$.[96] As expected, the intrinsic attenuation factor, [κ], scales proportionally with the polymer molecular weight. Therefore, the conductivity reduction in the dilute regime is simply determined by the polymer weight concentration, in agreement with earlier studies.[97, 106, 107]

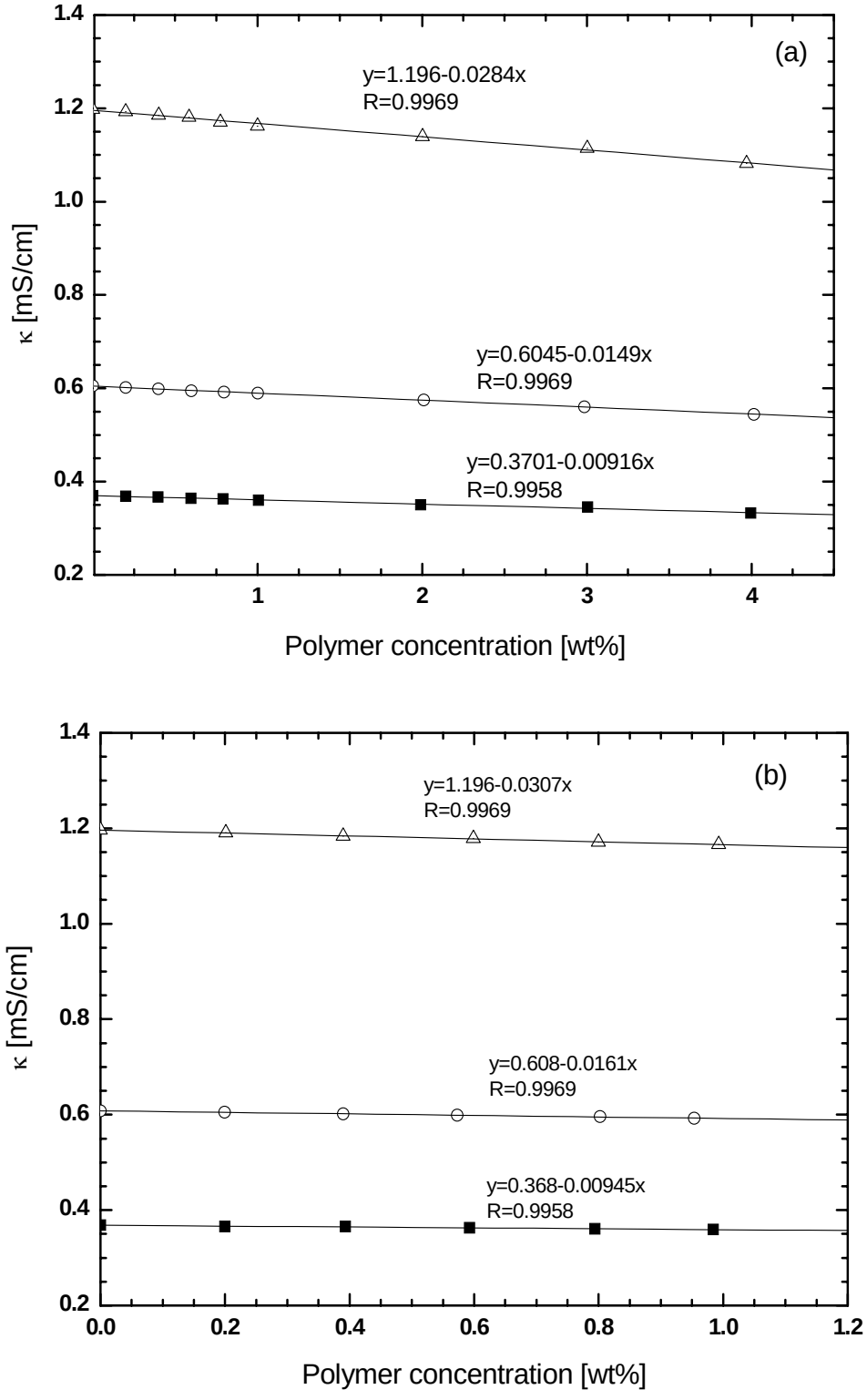

Figure 6.2: Plot of electric conductivity against the polymer concentration of (a) HEC9 and of (b) HMHEC, using sodium chloride as the probe ions. The three concentrations of NaCl used are 3 mM, 5 mM and 10 mM (data from bottom to top). Temperature is at 25 °C.

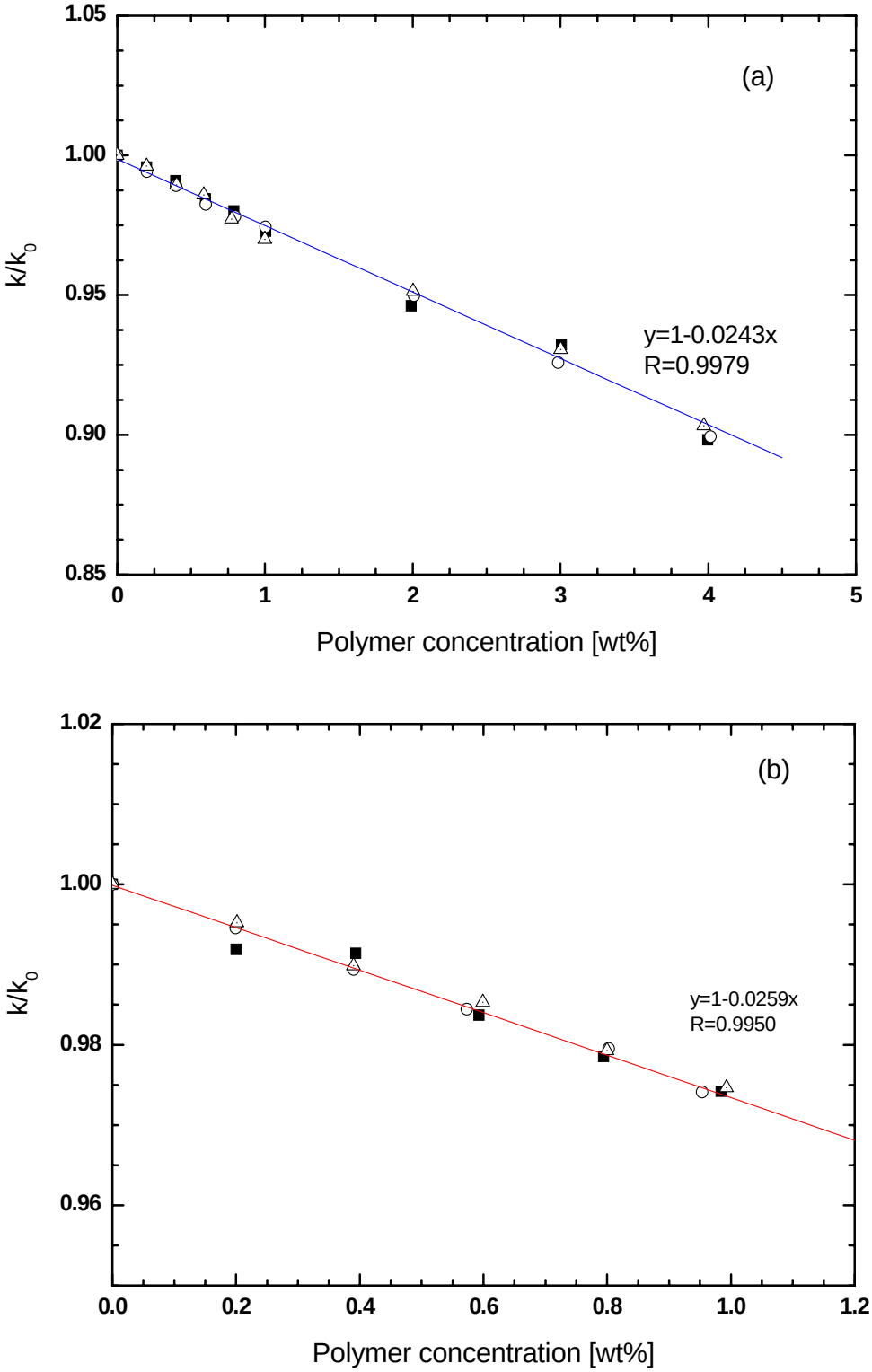

Figure 6.3: Variation of the reduced conductivity against the polymer concentration of (a) HEC9 and of (b) HMHEC, using sodium chloride as the probe ions. The three concentrations of NaCl are 3 mM, 5 mM and 10 mM (data from bottom to top). Temperature is 25 °C.

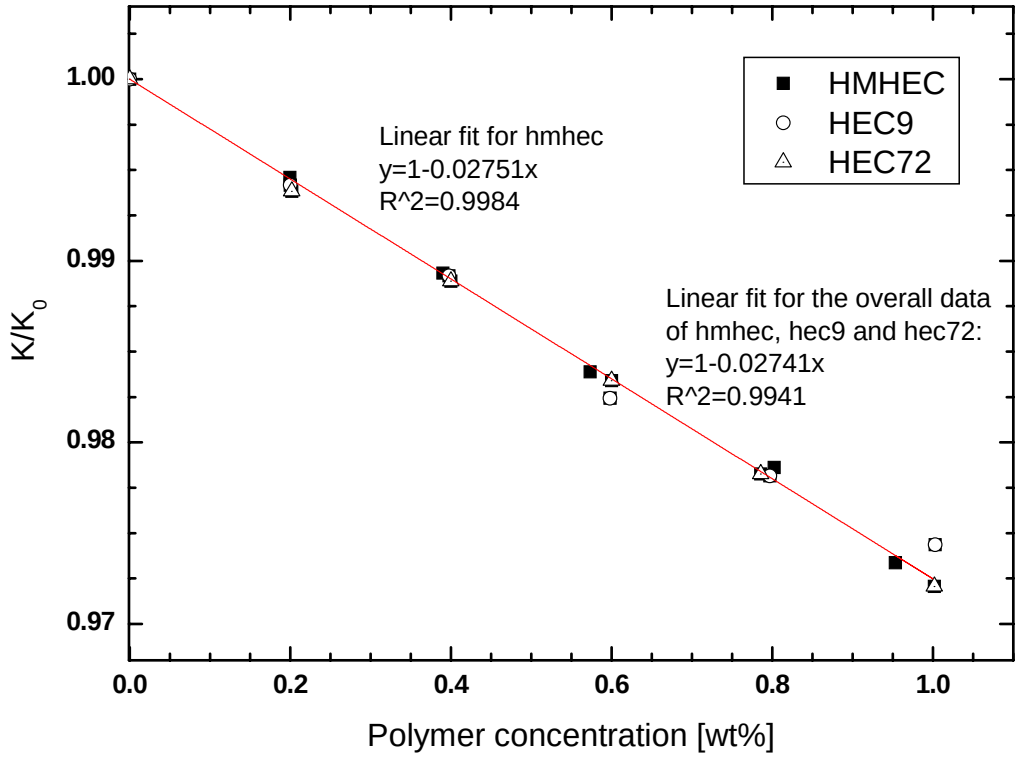

Figure 6.4: Plot of the reduced conductivity κ/κ0for 5mM NaCl against the polymer weight concentration c_p in both the dilute and semidilute regimes. The temperature is 25 °C. The polymers used here differ in molecular weight and hydrophobic modification. The conductivity of 5mM NaCl in water is 0.607±0.002 mS/cm.

Here our results support the above conclusion even for HEC and HMHEC solutions well beyond the dilute regime (cf. Figure 5.3, Figure 6.3b and Figure 6.4).

6.2.3 Comparison between Microviscosity and Bulk Viscosity

Based on the results shown in Figure 6.4, the microviscosity of the three investigated polymer solutions was calculated and presented in Figure 6.5a. The bulk viscosity was also shown in Figure 6.5b for comparison. As the concentration of the polymers increases, the bulk viscosity of all solutions increases exponentially, especially for HMHEC, whose solution viscosity can become nearly 4 orders of magnitude higher than the viscosity of water. In great contrast, the microviscosity of all solutions increases linearly with the polymer concentration, with the same slope

for all polymers studied here. The increase of the microviscosity is only ~2.8% at 1wt% concentration. In other words, the probe ion feels almost no obstruction by the polymer segments during the migration. The mnemonic image, which was frequently implied in theoretical models, takes the probe ion as like a fish moving through a fishnet.[103-105] The image fits well with the ions in our HMHEC solution, with the fishnet being quite widely open. It is concluded that the microenvironment inside the HMHEC solution is essentially approaching pure water, with the segments of the polymer only occasionally encountered by the probe ions. The hydrophobic modification of the parent polymer HEC does not give rise to any noticeable increase in the solutions' microviscosity.

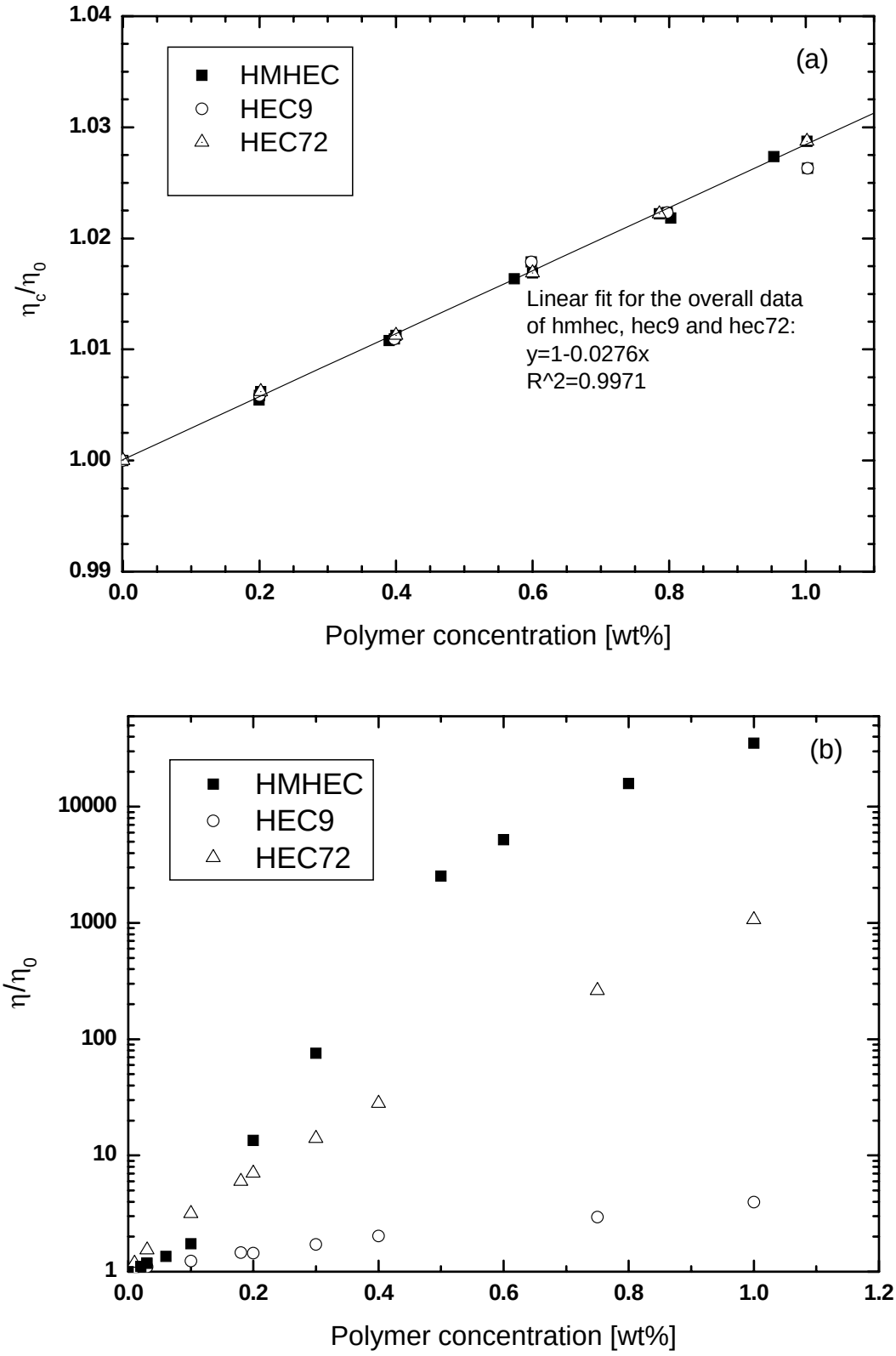

Figure 6.5: Plot of (a) the microviscosity; and (b) the bulk viscosity against the polymer concentration. The viscosity test is undertaken at the temperature of 25 °C. The polymers used are HEC9, HEC72 and HMHEC.

6.3 Conclusions

The microviscosity of HMHEC aqueous solutions was experimentally measured. Compared to its bulk viscosity, the microviscosity was significantly lower by more than 4 orders of magnitude. The hydrophobic modification was found to have no effect on the solutions' microviscosity, based on the same electric conductivity reduction of a simple salt NaCl in both HMHEC and HEC solutions. This interesting result was explained by the fact that the conductivity reduction is merely resulted from the hydrodynamic interactions between the probe ions and the polymer segments.

CHAPTER 7 Conclusions and Recommendations for Further Research

7.1 Conclusions

This research shed light on elucidating the interactions between associative polymers and surfactants, through studing the phase behavior and rheological properties of their aqueous mixtures. In particular, the clouding phenomena, phase separation behavior, steady and dynamic shear viscosity, and nonlinear rheology were measured and quantified for mixtures of hydrophobically modified hydroxyethyl cellulose (HMHEC) and nonionic surfactants.

Analyses for the formed macroscopic phases provided support for associative phase separation for the case of HMHEC mixed with surfactant, in contrast to segregative phase separation for the case of HEC. An interesting three-phase separation phenomenon was reported for the first time in some HMHEC/Triton X-100 mixtures at high enough surfactant concentrations and investigated in detail.

The viscosity behavior of HMHEC solutions were investigated experimentally. With increasing temperature, the viscosity of a HMHEC-surfactant mixture in aqueous solution first decreased, but then rose considerably until around the cloud point. The observed viscosity increase could be explained by the interchain association due to micellar aggregation. Then shear thickening and strain hardening behavior of HMHEC solutions were also examined. Dynamic oscillatory tests of the transient network on addition of surfactants showed that the enhanced zero-shear viscosity was due to an increase in the network junction strength, rather than their number, which in fact decreases. The reduction in the junction number could partly explain the weak variation of strain hardening extent for low surfactant concentrations, because of longer and looser bridging chain segments, and hence lesser nonlinear chain stretching.

The microviscosity of HMHEC aqueous solution was experimentally measured

by conductometry. The microviscosity was significantly lower by more than 4 orders of magnitude than its bulk viscosity. The hydrophobic modification was found to have no effect on the solutions' microviscosity.

7.2 Recommendations for Further Research

The ultimate goal of the research on the interactions of associative polymer and surfactant is to understand, from fundamental principles, how the macroscopic properties, such as viscosity, viscoelasticity and phase behavior are related to the microstructure of the mixture. Examing the macroscopic properties of associative polymer in the presence/absence of surfactant are relatively easier and have been done in this work quite successfully. However, probing the microscopic structure of the formed network is not an easy task. It is around this area and along this direction that further research needs to be done for a complete understanding of associative polymer mixed with surfactant.

Here we discuss and propose the future research in the following three topics: 1) the aggregation number of the mixed micelles; 2) the spacial configuration of the mixed micelles. Basically these two areas concern with the microstructure of the associative/surfactant aqueous solutions; 3) the surfactant effect on the microviscosity of HMHEC solutions.

In Chapter 4, we found an interesting correlation between the solution viscosity maximum and the cloud point temperature. It was proposed that the aggregation number growth of the mixed micelles upon temperature increase contribute to the observed viscosity increase. A further study on the aggregation number by fluorescence probe technique may provide important information to elucidate the underlying mechanism. As expected, the aggregation number will increase with temperature in an associative polymer/nonionic surfactant mixture solution. Then a correlation between the viscosity increase and the aggregation number could possibly be established. By knowing the aggregation number, the number of association junctions can also be figured out, thus a directly comparison with the high frequency storage modulus as could be obtained from a frequency sweep on a rheometer

becomes possible.

The spacial configuration of the mixed micelles is believed to be the main factor for the observed shear thickening and strain hardening behavior of HMHEC in the presence of nonionic surfactant. A powerful equipment, small-angle neutron scattering technique (SANS), can provide such information on a 0.1nm ~1000nm scale. Further study is recommended in this area. An immediate experimental challenge arises from the fact that the nonlinear rheological behavior can only show up under a certain shear rate or shear stress. To overcome this, one possible way is to increase the relaxation time of the associative polymer by using stronger hydrophobes attached to the backbone of the polymer, thus a transient network of much higher association strength can form. Then SANS characterization could become possible for a gel sample immediately after a shear rate has been applied. Relaxation of chains could also be monitored and thus provides information on how the chains relax and what is the relaxation time. This correlation of microstructure to the macroscopic nonlinear behavior will be an interesting and challenging research area in the coming years.

Finally, the impact of the presence of surfactant on the microviscosity would be a great idea deserving to be further explored. And possible comparison could be made with the results in Chapter 4 and 5 where the surfactant effect on the bulk viscosity of HMHEC solutions has been studied. However, it is not expected that the surfactant will have significant effect on the microviscosity of HMHEC solutions.

References

1. Schaller, E.J. Rheology Modifiers for Water Borne Paints, *Surface Coatings Australia*, **1985**, *22*(10), 6.

2. Maestro, A.; Gonzalez, C.; Gutierrez, J. M. *J. Rheo*. **2002**, *46*, 127-143.

3. Maestro, A.; Gonzalez, C.; Gutierrez, J. M. *J. Rheo*. **2002**, *46*, 1445-1457.

4. Linse, P.; Piculell, L.; Hansson, P. In *Polymer-Surfactant Systems*; Kwak, J. C. T., Ed.; Marcel Dekker, New York, **1998**,193.

5. Thuresson, K. and Lindman B. *J. Phys. Chem. B* **1997**, *101*, 6460-6468.

6. Alami, E.; Almgren, M.; Brown, W. *Macromolecules* **1996**, *29*, 5026-5035.

7. Appell, J.; Porte, G.; Rawiso, M. *Langmuir* **1998**, *14*, 4409-4414.

8. Zhao, G.; Khin, C. C.; Chen, S. B.; Chen, B. H. *J. Phys. Chem. B* **2005**, *109*, 14198-14204.

9. Thuresson, K.; Lindman B. and Nystrom B. *J. Phys. Chem. B* **1997**, *101*, 6450-6459

10. Bai, D.; Khin, C. C.; Chen, S. B.; Tsai, C. C.; Chen, B. H. *J. Phys. Chem. B* **2005**, *109*, 4909-4916.

11. Piculell, L.; Thuresson, K.; Lindman, B. *Polym. Adv. Technol.* **2001**, *12*, 44-69.

12. Zhang, K.; Karlstrom, G.; Lindman, B. *J. Phys. Chem.* **1994**, *98*, 4411-4421.

13. Joabsson, F.; Rosen, O.; Thuresson, K.; Piculell, L.; Lindman, B. *J. Phys. Chem. B* **1998**, *102*, 2954-2959.

14. Zhao, G.; Chen, S. B. *Langmuir* **2006**, *22*, 9129-9134.

15. Piculell, L.; Lindman, B. *Adv. Colloid Interface Sci.* **1992**, *41*, 149-178.

16. Goddard, E. D.; Leung, P. S. *Langmuir* **1992**, *8*, 1499-1500.

17. Guillemet, F.; Piculell, L. *J. Phys. Chem.* **1995**, *99*, 9201-9029.

18. Hashidzume, A.; Ohara, T.; Morishima, Y. *Langmuir* **2002**, *18*, 9211-9218.

19. Robb, I. D.; Williams, P. A.; Warren, P.; Tanaka, R. *J. Chem. Soc. Faraday Trans.* **1995**, *91*, 3901-3906.

20. Gerharz, B.; Horst, R. *Colloid Polym. Sci.* **1996**, *274*, 439-445.

21. Drummond, C. J.; Albers, S and Furlong, D. N. *Colloids Surf.* **1992**, 62*,* 75-85.

22. Sivadasan, K. and Somasundaran, P. *Colloids Surf.* **1990**, *49,* 229-239.

23. Pandit, N. K.; Kanjia, J.; Patel, K.; Pontikes, D. G. *Int. J. Pharm.* **1995,** *122,* 27-33.

24. Pandit, N. K.; Kanjia, J. *Int. J. Pharm.* **1996,** *141,* 197-203.

25. Aubry, T.; Moan, M. *J. Rheo*. **1996**, *40*, 441-448.

26. Nilsson, S.; Thuresson, K.; Hansson, P.; Lindman, B. *J. Phys Chem. B* **1998**, *102*, 7099-7105.

27. Patruyo, L. G.; Muller, A. J.; Saez, A. E. *Polymer*. **2002**, *43*, 6481-6493.

28. Piculell, L.; Egermayer, M.; Sjostrom, J. *Langmuir* **2003**, *19*, 3643-3649.

29. Jenkins, R.D. *PhD Thesis*, Lehigh University, **1991**.

30. Annable, T.; Buscall, R.; Ettelaie, R.; Shepherd, P. Whittlestone, D., *J. Rheol.* **1993**, 37, 695.

31. Ma, S.X.; Cooper, S.L. *Macromolecules* **2001**, *34*, 3294.

32. Tam, K.C.; Jenkins, R.D.; Winnik, M.A.; Bassett, D.R. *Macromolecules* **1998,** *31,* 4149.

33. Witten, T.A.; Cohen, M.H. *Macromolecules* **1985**, *18,* 1915.

34. Ballard, M.J.; Buscall, R.; Waiter, F.A. *Polymer* **1988**, *29*, 1287

35. Wang, S.Q. *Macromolecules* **1992**, *25,* 7003.

36. Marrucci, G.; Bhargava, S.; Cooper, S.L. *Macromolecules* **1993**, 26, 6483.

37. van den Brule, B.; Hoogerbrugge, P. *J. Non-Newtonian Fluid Mech.* **1995**, *60,* 303.

38. Ma, S.X.; Cooper, S.L. *Macromolecules* **2002**, *35*, 2024.

39. English, R.J.; Gulati, H.S.; Jenkins, R.D.; Khana, S.A. *J. Rheol.* **1997**, *41,* 427.

40. Tirtaatmadja, V.; Tam, K.C.; Jenkins, R.D. *Macromolecules* **1997,** *30,* 1426.

41. Abdala, A.A.; Wu, W.; Olesen, K.R.; Jenkins, R.D.; Tonelli, A.E.; Khan, S.A. *J. Rheol.* **2004,** *48,* 979.

42. Snowden, M. J.; Phillips, G. O.; Williams, P. A. *Food Hydrocolloids* **1987,** *1*, 291-300.

43. Morse, E. E. *Anal. Chem.* **1947**, *19*, 1012-1013.

44. Morris, D. L. *Science* **1948**, *107*, 254-255.

45. Louis Sattler; Zerban, F. W. *Science* **1948,** *108*, 207-208.

46. Hackley V.A., Ferraris C.F. *Guide to Rheological Nomenclature* **2001,** 1-36

47. Marin G. *Oscillatory Rheometry*. In *Rheological Measurements (2nd edition),* Collyer, A.A. & Clegg, D.W. (Eds.), London. Chapman & Hall Ltd. **1998**, 3-46

48. Walters, K. *Rheometry*. Chapman and Hall Ltd, London. **1975**.

49. Darby, R. *Viscoelastic Fluids: An Introduction to Their Properties and Behavior*. Macrel Dekker, New York, **1975**.

50. Ferry, J.D. "Viscoelastic Properties of Polymers", second edition, John Wiley and Sons: New York, **1970**.

51. Goddard, E.D. and Ananthapadmanabhan, K.P. *Interactions of Surfactants with Polymers and Proteins.* CRC Press, **1992.** 1-10.

52. Lindman,B.; Thalberg,K. *Polymer-Surfactant Interactions-Recent Developments*, in *Interactions of Surfactants with Polymers and Proteins,* Goddard, E.D. & Ananthapadmanabhan, K.P. (Eds.), CRC Press, **1992**. 205-268.

53. Miller, C. A.; Neogi, P. *Interfacial Phenomena, Equilibrium and Dynamic Effects*; Marcel Dekker, New York, **1985**, *33*, p140.

54. Alami, E.; Almgren, M.; Brown, W. *Macromolecules* **1996**, *29*, 5026-5035.

55. Iliopoulos, I.; Olsson, U. *J. Phys. Chem.* **1994**, *98*, 1500-1505.

56. Loyen, K.; Iliopoulos, R.; Audebert, R.; Olsson, U. *Langmuir* **1995**, *11*, 1053-1056.

57. Loyen, K.; Iliopoulos, R.; Olsson, U.; Audebert, R. *Progr. Colloid Polym. Sci.* **1995**, *98*, 42-46.

58. Penders, M. H. G. M.; Nilsson, S.; Piculell, L.; Lindman, B. *J. Phys. Chem.* **1993**, *97*, 11332-11338.

59. Goddard, E. D. *Colloids Surf.* **1986**, 1*9,* 255-300.

60. Clegg, S. M.; Williams, P. A.; Warren, P.; Robb, I. D. *Langmuir* **1994,** *10,* 3390-3394.

61. Piculell, L.; Bergfeldt, K.; Gerdes, S. *J. Phys. Chem.* **1996,** *100,* 3675-3679.

62. Effing, J. J.; McLennan, I. J.; Kwak, J. C. T. *J. Phys. Chem.* **1994,** *98,* 2499-2502.

63. Thuresson, K.; Nystrom, B.; Wang, G.; Lindman, B. *Langmuir* **1995**, *11*, 3730-3736.

64. McCarroll, M; Toerne, K.; Wandruszka, R. *Langmuir* **1998**, *14*, 6096-6100.

65. McCarroll, M; Toerne, K.; Wandruszka, R. *Langmuir* **1998**, *14*, 2965-2969.

66. Toerne, K.; Rogers, R.; Wandruszka, R. *Langmuir* **2000**, *16*, 2141-2144.

67. Maclay, W. *J. Colloid Sci.* **1956,** *11*, 272-285.

68. Strey, R. Ber. Bunsenges. Phys. Chem. **1996**, 100, 182-189.

69. Nilsson, P. G.; Wennerstrom, H.; Lindman, B. *J. Phys. Chem.* **1983**, 87, 1377-1385.

70. Hiller,G. K.; Calkins, N.; Wandruszka, R. *Langmuir* **1996,** *12,* 916-920.

71. Groswasser, A. B.; Wachtel, E.; Talmon, Y. *Langmuir* **2000,** *16,* 4131-4140.

72. Panayatova, S.; Bivas, I. *Bulg. J. Phys.* **2004**, *31*, 83-86.

73. Tsianon, M.; Thuresson, K.; Piculell, L. *Colloid Polym. Sci.* **2001***, 279*, 240-347.

74. Thuresson, K.; Soderman P. O.; Hansson, E.; Wang, G. *J. Phys. Chem.* **1996**, *100*, 4909-4918.

75. Behera, K.; Dahiya, P.; Pandey, S. *J Colloid Interface Sci.* **2007**, *307*, 235–245.

76. Streletzky, K.; Phillies, G. *Langmuir* **1995**, *11*, 42-47.

77. Tirtaatmadja, V.; Tam, K. C.; Jenkins, R. D. *Langmuir* **1999**, *15*, 7537-7545.

78. Nishikawa, K.; Yekta, A.; Pham, H. H.; Winnik, M. A. *Langmuir* **1998**, *14*, 7119-7129.

79. Ma, S. X.; Cooper, S. L. *J. Rheol.* **2002**, *46*, 339-350.

80. Talwar, S., Scanu, L.F., Khan, S.A. *J. Rheol.* **2006**, *50***,** 831.

81. Maestro, A., Gonzalez, C., Gutierrez*,* J.M. *J. Colloid Interface Sci.* **2005**, *288***,** 597.

82. Xu, B.; Yekta, A.; Li, L.; Masoumi, Z.; Winnik, M. A. *Colloid Surface A* **1996**, *112*, 239-250.

83. Yekta, A.; Xu, B.; Duhamel, J.; Adiwidjaja, H.; Winnik, M. A. *Macromolecules* **1995**, *28*, 956-966.

84. Tripathi, A.; Tam, K. C.; McKinley, G. H. *Macromolecules* **2006**, *39*, 1981-1999.

85. Aubry, T.; Moan, M. *J. Rheol.* **1994**, *38*, 1681-1692.

86. Mewis, J.; Kaffashi. B.; Vermant, J.; Butera, R. J. *Macromolecules* **2001**, *34*, 1376-1383.

87. Pellens, L.; Corrales, R. G.; Mewis, J. *J. Rheol.* **2004**, *48*, 379-393.

88. Tirtaatmadja, V.; Tam, K. C.; Jenkins, R. D. *Macromolecules* **1997**, *30*, 3271-3282.

89. Serero, Y., Jacobsen, V., Berret, J.-F., May, R. *Macromolecules* **2000,** *33,* 1841.

90. J.-F. Berret, Y. Serero, B. Winkelman, D. Calvet, A. Collet, M. Viguier, *J. Rheol.* **2001,** *45***,** 477-492.

91. R. Tanaka, J. Meadows, P.A. Williams, G.O. Phillips, *Macromolecules* **1992,** *25*, 1304-1310.

92. S.C. Wang, T.C. Wei, W.B. Chen, H.K. Tsao, *J. Chem. Phys.* **2004**, *120***,** 4980-4988.

93. F. Tanaka, S.F. Edwards, J. Non-Newtonian Fluid Mech. **1992**, *43*, 247.

94. M.S. Green, A.V. Tobolsky, *J. Chem. Phys.* **1946**, *14***,** 80-92.

95. Annable, R. Buscall, R. Ettelaie, P. Shepherd, D. Whittlestone, *Langmuir* **1994**, *10*, 1060-1070.

96. Wang, S.C.; Tsao, H.K. *Macromolecules* **2003**, *36*, 9128.

97. Stojilkovic, K.S.; Berezhkovskii, A.M.; Zitserman, V.Y.; Bezrukov, S.M. *J. Chem. Phys.* **2003**, *119,* 6973.

98. Barshtein, G.; Almagor, A.; Yedgar, S.; Gavish, B. *Phys. Rev. E.* **1995**, *52*, 555.

99. Phillies, G.D.J. *J. Phys. Chem.* **1989**, *93*, 5029.

100. Lin, T.-H.; Phillies, G.D.J. *J. Phys. Chem.* **1982***, 86*, 4073.

101. Lin, T.-H.; Phillies, G.D.J. *J. Colloid Interface Sci.* **1984**, *100*, 82-95.

102. Radko, S.P.; Chrambach, A. *J. Phys. Chem.* **1996**, *100*, 19461.

103. Radko, S.P.; Chrambach, A. *Macromolecules* **1999**, *32*, 2617.

104. De Gennes, P.-G. *Scaling Concepts in Polymer Physics.* Cornell Universtiy Press: Ithaca, NY, **1993**.

105. Langevin, D.; Rondelez, F. *Polymer* **1978**, *19*, 875.

106. K. R. Foster, E. Cheever, and J. B. Leonard, *Biophys. J.* **1984**, *45*, 975.

107. F. Bordi, C. Cametti, and A. Di Biasio, *J. Phys. Chem.* **1988**, *92*, 4772.

108. Doi, M. and Edwards, S.F. *The Theory of Polymer Dynamics.* Clarendon, Oxford, **1986**

PUBLICATIONS

Journal Publications

- **Zhao, G.-Q.**, Chen, S. B. Microviscosity of Hydrophobically Modified Hydroxyethyl Cellulose Aqueous Solutions. ***J Colloid Interface Sci. 322*** (2008). 678-680.
- **Zhao, G.-Q.**, Chen, S. B. Three-phase separation in nonionic surfactant/ hydrophobically modified polymer aqueous mixtures. ***Langmuir 23*** (2007) 9967-9973.
- **Zhao, G.-Q.**, Chen, S. B. Nonlinear rheology of aqueous solutions of hydrophobically modified hydroxyethyl cellulose with nonionic surfactant. ***J Colloid Interface Sci. 316*** (2007). 858-866.
- **Zhao, G.-Q.**, Chen, S. B. Phase behavior and shear thickening of HM-HEC solutions with addition of nonionic surfactant $C_{12}E_5$. ***Journal of Central South University of Technology 14*** (2007). 202-205
- **Zhao, G.-Q.**, Chen, S. B. Clouding and phase behavior of nonionic surfactants in hydrophobically modified hydroxyethyl cellulose solutions. ***Langmuir* 22** (2006) 9129-9134.
- **Zhao, G.-Q.**, Khin, C. C., Chen, S. B., Chen, B. H.. Nonionic surfactant and temperature effects on the viscosity behavior of hydrophobically modified hydroxyethyl cellulose solutions. ***J. Phys. Chem. B* 109** (2005) 14198-14204.

Conference Proceedings

- Chen, S. B. and **Zhao, G.-Q.** Three-phase behavior of surfactant-polymer mixture. *6th European Congress of Chemical Engineerin*g, Copenhagen, Denmark, Sept. 2007
- **Zhao, G.-Q.**, Chen, S. B. Temperature and Nonionic Surfactant Effects on Shear Thickening of Hydrophobically Modified Hydroxyethyl Cellulose Aqueous Solutions. *4th International Congress on Materials for Advanced Technologies,* Singapore, July 2007
- **Zhao, G.-Q.**, Chen, S. B. Nonionic surfactant and temperature effects on the viscosity behavior of HMHEC solutions. *17th International Congress of Chemical and Process Engineering,,* Prague, Czech Republic, Aug. 2006

- **Zhao, G.-Q.**, Chen, S. B. Phase Behavior and Shear Thickening of HMHEC Solutions with Addition of Nonionic Surfactant $C_{12}E_5$. *Proceedings of the 4th Pacific Rim Conference on Rheology*, Shanghai, China, Aug. 2005

- Chen, S. B. and **Zhao, G.-Q.** Rheology and Phase Behavior of Hydrophobically Modified Polymer in Nonionic Surfactant Solutions. *3rd International Conference on Materials for Advanced Technologies,* Singapore, Jul. 2005